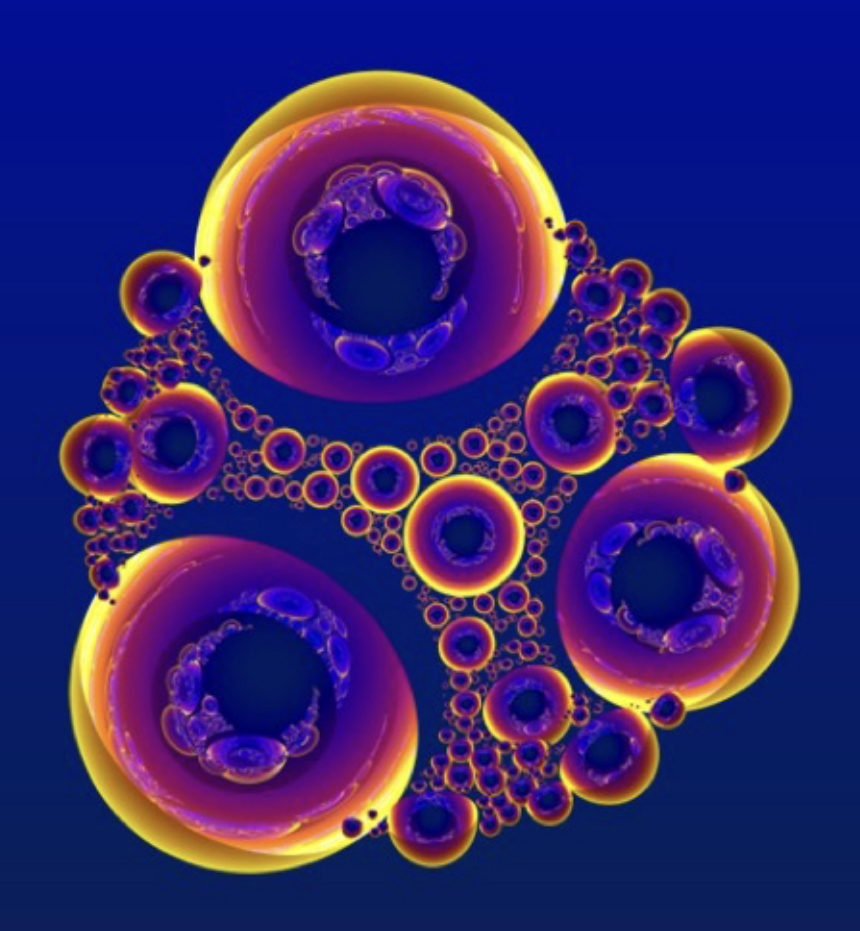
ARNOLD MATHEMATICAL JOURNAL







2025 Volume 11, Issue 3



Arnold Mathematical Journal

Editor in Chief:

Sergei Tabachnikov, Pennsylvania State University (USA)

Managing Editor:

Maxim Arnold, University of Texas at Dallas (USA)

Editorial Board:

Andrei Agrachev, International School for Advanced Studies (Italy)

Peter Albers, Heidelberg University (Germany)

Gal Binyamini, Weizmann Institute of Science (Israel)

Gil Bor, Centro de Investigación en Matemáticas (Mexico)

Felix Chernous'ko, Institute for Problems in Mechanics, RAS (Russia)

Bertrand Deroin, Cergy Paris Université (France)

David Eisenbud, University of California, Berkeley (USA)

Uriel Frisch, Observatoire de la Cote d'Azur, Nice (France)

Dmitry Fuchs, University of California, Davis (USA)

Alexander Gaifullin, Steklov Mathematical Institute, Moscow (Russia)

Victor Goryunov, University of Liverpool (UK)

Sabir Gusein-Zade, Moscow State University (Russia)

Yulij Ilyashenko, Higher School of Economics, Moscow (Russia)

Oleg Karpenkov, University of Liverpool (UK)

Askold Khovanskii, University of Toronto (Canada)

Evgeny Mukhin, IUPU, Indianapolis (USA)

Anatoly Neishtadt, Loughborough University (UK)

Evita Nestoridi, Stony Brook University (USA)

Greta Panova, University of Southern California (USA)

Dan Romik, University of California, Davis (USA)

Alexander Shnirelman, Concordia University (Canada)

Frank Sottile, Texas A&M University (USA)

Vladlen Timorin, Higher School of Economics, Moscow (Russia)

Alexander Varchenko, University of North Carolina, Chapel Hill (USA)

Oleg Viro, Stony Brook University (USA)

Michael Yampolsky, University of Toronto (Canada)

Advisors:

Artur Avila, University of Zurich (Switzerland) and IMPA (Brazil)

Etienne Ghys, Ecole normale superieure de Lyon (France)

Dennis Sullivan, Stony Brook University and Graduate Center, CUNY (USA)

Journal of **Institute of Mathematical Sciences**, Stony Brook University, NY Published by **Association for Mathematical Research**, Davis, CA; Jenkintown PA.

Contents

E. G. Malkovich	1
Discretization of the sub-Riemannian Heisenberg Group	_
O. Karpenkov, A. Pratoussevitch, R. Sheppard	17
Circumscribed Circles in Integer Geometry	
T. Kogiso, K. Miyamoto, X. Ren, M. Wakui, K. Yanagawa	40
Arithmetic on q-deformed rational numbers	42
M. Langford, Yu. Liu, G. McNamara	
Ancient curve shortening flow in the disc	93
with mixed boundary condition	
A. Gogolev, L. Keck, K. Lewis	117
Bouncing Outer Billiards	117



Arnold Mathematical Journal Volume 11, Issue 3, 2025



Discretization of the sub-Riemannian Heisenberg Group

Evgeny G. Malkovich®

Received 22 Sept 2024; Accepted 9 Feb 2025

Abstract: In this article, we present a discrete model of the sub-Riemannian Heisenberg group \mathcal{H} , which serves as an analog of a triangulation of a two-dimensional surface embedded in \mathbb{R}^3 . The constructed discrete model is represented by a spatial graph Γ_r with weighted edges. The shortest paths within Γ_r approximate geodesics in \mathcal{H} .

Keywords: Nonholonomic distribution, Heisenberg group, discrete geometry, computational geometry, sub-Riemannian spheres, geodesics, shortest paths in a graph, tortuosity.

AMS Classification: 52C35, 53C17

Key words and phrases: Nonholonomic distribution, Heisenberg group, discrete geometry, computational geometry, sub-Riemannian spheres, geodesics, shortest paths in a graph, tortuosity

1 Introduction

The Heisenberg group \mathcal{H} is one of the best known and straightforward examples of nonholonomic geometry. It consists of the three-dimensional space \mathbb{R}^3 equipped with a two-dimensional non-integrable subbundle of the tangent bundle $T\mathbb{R}^3$. In the context of the Heisenberg group, the planes Π of admissible directions are spanned by two vector fields, X and Y:

$$X = \frac{\partial}{\partial x} - \frac{y}{2} \frac{\partial}{\partial z}, \quad Y = \frac{\partial}{\partial y} + \frac{x}{2} \frac{\partial}{\partial z}.$$
 (1)

It is straightforward to verify that the Lie bracket $[X,Y]=\frac{\partial}{\partial z}$. According to Frobenius theorem, there is no foliation of \mathbb{R}^3 into a family of two-dimensional surfaces Σ such that X and Y are tangent to Σ ; this is equivalent to the non-integrability of distribution. In this scenario, it is quite clear that the normal vector \vec{n} of the plane Π would need to be the gradient of some function F = F(x, y, z) up to multiplication by a scalar function $\lambda = \lambda(x, y, z)$:

$$\lambda \vec{n} = \lambda X \times Y = \lambda(\frac{y}{2}, -\frac{x}{2}, 1) = (F'_x, F'_y, F'_z).$$

It is not hard to check that there are no solutions $\lambda(x,y,z)$ and F(x,y,z) of this system of PDEs: from the first two equations it easy to show that F should be a function depending only on $\phi = \arctan \frac{y}{x}$ and z; usind the third equation one will find that F doesn't depend on ϕ either; after that it is clear that there are no non-trivial solutiouns. In contrast, in the integrable (or holonomic) case the family of surfaces Σ is defined as the level sets of some function F

$$\Sigma = \{ p \in \mathbb{R}^3 | F(p) = \text{const} \}.$$

To discretize a smooth surface Σ , one can simply define a triangulation of this surface. If the triangles in this triangulation are sufficiently small, they can approximate the pieces of the surface accurately.

For the non-holonomic geometry on \mathcal{H} , we can consider a small disk $D_{\varepsilon} = \{\alpha X + \beta Y | \alpha^2 + \beta^2 < \varepsilon^2\} \subset \Pi$ as a "two-dimensional piece of the Heisenberg group" [1]. However, it turns

out that a discrete model of the Heisenberg group, represented as a set of intersecting disks, fails to capture the essential geometric features of \mathcal{H} .

To construct a viable discrete model of \mathcal{H} , we define a local sub-Riemannian distance between sufficiently close points. This distance is generated by the distribution (1), similar to how it is approached in Heron's problem. Subsequently, we define a spatial graph Γ_r as a discretization of the sub-Riemannian Heisenberg group. Numerical experiments indicate that the metric properties of this graph — such as the shape of the shortest paths — effectively simulate the corresponding properties of the Heisenberg group.

There is a series of works [2, 3, 4] that explore discrete non-holonomic systems from the perspectives of finite-difference operators and computational methods. For instance, in the article titled "On Discrete Geometry of Non-Holonomic Spaces" [5], the authors examine a discrete version of the Lagrange-d'Alembert-Chaplygin equations without delving into specific discrete geometric objects. This work aims to construct a tangible discrete model for $\mathcal H$ — the simplest example of sub-Riemannian geometry.

2 Local sub-Riemannian Distance

Consider two arbitrary points $p_i = (x_i, y_i, z_i)$ and $p_j = (x_j, y_j, z_j)$ in \mathcal{H} . Each point defines a plane spanned by the vectors $X_i = (1, 0, -\frac{y_i}{2})$ and $Y_i = (0, 1, \frac{x_i}{2})$. A normal vector to this plane is given by $N_i = (\frac{y_i}{2}, -\frac{x_i}{2}, 1)$. The corresponding planes are:

$$\Pi_i$$
: $\frac{y_i}{2}(x - x_i) - \frac{x_i}{2}(y - y_i) + (z - z_i) = 0$

$$\Pi_j: \frac{y_j}{2}(x-x_j) - \frac{x_j}{2}(y-y_j) + (z-z_j) = 0.$$

The intersection of these planes defines a line $l_{ij} = \Pi_i \cap \Pi_j$, which can be expressed in parametric form:

$$l_{ij}(t) = \begin{pmatrix} \frac{(z_j - z_i)(x_i + x_j)}{x_i y_j - x_j y_i} \\ \frac{(z_j - z_i)(y_i + y_j)}{x_i y_j - x_j y_i} \\ \frac{z_i + z_j}{2} \end{pmatrix} + t \begin{pmatrix} 2x_j - 2x_i \\ 2y_j - 2y_i \\ x_i y_j - x_j y_i \end{pmatrix}.$$

We define the *local sub-Riemannian (lsR) distance* between the two points p_i and p_j as the length of the shortest broken line consisting of two segments that connect these points within the union of the two planes $\Pi_i \bigcup \Pi_j$.

$$\mathbf{d}_{lsR}(p_i, p_j) = \min_{q \in l_{ij}} (\rho(p_i, q) + \rho(q, p_j)),$$

where ρ is the standard Euclidean distance in \mathbb{R}^3 . This approach generalizes the classic Heron's problem of finding a point q on a fixed line that minimizes the sum of distances to two fixed points. One of the planes, let's say Π_i , can be rotate about the line l_{ij} until it coincides with the another plane Π_j and the points p_i and p_j will be placed in the different half-planes defined by the line l_{ij} . Then

$$\mathbf{d}_{lsR}(p_i, p_j)^2 = \rho(p_i', p_j)^2 = (\rho_i + \rho_j)^2 + (\rho(p_i^{\perp}, p_j^{\perp}))^2,$$
(2)

as can be seen in the Fig.1. Here p_i^{\perp} is the projection of p_i onto l_{ij} and $\rho_i = \rho(p_i, p_i^{\perp})$.

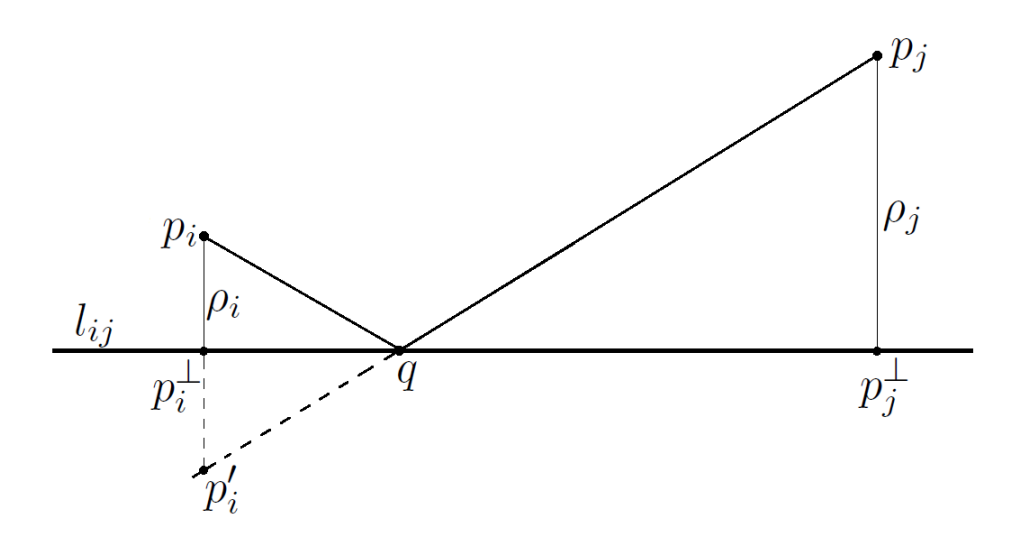


Figure 1: The local sub-Riemannian distance $\mathbf{d}_{lsR}(p_i, p_j)$ and Heron's problem.

The distances ρ_i and ρ_j can be calculated easily

$$\rho_i = \frac{|x_i y_j - x_j y_i + 2z_i - 2z_j|}{\sqrt{4(x_i - x_j)^2 + 4(y_i - y_j)^2 + (x_i y_j - x_j y_i)^2}} \sqrt{4 + x_i^2 + y_i^2},$$
(3)

Discretization of the sub-Riemannian Heisenberg Group

$$\rho_j = \frac{|x_i y_j - x_j y_i + 2z_i - 2z_j|}{\sqrt{4(x_i - x_j)^2 + 4(y_i - y_j)^2 + (x_i y_j - x_j y_i)^2}} \sqrt{4 + x_j^2 + y_j^2}.$$
 (4)

The distance $\rho(p_i^{\perp}, p_j^{\perp})$ between the projections of the points on the line l_{ij} is

$$\rho(p_i^{\perp}, p_j^{\perp})^2 = \frac{\left(2(x_i - x_j)^2 + 2(y_i - y_j)^2 + (z_j - z_i)(x_i y_j - x_j y_i)\right)^2}{4(x_i - x_j)^2 + 4(y_i - y_j)^2 + (x_i y_j - x_j y_i)^2}.$$
 (5)

Gathering (3) - (5) and substituting them into (2) gives the lsR-distance:

$$\mathbf{d}_{lsR}(p_i, p_j) = \frac{1}{\sqrt{4(x_i - x_j)^2 + 4(y_i - y_j)^2 + (x_i y_j - x_j y_i)^2}} \cdot \left((x_i y_j - x_j y_i + 2z_i - 2z_j)^2 (\sqrt{4 + x_i^2 + y_i^2} + \sqrt{4 + x_j^2 + y_j^2})^2 + (6) + (2(x_i - x_j)^2 + 2(y_i - y_j)^2 + (z_j - z_i)(x_i y_j - x_j y_i)^2 \right)^{\frac{1}{2}}.$$

We will use formula (6) to define weights of the edges in a graph Γ_r . Next we set p_1 as an origin point $O \in \mathcal{H}$ and examine the ball B(O,1) with respect to the lsR-distance.

$$\mathbf{d}_{lsR}(O,(x,y,z)) = \sqrt{x^2 + y^2} \cdot \sqrt{1 + \frac{z^2}{(x^2 + y^2)^2} (2 + \sqrt{4 + x^2 + y^2})^2}.$$
 (7)

It is evident that the vertical axis Oz is 'forbidden' — points p_i and p_j having different z coordinate define parallel planes Π_i and Π_j . Consequently, the lsR-distance $\mathbf{d}_{lsR}(O,(0,0,z))$ becomes infinite (as illustrated in Fig. 2). This contrasts with the standard sub-Riemannian ball in the Heisenberg group, which takes on an 'apple' shape [6, 7]. In contrast, the lsR-distance results in a pinched ball resembling a donut with an infinitely small hole.

The sub-Riemannian distance \mathbf{d}_{sR} from the origin O to the point (x, y, z) in the Heisenberg group \mathcal{H} is defined as follows [7]:

a) if
$$z = 0$$
, then $\mathbf{d}_{sR}(O, (x, y, 0)) = \sqrt{x^2 + y^2}$,

b) if
$$z \neq 0$$
 and $x = y = 0$, then $\mathbf{d}_{sR}(O, (0, 0, z)) = \sqrt{2\pi |z|}$,

c) if
$$z \neq 0$$
 and $x^2 + y^2 > 0$, then $\mathbf{d}_{sR}(O, (x, y, z)) = \frac{q}{\sin q} \sqrt{x^2 + y^2}$,

where

$$\frac{2q - \sin 2q}{4\sin^2 q} = \frac{z}{x^2 + y^2}. (8)$$

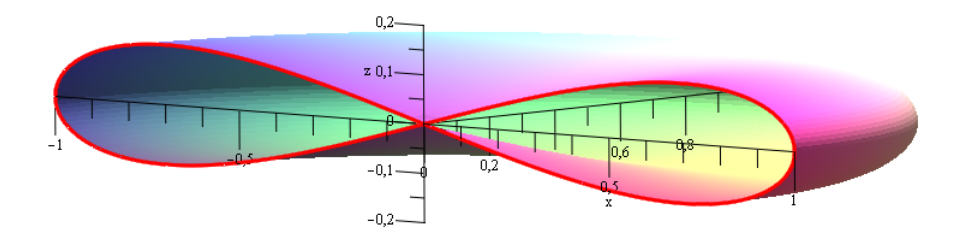


Figure 2: The hemisphere in the \mathbf{d}_{lsR} -distance and its ∞ -shaped Oxz-section (red).

The Taylor expansion of (7) gives

$$\mathbf{d}_{lsR}(O,(x,y,z)) = \sqrt{x^2 + y^2} \Big(1 + \frac{1}{2} \frac{z^2}{(x^2 + y^2)^2} (2 + \sqrt{4 + x^2 + y^2})^2 + \ldots \Big).$$

In the general case \mathbf{c}) of the sub-Riemannian distance, assuming that q is small enough, from (8) one gets

$$q \sim \frac{3z}{x^2 + y^2}.$$

Then

$$\mathbf{d}_{SR}(O,(x,y,z)) = \sqrt{x^2 + y^2} \left(1 + \frac{1}{2} \frac{3z^2}{(x^2 + y^2)^2} + \dots \right).$$

The second term in this expansion can be interpreted as a sub-Riemannian correction to the 2-dimensional Euclidean distance function $\sqrt{x^2+y^2}$. Notably, both corrections share a common multiplier of the form $\frac{3z^2}{(x^2+y^2)^2}$, which is a positive indication. It is possible to introduce an additional parameter Λ into the lsR-distance (7) that changes the weight of the $(\rho(p_i^\perp,p_i^\perp))^2$ summand, namely

$$\sqrt{x^2 + y^2} \cdot \sqrt{1 + \Lambda \frac{z^2}{(x^2 + y^2)^2} (2 + \sqrt{4 + x^2 + y^2})^2}.$$

As Λ approaches zero, the ball B(O,1) becomes thicker; conversely, as $\Lambda \to \infty$, it flattens out — transforming from a donut to a pancake: $B(O,1) \to D_1$. It is crucial to note that if the lsR-ball B(O,1) were merely a 2-dimensional disc D_1 , then the distance between almost any pair of random points would be infinite.

If the center of the ball shifts from the origin to the point p_i , the ball bends in such a way that its central plane of symmetry coincides with the plane Π_i of admissible directions at p_i (Fig.3).

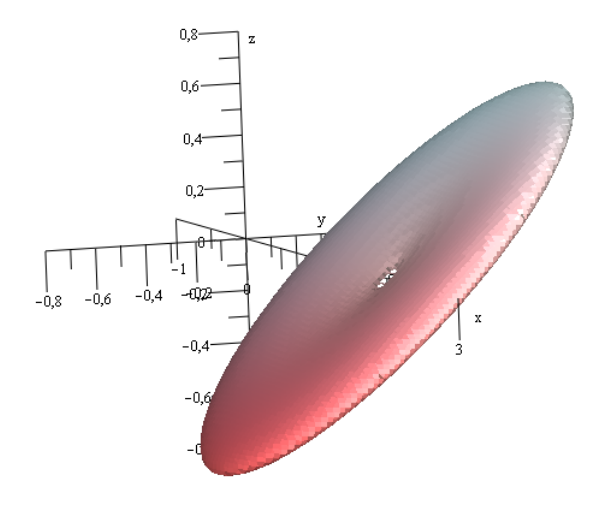


Figure 3: The ball B((2,0,0),1) in the \mathbf{d}_{lsR} -distance.

3 A spatial graph and a discrete sub-Riemannian distance

Consider the cubic domain $\Omega = [-1,1]^3 \subset \mathcal{H}$ with a set $D = \{p_i \in \Omega | i = 1, ..., N\}$ of N points. These points can form either a regular lattice or they can be randomly and uniformly distributed in Ω . We will consider the scenario with random points. Calculate all distances $\mathbf{d}_{\mathrm{lsR}}(p_i, p_j)$ using (6) and consider the weighted spatial graph Γ_r with vertices p_i and edges v_{ij} of weight $\mathbf{d}_{\mathrm{lsR}}(p_i, p_j) \leq r$, it means that vertices $p_i \in D$ and p_j are connected by the edge v_{ij} in the graph Γ_r if and only if the local sub-Riemannian distance $\mathbf{d}_{\mathrm{lsR}}(p_i, p_j)$ between them is smaller than a fixed value r.

The graph Γ_r serves as a discrete model for the Heisenberg group. When the parameter r is too small, most vertices in Γ_r tend to be disjoint. Conversely, if r is excessively large, nearly all pairs of points (p_i, p_j) will be connected by an edge. The critical threshold value r^* is influenced by both the number of vertices N and the domain Ω . Here, r^* refers to

the specific value of r such that for any $r > r^*$, the graph Γ_r becomes connected for an average distribution of the points p_i .

Next we perform a number of numerical experiments demonstrating that the presented discrete model possesses features specific for the sub-Riemannian Heisenberg group. Firstly, using the standard Dijkstra algorithm [8] for finding shortest paths in a graph, one can find the shortest path in Γ_r . The shortest path is a broken line with vertices at the points $p_1, p_{i_1}, \dots, p_{i_k}, p_2$, thus the *discrete sub-Riemannian (dsR) distance* between p_1 and p_2 in Γ_r is

$$\mathbf{d}_{dsR}(p_1, p_2) = \mathbf{d}_{lsR}(p_1, p_{i_1}) + \mathbf{d}_{lsR}(p_{i_1}, p_{i_2}) + \dots + \mathbf{d}_{lsR}(p_{i_k}, p_2).$$
(9)

The distance between close vertices is defined via the local sub-Riemannian distance, while the distance between arbitrary vertices is the length of the shortest path in Γ_r .

Numerical calculations show that the shortest path between $p_1 = (0,0,0)$ and $p_2 = (0,0,z_2)$ has a form of a single-wind helix (Fig.4) — a typical form for the Heisenberg geodesics [7, 9]:

$$x(t) = (\sin(\theta_0 + h_3 t) - \sin \theta_0)/h_3,$$

$$y(t) = (\cos \theta_0 - \cos(\theta_0 + h_3 t))/h_3,$$

$$z(t) = (h_3 t - \sin h_3 t)/h_3^2.$$
(10)

In (10) the parameter θ_0 can be chosen in such a way that the initial velocity vector at t=0 coincides with the first interval $[p_1,p_{i_1}]$ and the varying parameter h_3 gives the necessary height $z(2\pi)$ of the helix (Fig.4, black curve). Note that the discrete sub-Riemannian distance between points having different z coordinate is finite, contrary to the local sub-Riemannian distance.

Next we compare the distance $\mathbf{d}_{\mathrm{dsR}}$ between points as the vertices of the graph Γ_r and the sub-Riemannian distance \mathbf{d}_{sR} in \mathcal{H} . We will consider two situations: horizontal and vertical. In the horizontal case, when $p_1=(0,0,0)$ and $p_2=(x_2,y_2,0)$, the geodesic in \mathcal{H} is a straight horizontal interval $[p_1,p_2]$ in the plane Oxy. The vertical situation is when $p_1=(0,0,0)$ and $p_2=(0,0,z_2)$ and the geodesic is a helix (10) with non-constant slope. In

Discretization of the sub-Riemannian Heisenberg Group

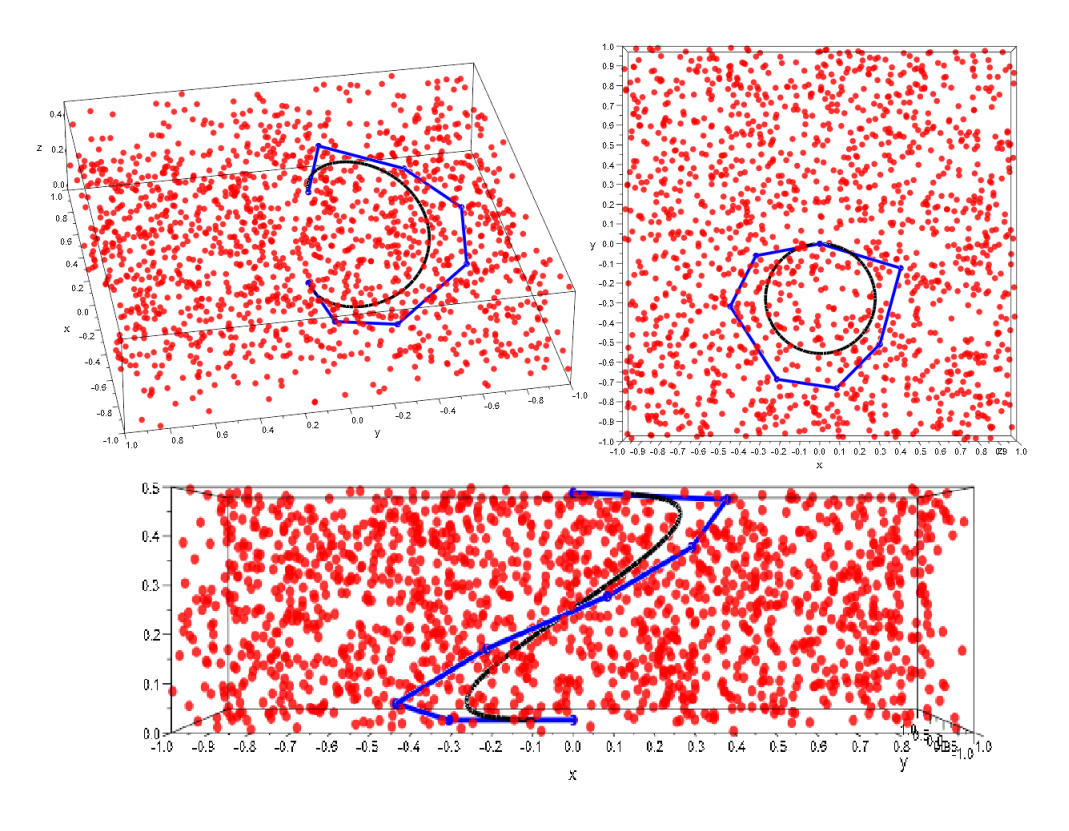


Figure 4: Sub-Riemannian geodesic (black, (10)) and typical shortest path (blue) in the graph $\Gamma_{\frac{1}{2}}$ with N=1500 vertices connecting points (0,0,0) and $(0,0,\frac{1}{2})$, various projections.

accordance with **a**) the sub-Riemannian distance in the horizontal case coincides with the Euclidean length $\mathbf{d}_{sR}((0,0,0),(x_2,y_2,0)) = \sqrt{x_2^2 + y_2^2}$.

	N = 1000	N = 2000	N = 4000	N = 6000	$\mathbf{d}_{sR}(p_1,p_2)$
$x_2 = y_2 = \frac{1}{2}$	1.8628	0.8971	0.8655	0.7752	$\frac{\sqrt{2}}{2} \approx 0.7071$
$x_2 = y_2 = 1$	∞	1.9839	1.7267	1.5965	$\sqrt{2} \approx 1.4142$

Table 1. Mean distance $\mathbf{d}_{dsR}((0,0,0),(x_2,y_2,0))$ for different N and sub-Riemannian distance, horizontal case.

If the number of vertices N is small, the graph Γ_r can be disconnected, in which case the distance between disconnected vertices is equal to infinity. In *Table 1* the value 0.8955

is the averaged distance of $\mathbf{d}_{dsR}(p_1, p_2)$ calculated for 10 numerical experiments with 4000 random vertices each. As N increases, the dispersion of $\mathbf{d}_{dsR}(p_1, p_2)$ decreases and its value gets closer to the value of $\mathbf{d}_{sR}(p_1, p_2)$. The convergence of the distances in the vertical case is shown in *Table 2*.

	N = 1000	N = 2000	N = 4000	N = 6000	$\mathbf{d}_{sR}(p_1,p_2)$
$z_2 = \frac{1}{9}$	1.717	1.3617	1.2929	1.2702	$\frac{\sqrt{2\pi}}{3} \approx 0.8355$
$z_2 = \frac{4}{9}$	3.2894	2.8339	2.5877	2.5209	$\frac{2\sqrt{2\pi}}{3} \approx 1.671$

Table 2. Mean distance $\mathbf{d}_{dsR}((0,0,0),(0,0,z_2))$ for different N and the sub-Riemannian distance, vertical case.

From Tables 1 and 2 one can see that, as N increases, the discrete sub-Riemannian distance gets closer to the standard sub-Riemannian distance in \mathcal{H} , but with different rates in the horizontal and vertical cases. A more detailed discussion on these results will be provided in the next section.

The last feature of geodesics in \mathcal{H} that is going to be checked for Γ_r is the fact that the coordinate z(t) of the geodesic that starts at O is proportional to the sectional area of the projection (x(t), y(t)) onto the Oxy plane. For the considered discrete model this projection is a polygon, see the upper right picture in Fig.4 The numerical experiment is the following:

- 1. Pick *M* test vertices *p* in Γ_r , whose third coordinate is z(p);
- 2. Find the shortest path from *O* to *p*;
- 3. Calculate the polygon area A(p) of the projected path.

For the Heisenberg group z(p) and A(p) are the same values, and, for example, the Dido's problem can easily be reformulated as a problem of finding geodesics [7]. The results for $\Gamma_{\frac{1}{2}}$ with N=3000 random vertices and with M=200 test vertices are presented in the Fig. 5. As the coordinate z(p) is uniformly distributed in [-1,1], the dots with coordinates (z(p),A(p)) on Fig. 5 lie quite close to the plot of |z(p)|.

Discretization of the sub-Riemannian Heisenberg Group

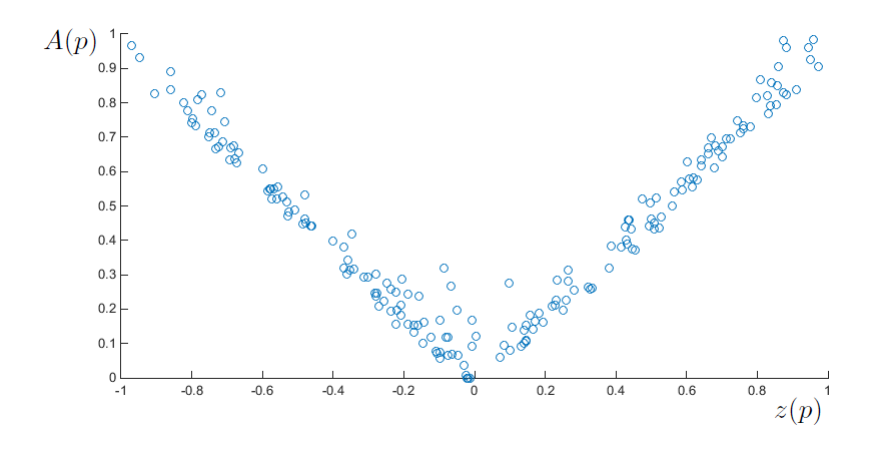


Figure 5: The coordinate z(p) and the area A(p) of the projected polygon for M=200 test vertices in $\Gamma_{\frac{1}{2}}$.

4 Tortuosity

First let us recall briefly what *tortuosity* is. Consider a domain $\Omega' \subset \mathbb{R}^3$ modeling a piece of porous media, such that there is a connected subset $P \subset \Omega'$ modeling the system of the media pores. Next, $\Omega' \setminus P$ simulates solid material. One can consider two arbitrary points $A, B \in P$ and the shortest path $\gamma(t)$, $t \in [0,1]$ connecting A and B that fully lies in the system of pores $P: \forall t \in [0,1] \ \gamma(t) \in P$. The ratio of the length of γ and the standard Euclidean distance between A and B

$$\frac{\int\limits_{0}^{1}|\dot{\gamma}(t)|dt}{\mathrm{dist}_{Eucl}(A,B)}$$

called the *tortuosity* τ *of the path* $\gamma(t)$. If the media is homogeneous and isotropic and if $\operatorname{dist}_{Eucl}(A,B)$ is sufficiently large, the tortuosity will be close to a limit value: it is greater than 1 and measures the level of entanglement of the system of pores. If the media is anisotropic then $\tau(A,B)$ will depend on the direction \overrightarrow{AB} .

Secondly, one can study the tortuosity of the Delaunay triangulation of uniformly distributed points [10]. It turns out that the ratio between the length $l_{triang}(A, B)$ of the shortest broken line connecting two points via edges of the triangulation and the Eu-

clidean distance,

$$\frac{l_{triang}(A, B)}{\operatorname{dist}_{Eucl}(A, B)}$$
,

converges from above to a fixed value $\tau_{Dln}\approx 1.05$ for a two-dimensional domain and $\tau_{Dln}\approx 1.09$ for a three-dimensional domain.

Next we come back to a domain Ω with the standard sub-Riemannian metric \mathbf{d}_{sR} and the spatial graph Γ_r in Ω with vertices $p_i \in D$ and metric \mathbf{d}_{dsR} . The following ratio

$$\tau(A,B) = \frac{\mathbf{d}_{dsR}(A,B)}{\mathbf{d}_{sR}(A,B)}$$
(11)

is called the *tortuosity* of the path from A to B. This value depends on the set D of vertices, on the coordinates of B and on the parameter r of the graph Γ_r . It is a straight-forward generalization of the previously mentioned tortuosity.

Let us consider again two points $A=p_1$ and $B=p_2$ from the previous section. From Table 1, when both points lie in the horizontal plane $\{z=0\}$ and the sub-Riemannian geodesic is a straight line, the tortuosity (11) gets close to τ_{Dln} in the three-dimensional case of the Delaunay tortuosity.

	N = 1000	N = 2000	N = 4000	N = 6000
$x_2 = y_2 = \frac{1}{2}$	2.6344	1.2687	1.2240	1.0963
$x_2 = y_2 = 1$	∞	1.4028	1.2210	1.1289

Table 3. The tortuosity $\tau((0,0,0),(x_2,y_2,0))$ for different N, horizontal case.

In the case of helicoidal geodesic, the difference between the sub-Riemannian and discrete sub-Riemannian distances becomes more evident:

	N = 1000	N = 2000	N = 4000	N = 6000
$z_2 = \frac{1}{9}$	2.0551	1.6298	1.5475	1.5203
$z_2 = \frac{4}{9}$	1.9685	1.6959	1.5486	1.5086

Table 4. The tortuosity $\tau((0,0,0),(0,0,z_2))$ for different N, vertical case.

Considering this 'anisotropic' behaviour of $\tau(A, B)$ we formulate the following

Discretization of the sub-Riemannian Heisenberg Group

Conjecture on the limit tortuosity. Consider a cubic domain $\Omega \subset \mathcal{H}$ with the sub-Riemannian distance \mathbf{d}_{sR} and the corresponding spatial graph Γ_r with N uniformly distributed vertices D and the discrete sub-Riemannian distance \mathbf{d}_{dsR} . Fix two points $A = (0,0,0) \in D$ and $B = (\cos \varphi, 0, \sin \varphi) \in D$. As $N \to \infty$ one can choose a parameter of the graph Γ_r with the asymptotic

$$r \sim c \cdot N^{-d}$$
 for some $c > 0$, $d > 0$, (12)

such that the tortuosity $\tau(A,B)$ converges to a limit tortuosity $\tilde{\tau}=\tilde{\tau}(\varphi)$ depending only on the coordinate φ of B for almost all positions of vertices in D. The limit tortuosity should be bounded

$$1 < \tilde{\tau} < C \quad \forall \varphi \in [0, 2\pi].$$

Due to the fact that all considered functions are random variables the convergence of the tortuosity in this conjecture should be almost sure convergence. Finding optimal bounds for the constants c, d and C is another problem to consider. Also, the connection between d and the dimension (topological or Hausdorf) of the Heisenberg group is not clear.

We will say that a broken line with vertices $A=p_{i_1},p_{i_2},\ldots,p_{i_k}=B$ is ε -close to a geodesic $\gamma(t),\,t\in[t_0,t_1]$, connecting A and B if there is a cylindrical neighbourhood of $\gamma(t)$

$$Cyl_{\varepsilon} = \bigcup_{t \in [t_0, t_1]} \{ \gamma(t) + v | \forall v \in \mathbb{R}^3, |v| \le \varepsilon \},$$

containing all vertices p_i and all edges $[p_{i_j}, p_{i_j+1}]$ of the broken line.

Finally, we can formulate the approximation conjecture:

Approximation Conjecture. Consider a cubic domain $\Omega \subset \mathcal{H}$ with the sub-Riemannian distance \mathbf{d}_{sR} , the orresponding spatial graph Γ_r with N uniformly distributed vertices D and the discrete sub-Riemannian distance $\mathbf{d}_{\mathrm{dsR}}$. Fix two points $A=O\in D$ and arbitrary $B\in D$ and a sub-Riemannian geodesic $\gamma(t)$ connecting $A=\gamma(t_0)$ and $B=\gamma(t_1)$. For any ε there is number N of vertices and a parameter r satisfying (12) such that there is a shortest path $A=p_{i_1},p_{i_2},\ldots,p_{i_k}=B$ in the graph Γ_r which is ε -close to $\gamma(t)$.

Note that if the point B lies on the Oz axis then there is no uniqueness of the sub-Riemannian geodesic connecting A = O and B, it is defined up to rotation as it was mentioned earlier. In this case in the approximate conjecture one should choose an appropriate geodesic. It seems to be clear how to prove that in a cylindric neighbourhood of the fixed geodesic there is a broken line with vertices and edges from Γ_r . But how to prove that this broken line will be globally shortest path in Γ_r ?

5 Conclusion.

Here we presented a discrete model Γ_r of the Heisenberg group \mathcal{H} as a spatial graph with weighted edges. The weight of the edge is defined by the local sub-Riemannian distance \mathbf{d}_{lsR} , generated by the non-integrable Heisenberg distribution (1). The discrete sub-Riemannian distance \mathbf{d}_{dsR} is the length of a shortest path in Γ_r . Numerical experiments give a motivation to formulate an approximation conjecture stating that shortest paths in the graph Γ_r will be sufficiently close to the geodesics in \mathcal{H} if the number of vertices N is large enough and the parameter r is appropriately small.

The constructed model can be considered as a 'triangulation of the sub-Riemannian Heisenberg group', but without triangles. The triangulation of a smooth two-dimensional surface embedded in \mathbb{R}^3 is a collection of vertices, edges and triangles. In the nonintegrable case there is no surface, so there should be no triangles. It is natural to choose a spatial graph Γ_r , consisting only of vertices and edges, as a model for non-integrable geometry.

We believe that the presented construction will be interesting both for specialists in discrete geometry and in sub-Riemannian geometry. The presented model can be useful for simulations of various processes in anisotropic medias, such as heat propagation, diffusion in anisotropic porous materials, deformations of layered solids, etc.

Acknowledgments

The research was carried out within the framework of a state assignment of the Ministry of Education and Science of the Russian Federation for the Sobolev Institute of Mathematics of the SBRAS (project no. FWNF-2022-0006)

References

- [1] E. Malkovich. On discrete sub-Riemannian geometry. International Conference on Geometric Analysis, 2022, p.82. 2
- [2] J.E. Marsden, M. West. Discrete mechanics and variational integrators. Acta Numerica, 2001, 357-514. 3
- [3] A.A. Simoes, J.C. Marrero, D.M. de Diego. Exact discrete Lagrangian mechanics for nonholonomic mechanics. Numerische Mathematik, Vol. 151, p. 49-98, 2022. 3
- [4] Yu.N. Fedorov, D.V. Zenkov. Discrete nonholonomic LL systems on Lie groups. Nonlinearity 18(2005), 2211-2241. 3
- [5] P.Popescu, M. Popescu. On discrete geometry of non-holonomic spaces. Proceedings of The International Conference "Differential Geometry and Dynamical Systems" (DGDS-2014), 1-4 September 2014, Mangalia, ROMANIA, BSG PROCEEDINGS 22 (2015) 69-74.
- [6] V.N. Berestovskii, I.A. Zubareva. Shapes of spheres of special nonholonomic left-invariant intrinsic metrics on some Lie groups. Siberian Math. J.42(2001), no.4, 613–628. 5
- [7] Yu. Sachkov. Introduction to Geometric Control. Springer Nature, 2022. 5, 8, 10

Evgeny G. Malkovich

- [8] E.W. Dijkstra. A note on two problems in connexion with graphs. Numerische Mathematik. (1959), 1: 269–271. 8
- [9] V.N. Berestovskii. Geodesics of nonholonomic left-invariant intrinsic metrics on the Heisenberg group and isoperimetric curves on the Minkowski plane. Siberian Math. J., 35:1 (1994), 1–8. 8
- [10] A.A. Bystrov, E.G. Malkovich. Tortuosity of Delaunay Triangulations and Statistics of Shortest Paths. Experimental Mathematics, 2024, October, 1–7. doi:10.1080/10586458.2024.2410189. 11

AUTHOR

Evgeny G. Malkovich Novosibirsk State University and

Sobolev Institute of Mathematics,

Russia

email: malkovicheugen@yandex.ru, malkovich@math.nsc.ru



Arnold Mathematical Journal Volume 11, Issue 3, 2025



Circumscribed Circles in Integer Geometry

Oleg Karpenkov Anna Pratoussevitch Rebecca Sheppardo

Received 17 Dec 2024; Accepted 7 May 2025

Abstract:

Integer geometry on a plane deals with objects whose vertices are points in \mathbb{Z}^2 . The congruence relation is provided by all affine transformations preserving the lattice \mathbb{Z}^2 . In this paper we study circumscribed circles in integer geometry. We introduce the notions of integer and rational circumscribed circles of integer sets. We determine the conditions for a finite integer set to admit an integer circumscribed circle and describe the spectra of radii for integer and rational circumscribed circles.

AMS Classification: 52B20, 11H06, 11P21

Key words and phrases: integer geometry, number theory, integer circumscribed circles

© 2025 Oleg Karpenkov, Anna Pratoussevitch, Rebecca Sheppard

Introduction

In this paper we introduce the notion of circumscribed circles in integer geometry and investigate their properties.

The integer distance between two points in the lattice \mathbb{Z}^2 is defined in terms of the number of lattice points on the segment between them; see Section 1.2 for more details. An *integer circle* is the locus of all lattice points at a fixed integer distance from a given lattice point. The properties of integer circles differ substantially from the properties of their Euclidean counterparts. In fact, using the Basel Problem [Ayo74], it can be shown that the density of a unit integer circle in \mathbb{Z}^2 is positive and equal to $6/\pi^2$ (see also [HW08]) Note that the chords of unit integer circles provide a tessellation which is combinatorially equivalent to the Farey tessellation of the hyperbolic plane, while their radial segments correspond to geodesics in the hyperbolic plane (see [Ser, MGO19]).

An *integer circumscribed circle* of a subset of \mathbb{Z}^2 is defined as an integer circle that contains this subset. While in Euclidean geometry every non-degenerate triangle has a unique circumscribed circle, this is no longer the case in integer geometry. In fact, the number of integer circumscribed circles of an integer triangle is infinite.

This paper aims to provide a comprehensive study of circumscribed circles in integer geometry. In Theorem 2.9 we introduce necessary and sufficient conditions for a finite integer set to admit a circumscribed circle. As a special case, we discuss the circumscribed circles of integer quadrangles and their Euclidean counterparts.

While a finite set might not admit an integer circumscribed circle, it will have integer dilates that do. The integer circumscribed circles of the dilates can be interpreted as integer circles with rational centres and radii. We call the set of all such rational radii the *rational spectrum*. In Theorem 3.10 we describe the structure of rational spectra of finite sets.

This paper is organized as follows. In Section 1, we begin with basic definitions of integer

Circumscribed Circles in Integer Geometry

geometry and introduce the notion of an integer circle. In Section 2 we state and prove the conditions under which a finite integer set admits an integer circumscribed circle. We extend the notion of circumscribed circles to the case of rational radii and rational centres and describe the spectra of the radii of such circles in Section 3. In Section 4 we discuss integer and rational circumscribed circles for segments, triangles and quadrangles in more detail.

1 Basic Notions of Integer Geometry

1.1 Objects in Integer Geometry

Consider the plane \mathbb{R}^2 with the fixed basis (1,0),(0,1). An *integer point* is a point in \mathbb{R}^2 whose coordinates in this basis are integers, i.e. the set of all integer points is the lattice \mathbb{Z}^2 . An *integer set* is a subset of \mathbb{Z}^2 . An *integer segment* is a segment in \mathbb{R}^2 with endpoints in \mathbb{Z}^2 . An *integer line* is a line in \mathbb{R}^2 that contains at least two integer points. An *integer vector* is a vector in \mathbb{R}^2 with integer endpoints. An *integer polygon* is a polygon in \mathbb{R}^2 whose vertices are integer points.

An *integer affine transformation* is an affine transformations that preserves the integer lattice \mathbb{Z}^2 . We denote the set of all integer affine transformations by Aff $(2,\mathbb{Z})$. Similar to the Euclidean isometries, Aff $(2,\mathbb{Z})$ contains *integer translations*, *integer rotations* and *integer symmetries*. They correspond to translations by integer vectors, multiplication by matrices in SL $(2,\mathbb{Z})$ and multiplication by matrices in GL $(2,\mathbb{Z})\setminus$ SL $(2,\mathbb{Z})$ respectively.

We say that two integer sets are *integer congruent* if there exists an integer affine transformation sending one set to another.

An angle in \mathbb{R}^2 with an integer point as its vertex is called an *integer angle*. An integer angle that contains an integer point other than its vertex on each of its sides is called a *rational integer angle*.

1.2 Some Integer Invariants

Let us recall some basic notions of integer geometry (see [Kar22]). The *integer length* $\mathcal{C}(AB)$ of a vector AB in \mathbb{Z}^2 is defined as the number of lattice points that the vector passes through, minus one. Note that the integer length is given by the greatest common divisor of the differences of coordinates. The *integer distance* $\mathrm{Id}(A,B)$ between integer points A and B is the integer lengths of AB. The *integer distance* $\mathrm{Id}(O,L)$ between an integer point A0 and an integer line A1 is the index of the sub-lattice generated by vectors A2 over A3.

The *integer area* IS(ABC) of a triangle ABC is the index of the sub-lattice generated by AB and AC in \mathbb{Z}^2 . In fact, the integer area is equal to the absolute value of the determinant det(AB, AC), and therefore it is twice the Euclidean area of the triangle ABC.

1.3 Integer Circles

We define an *integer circle* with centre $O \in \mathbb{Z}^2$ and radius $r \in \mathbb{Z}$, r > 0 as the locus of all points P such that $\mathcal{U}(OP) = r$.

Proposition 1.1. The intersection of an integer line L with an integer circle is either empty, or an infinite periodic subset of integer points on L, or two points.

The *integer radial line* of an integer circle C is an integer line passing through the centre of C. An integer radial line of C intersects C in two points. An *integer tangent line* to an integer circle C of radius r with centre O is an integer line C such that C is an integer line C.

Remark 1.2. For every pair of integer tangent lines of an integer circle there exists an integer isometry of the circle mapping one integer tangent line to the other.

Remark 1.3. Two integer circles of the same radius are integer congruent. Moreover, one can be mapped to the other by a translation by an integer vector.

Figure 1 shows in bold those points of the integer unit circle S_0 centred at the origin O whose coordinates do not exceed 5 in absolute value. The polygon in Figure 1 is called a

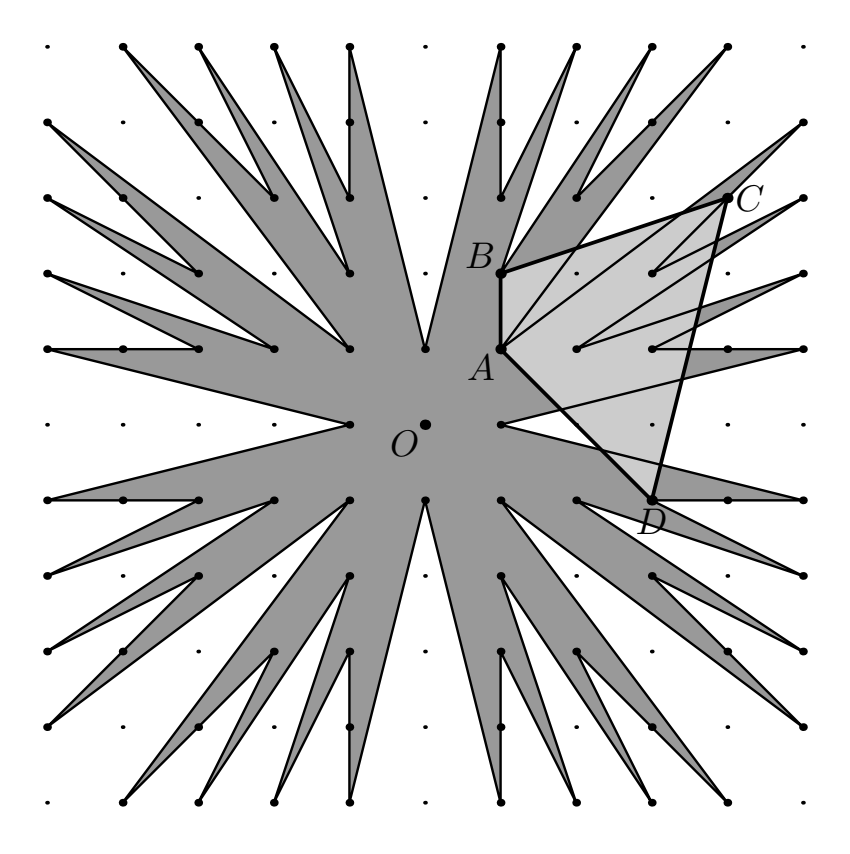


Figure 1: An integer circle circumscribed about an integer quadrangle.

Farey starburst and is obtained by connecting these points by straight segments in the order of increasing argument. The vertices A, B, C, D belong to the integer circle S_0 , hence S_0 is a circumscribed circle of the quadrangle ABCD.

Remark 1.4. Consider the integer unit circle S_0 centred at the origin O. Let α be some integer angle and A the point (1,0). Then it is possible to find infinitely many points B in S_0 such that the angle $\angle AOB$ is integer congruent to α . Note the difference with the Euclidean case, where there are exactly two such points B.

1.4 Integer Trigonometry

Let us discuss basic definitions of integer trigonometry introduced in [Kar09, Kar08] (for the multi-dimensional trigonometry see [BKD23]).

Definition 1.5. Let p, q be co-prime integers with $q \ge p > 0$. The *integer arctangent of* q/p is the angle $\angle AOB$, where

$$A = (1,0), O = (0,0), and B = (p,q).$$

We define integer sine, integer cosine and integer tangent as

$$\operatorname{lsin} \angle AOB = q$$
, $\operatorname{lcos} \angle AOB = p$, and $\operatorname{ltan} \angle AOB = q/p$.

Note that any rational angle is integer congruent to exactly one integer arctangent. So the values of integer trigonometric functions form in fact a complete set of invariants of rational angles up to integer congruence.

The integer sine has a nice geometric definition:

$$\operatorname{lsin} \angle ABC = \frac{\operatorname{lS}(ABC)}{\operatorname{l}\ell(AB)\operatorname{l}\ell(AC)}$$

which directly corresponds to the Euclidean formula for the area of a parallelogram in terms of the sine of its angle. The integer tangent is closely related to the geometry of numbers and their connections to continued fractions [Kar13].

2 Integer Circumscribed Circles

In this section we generalise the notion of a circumscribed circle in the context of integer geometry.

Definition 2.1. An *integer circumscribed circle* of $S \subset \mathbb{Z}^2$ is an integer circle that contains S.

In the Euclidean geometry there exists at most one circumscribed circle for a given set S with |S| > 2. This is not the case in integer geometry where a set can have several circumscribed circles. The radius of the circumscribed circle is an important quantity in Euclidean geometry. A suitable replacement for this quantity in integer geometry is the integer circumscribed spectrum.

Definition 2.2. Let *S* be an integer set. The set of all radii of integer circumscribed circles of *S* is called the *integer circumscribed spectrum* of *S* and denoted by $\Lambda_{\mathbb{Z}}(S)$.

Note the following.

Proposition 2.3. Let $a, b \in S$ and let r be the radius of a circumscribed circle of S. Then r divides Id(a, b).

Proof. Let *x* be the centre of the circumscribed circle of *S*. Then

$$a - x \equiv b - x \equiv (0, 0) \mod r$$
.

Hence $a - b \equiv (0,0) \mod r$, and therefore r divides ld(a,b).

This proposition implies that the integer spectrum is bounded:

Corollary 2.4. The integer spectrum $\Lambda_{\mathbb{Z}}(S)$ of an integer set S that contains at least 2 points is bounded.

The first natural question in the study of integer circumscribed circles is whether $\Lambda_{\mathbb{Z}}(S)$ is empty. In this section we will introduce a criterion that answers this question

Oleg Karpenkov, Anna Pratoussevitch, Rebecca Sheppard

for a finite set S in terms of projections of S to integer tori as defined below. Later in Subsection 3.2 we will study the structure of $\Lambda_{\mathbb{Z}}(S)$.

Definition 2.5. For an integer $m \ge 2$, let the (mod m) integer torus be

$$\mathcal{T}_m = \mathbb{Z}^2/\langle (m,0), (0,m)\rangle \cong \mathbb{Z}/m\mathbb{Z} \times \mathbb{Z}/m\mathbb{Z}.$$

The *projection* $\pi_m : \mathbb{Z}^2 \to \mathcal{T}_m$ is given by $(x, y) \to (x \mod m, y \mod m)$.

We say that two integer points v_1 and v_2 in \mathbb{Z}^2 are *equivalent mod* m if $\pi_m(v_1) = \pi_m(v_2)$, denoted by $v_1 \equiv v_2 \mod m$.

In the statement of the main result of this section we use the following terminology.

Definition 2.6. We say that an integer set S is a *covering set* of \mathcal{T}_m if $\pi_m(S) = \mathcal{T}_m$.

Definition 2.7. We say that an integer set *S* is *tori-transparent* if for every integer $m \ge 2$ we have that *S* is not a covering set of \mathcal{T}_m .

Remark 2.8. Note that a covering set of an integer torus \mathcal{T}_t with $t \ge 2$ must consist of at least $|\mathcal{T}_t| = t^2 \ge 4$ points, hence all integer sets S with $|S| \le 3$ are tori-transparent.

Now we are ready to write down the existence criterion.

Theorem 2.9. Consider a finite integer set $S \subset \mathbb{Z}^2$. Then the following three statements are equivalent:

(i) There exists an integer circumscribed circle of S, i.e.

$$\Lambda_{\mathbb{Z}}(S) \neq \emptyset$$
.

(ii) There exists an integer unit circumscribed circle of S, i.e.

$$1 \in \Lambda_{\mathbb{Z}}(S)$$
.

(iii) The set S is tori-transparent.

We start the proof with the following four lemmas.

Circumscribed Circles in Integer Geometry

Lemma 2.10. Let $v_1, v_2 \in \mathbb{Z}^2$. Consider two integers d and m such that d is a divisor of m. Then $\pi_m(v_1) = \pi_m(v_2)$ implies $\pi_d(v_1) = \pi_d(v_2)$.

Proof. If $\pi_m(v_1) = \pi_m(v_2)$, then $v_1 - v_2 \equiv 0 \mod m$ and hence $v_1 - v_2 \equiv 0 \mod d$, since d is a divisor of m. Therefore $\pi_d(v_1) = \pi_d(v_2)$.

Lemma 2.11. Let S be any subset of \mathbb{Z}^2 . If S is a covering set of \mathcal{T}_m then it is a covering set of \mathcal{T}_p for any prime divisor p of m.

Proof. The set S is a covering set of \mathcal{T}_m , hence for each $v \in \mathbb{Z}^2$ there exists some $s \in S$ such that $\pi_m(v) = \pi_m(s)$. By Lemma 2.10, $\pi_p(v) = \pi_p(s)$. Hence, S is a covering set of \mathcal{T}_p .

Lemma 2.12. For any integer set S the following statements are equivalent:

- (i) The set S is tori-transparent.
- (ii) The set S is not a covering set of any torus \mathcal{T}_p for prime p.

Proof. (i) \Rightarrow (ii) If the set S is tori-transparent then S is not a covering set of any torus \mathcal{T}_m for integer $m \geq 2$, hence S is not a covering set of any torus \mathcal{T}_p for prime p.

(ii) \Rightarrow (i) Consider any integer $m \ge 2$ and let p be a prime divisor of m. By assumption, S is not a covering set of \mathcal{T}_p . Hence, by Lemma 2.11, S is not a covering set of \mathcal{T}_m .

Lemma 2.13. Consider a finite, tori-transparent integer set S. Then for any finite subset M of \mathbb{Z} there exists a point $v \in \mathbb{Z}^2$ such that $\pi_m(v) \notin \pi_m(S)$ for all $m \in M$.

Proof. Let $\{p_1, ..., p_n\}$ be the set of all prime divisors of all elements in M. By Lemma 2.11 for every i = 1, ..., n the set S is not a covering set of \mathcal{T}_{p_i} . Hence for every i = 1, ..., n there exists a point $v_i \in \mathbb{Z}^2$ such that for any $s \in S$ we have

 $v_i \not\equiv s \bmod p_i$.

Then by the Chinese Remainder Theorem (applied coordinate-wise) there exists a point v such that for every i = 1, ..., n it holds:

 $v \equiv v_i \bmod p_i$.

Oleg Karpenkov, Anna Pratoussevitch, Rebecca Sheppard

Hence for every i = 1, ..., n we have

$$\pi_{p_i}(v) = \pi_{p_i}(v_i) \notin \pi_{p_i}(S).$$

Therefore, by Lemma 2.11 $\pi_{p_i}(v) \notin \pi_m(S)$ for all $m \in M$.

Proof of Theorem 2.9 (iii) \Rightarrow **(iii)** \Rightarrow **(ii).** The existence of a circumscribed circle and the property of being a covering set of integer tori \mathcal{T}_m are invariant under translation by integer vectors. Thus we can assume that the set S is contained in the positive quadrant of \mathbb{Z}^2 . Choose N satisfying the following two conditions:

- *S* is completely contained in the box $[1, N] \times [1, N]$;
- the number of elements in S does not exceed N.

Consider $Z = \{1, 2, ..., N\} = [1, N] \cap \mathbb{Z}$. By Lemma 2.13 there exists (a, b) such that $\pi_m(a, b)$ is not in $\pi_m(S)$ for all $m \in Z$.

Set
$$\beta = b + N!$$
.

Let p_1, \ldots, p_k be all prime numbers in the segment $[N+1,\beta]$. Now note that the size of the set S is $|S| \le N < p_i$. Hence the set of first co-ordinates of points in S has fewer than p_i elements. Therefore, for any $i=1,\ldots,k$ we can choose c_i such that c_i is not equal modulo p_i to the first coordinate of any point in S.

By Chinese Remainder Theorem there exists a solution α of the following system of equations:

$$\begin{cases} \alpha \equiv a \bmod N! \\ \alpha \equiv c_i \bmod p_i \end{cases}$$

Then we will show that the point (α, β) has the property that $\pi_m(\alpha, \beta) \notin \pi_m(S)$ for every integer m, and therefore (α, β) belongs to the unit integer circle with centre at (x, y) for every $(x, y) \in S$.

Circumscribed Circles in Integer Geometry

- If $m \le N$ then $\pi_m(\alpha, \beta) = \pi_m(a, b) \notin \pi_m(S)$.
- If $m \in [N+1,\beta]$ and m is a prime, say $m=p_i$, then $\alpha \equiv c_i \mod p_i$ and hence is not equal to the first coordinate of any point in S modulo p_i (by the above). Therefore $\pi_m(\alpha,\beta) \notin \pi_m(S)$.
- If $m \in [N+1,\beta]$ and m is not a prime then $\pi_m(\alpha,\beta) \notin \pi_m(S)$ by Lemma 2.12 and by the cases considered above.
- If $m > \beta$ then the second co-ordinate of any point in S is in the interval [1, N] while $\beta > N! > N$. Hence the difference of the second coordinates is contained in $[\beta N, \beta 1] \subset [1, m 1]$ and is therefore not equal to zero modulo m. Thus $\pi_m(\alpha, \beta) \notin \pi_m(S)$.

Proof of Theorem 2.9 (ii) \Rightarrow **(i).** This is straightforward.

Proof of Theorem 2.9 (i) \Rightarrow **(iii).** Assume that there exists a circumscribed circle of S of some radius r centred at O. Suppose that S is a covering set of \mathcal{T}_m for some integer $m \geq 2$. Let p be a prime divisor of m. Lemma 2.11 implies that S is a covering set of \mathcal{T}_p .

On the one hand there exists $s_1 \in S$ such that $\pi_p(s_1) = \pi_p(O)$. Therefore, p divides r.

On the other hand there exists $s_2 \in S$ such that $\pi_p(s_2) \neq \pi_p(O)$. Therefore, p does not divide $l\ell(s_2, O) = r$.

This is a contradiction. Hence *S* is tori-transparent.

Remark 2.14. The finiteness of the set *S* is crucial in Theorem 2.9. For instance, the set

$$S = \{0, 6\} \times \mathbb{Z}$$

is an example of an infinite set, for which Theorem 2.9 does not hold.

Indeed, for every m, the set S is not a covering set of \mathcal{T}_m as $[1,0]_m \notin \pi_m(S)$ for $m \neq 5$ and $[2,0]_m \notin \pi_m(S)$ for m=5. Assume that there exists a circle through all points of S with centre (x,y). The point (x,y) is at integer distance one from all points of $\{0\} \times \mathbb{Z}$,

Oleg Karpenkov, Anna Pratoussevitch, Rebecca Sheppard

hence $\gcd(x, y - n) = 1$ for all $n \in \mathbb{Z}$ and therefore $x = \pm 1$. Similarly, (x, y) is at integer distance one from all points of $\{6\} \times \mathbb{Z}$, hence $\gcd(x - 6, y - n) = 1$ for all $n \in \mathbb{Z}$ and therefore $x - 6 = \pm 1$. We arrive at a contradiction.

Finally let us say a few words about the $Aff(2, \mathbb{Z})$ -invariance of the property of being a covering set of a torus.

Proposition 2.15. Let S be an integer set and m an integer number. The property of S to be a covering set of \mathcal{T}_m is preserved under $Aff(2, \mathbb{Z})$.

Proof. Any element of Aff $(2, \mathbb{Z})$ can be written as a map $v \mapsto Av + b$ for some matrix $A \in GL(2, \mathbb{Z})$ and vector $b \in \mathbb{Z}^2$. Note that the equation $v_1 \equiv v_2 \mod m$ (coordinate-wise) is equivalent to the equation $Av_1 + b \equiv Av_2 + b \mod m$. So the number of points in the image under the projection π_m is preserved under Aff $(2, \mathbb{Z})$.

Corollary 2.16. The property of a finite set to be tori-transparent is invariant under $Aff(2, \mathbb{Z})$.

Definition 2.17. Let S be an integer set and k a positive integer. We say that S is *shift-divisible* by k if there exists an integer point x and an integer set \hat{S} such that

$$S = x + k\hat{S}$$
.

We then say that $\hat{S} \approx S/k$. Note that S is shift-divisible by k if and only if any two points in S are equivalent modulo k. Note that the set \hat{S} is uniquely defined up to a translation by an integer vector. We define S/k as the equivalence class of \hat{S} under translations by integer vectors. The property of an integer set to be a covering set of \mathcal{T}_m is preserved under translations by integer vectors, hence we can say that S/k is a covering set of \mathcal{T}_m or is tori-transparent if the set \hat{S} has this property.

Proposition 2.18. Let S be a finite integer set and a, b integers. If S is shift-divisible by a and b then S is shift-divisible by lcm(a,b).

Circumscribed Circles in Integer Geometry

Proof. If *S* is shift-divisible by *a* and *b* then any two points in *S* are equivalent modulo *a* and modulo *b* and therefore equivalent modulo lcm(a, b). Hence *S* is shift-divisible by lcm(a, b).

Proposition 2.19. Let S be a finite integer set and r an integer. Then S has a circumscribed circle of radius r if and only if S is shift-divisible by r and S/r is tori-transparent.

Proof. Suppose that the set S has a circumscribed circle C of radius r with centre x. Then $S-x\subset r\mathbb{Z}^2$ and $\hat{S}=(S-x)/r$ is an integer set such that $S=x+r\hat{S}$, i.e. S is shift-divisible by r and $S/r\approx \hat{S}$. Moreover, $\hat{C}=(C-x)/r$ is a unit integer circumscribed circle of \hat{S} , hence $1\in\Lambda_{\mathbb{Z}}(\hat{S})$. Theorem 2.9 implies that S/r is tori-transparent.

Now suppose that S is shift-divisible by r and S/r is tori-transparent, i.e. there exists an integer point x and an integer tori-transparent set \hat{S} such that $S = x + r\hat{S}$. By Theorem 2.9, the set \hat{S} admits a unit integer circumscribed circle \hat{C} . Then $C = x + r\hat{C}$ is an integer circumscribed circle of S of radius r.

Proposition 2.20. Let S be a finite integer set and a,b integers. If $a,b \in \Lambda_{\mathbb{Z}}(S)$ then $lcm(a,b) \in \Lambda_{\mathbb{Z}}(S)$.

Proof. If $a, b \in \Lambda_{\mathbb{Z}}(S)$ then Proposition 2.19 implies that S is shift-divisible by a and b and S/a, S/b are tori-transparent. Proposition 2.18 implies that S is shift-divisible by $\operatorname{lcm}(a,b)$. Let $\hat{S} = S/(\operatorname{lcm}(a,b))$. Let $d = \gcd(a,b)$, $\hat{a} = a/d$ and $\hat{b} = b/d$, so that $\gcd(\hat{a},\hat{b}) = 1$ and $\operatorname{lcm}(a,b) = d\hat{a}\hat{b}$. The set

$$\hat{a}\hat{S} = \hat{a}(S/(d\hat{a}\hat{b})) = S/(d\hat{b}) = S/b$$

is tori-transparent, hence \hat{S} is not a covering set of \mathcal{T}_m for all m co-prime with \hat{a} . Similarly, the set

$$\hat{b}\hat{S} = \hat{b}(S/(d\hat{a}\hat{b})) = S/(d\hat{a}) = S/a$$

is tori-transparent, hence \hat{S} is not a covering set of \mathcal{T}_m for all m co-prime with \hat{b} . The integers \hat{a} and \hat{b} are co-prime, hence every integer m is co-prime with at least one of \hat{a} and \hat{b} . Therefore \hat{S} is not a covering set of any \mathcal{T}_m for $m \geq 2$, i.e. $\hat{S} = S/(\text{lcm}(a,b))$ is tori-transparent. Proposition 2.19 implies that $\text{lcm}(a,b) \in \Lambda_{\mathbb{Z}}(S)$.

3 Rational Circumscribed Circles

Some sets do not have integer circumscribed circles. However we can extend the definition of integer circumscribed circles to circles with rational radii. We will see that every finite set has at least one rational circumscribed circle.

3.1 Definition of a Rational Circumscribed Circle

Definition 3.1. We call a fraction $\frac{p}{q}$ *irreducible* if gcd(p,q) = 1.

Definition 3.2. Consider an integer set S and let p and q be two integers. We say that S has a *rational circumscribed circle* of radius $\frac{p}{q}$ if the set qS has a circumscribed circle of radius p.

Definition 3.3. The *rational circumscribed spectrum* $\Lambda_{\mathbb{Q}}(S)$ of an integer set S is the set of all rational values $\frac{p}{q}$ such that S admits a rational circumscribed circle of radius $\frac{p}{q}$.

Remark 3.4. Since every integer circle is also a rational circle, we have

$$\Lambda_{\mathbb{Z}}(S) \subset \Lambda_{\mathbb{Q}}(S).$$

Proposition 3.5. Let S be an integer set. If $\frac{p}{q}$ is an irreducible fraction in $\Lambda_{\mathbb{Q}}(S)$ and $a, b \in S$ then p divides $\mathrm{ld}(a,b)$.

Proof. By definition, $\frac{p}{q} \in \Lambda_{\mathbb{Q}}(S)$ implies $p \in \Lambda_{\mathbb{Z}}(qS)$, i.e. the set qS has an integer circumscribed circle of radius p. Proposition 2.3 implies that p is a divisor of $\mathrm{Id}(qa,qb) = q \cdot \mathrm{Id}(a,b)$ for any $a,b \in S$. As p and q are co-prime, it follows that p is a divisor of $\mathrm{Id}(a,b)$.

This proposition implies that the rational spectrum is bounded.

Corollary 3.6. Let S be an integer set, $|S| \ge 2$. Then the rational spectrum $\Lambda_{\mathbb{Q}}(S)$ of S and the set of numerators of irreducible fractions in $\Lambda_{\mathbb{Q}}(S)$ are bounded.

Proposition 3.7. Let S be a finite integer set. If $\frac{p_1}{q_1}$ and $\frac{p_2}{q_2}$ are two irreducible fractions in $\Lambda_{\mathbb{Q}}(S)$ then

$$\frac{\operatorname{lcm}(p_1q_2,p_2q_1)}{q_1q_2} = \frac{\operatorname{lcm}(p_1,p_2)}{\gcd(q_1,q_2)} \in \Lambda_{\mathbb{Q}}(S).$$

Circumscribed Circles in Integer Geometry

Proof. If $\frac{p_1}{q_1} \in \Lambda_{\mathbb{Q}}(S)$ then $p_1 \in \Lambda_{\mathbb{Z}}(q_1S)$, hence $p_1q_2 \in \Lambda_{\mathbb{Z}}(q_1q_2S)$. Similarly, $p_2q_1 \in \Lambda_{\mathbb{Z}}(q_1q_2S)$. Proposition 2.20 implies $lcm(p_1q_2, p_2q_1) \in \Lambda_{\mathbb{Z}}(q_1q_2S)$, hence

$$\frac{\operatorname{lcm}(p_1q_2, p_2q_1)}{q_1q_2} \in \Lambda_{\mathbb{Q}}(S).$$

Finally, we will use the following identity known in elementary number theory

$$\frac{\text{lcm}(p_1q_2, p_2q_1)}{q_1q_2} = \frac{\text{lcm}(p_1, p_2)}{\text{gcd}(q_1, q_2)}.$$

3.2 Structure of Rational Spectra

Proposition 3.8. Let S be a finite integer set. If $\frac{p}{q}$ and $\frac{p'}{q'}$ are two irreducible fractions in $\Lambda_{\mathbb{Q}}(S)$ and $\max(\Lambda_{\mathbb{Q}}(S)) = \frac{p}{q}$, then $p' \mid p$ and $q \mid q'$.

Proof. By Proposition 3.7, the number

$$\frac{\operatorname{lcm}(p, p')}{\gcd(q, q')}$$

is in $\Lambda_{\mathbb{Q}}(S)$, hence

$$\frac{\operatorname{lcm}(p, p')}{\gcd(q, q')} \le \max(\Lambda_{\mathbb{Q}}(S)) = \frac{p}{q}.$$

Note that $lcm(p, p') \ge p$ and $gcd(q, q') \le q$, hence the inequality above can only hold if

$$lcm(p, p') = p,$$
 $gcd(q, q') = q.$

Therefore $p' \mid p$ and $q \mid q'$.

Corollary 3.9. Let S be a finite integer set. If $\frac{p}{q}$ is an irreducible fraction in $\Lambda_{\mathbb{Q}}(S)$ and $\max(\Lambda_{\mathbb{Q}}(S)) = \frac{p}{q}$, then p is the largest possible numerator and q is the smallest possible denominator of an irreducible fraction in $\Lambda_{\mathbb{Q}}(S)$.

Theorem 3.10. Let S be a finite integer set. Let $\{t_1, ..., t_n\}$ be the set of all primes t such that S is a covering set of \mathcal{T}_t . Let $\tau = \prod_{i=1}^n t_i$. Then there exists $p \in \mathbb{Z}_+$ such that

$$\Lambda_{\mathbb{Q}}(S) = \left\{ \frac{1}{c} \cdot \frac{p}{\tau} \,\middle|\, c \in \mathbb{Z}_+ \right\}.$$

Oleg Karpenkov, Anna Pratoussevitch, Rebecca Sheppard

In fact, $p = \max(\Lambda_{\mathbb{Z}}(\tau S))$, $p/\tau = \max(\Lambda_{\mathbb{Q}}(S))$, and the greatest common divisor of all integer distances between pairs of points in S is a multiple of p.

If S *is tori-transparent then* $\tau = 1$,

$$\Lambda_{\mathbb{Q}}(S) = \left\{ \frac{p}{c} \middle| c \in \mathbb{Z}_+ \right\}$$

and $p = \max(\Lambda_{\mathbb{Z}}(S)) = \max(\Lambda_{\mathbb{Q}}(S))$.

Proof. Let $\frac{p}{q}$ be an irreducible fraction such that $\max(\Lambda_{\mathbb{Q}}(S)) = \frac{p}{q}$.

- 1. We will show that q is a divisor of τ : We know that S and hence τS is not a covering set of \mathcal{T}_t for any prime $t \notin \{t_1, \dots, t_n\}$. For $i = 1, \dots, n$, the set $t_i S$ and hence τS is not a covering set of \mathcal{T}_{t_i} . In summary, the set τS is not a covering set of \mathcal{T}_t for every prime t, i.e. τS is tori-transparent. Theorem 2.9 implies $1 \in \Lambda_{\mathbb{Z}}(\tau S)$ and hence $\frac{1}{\tau} \in \Lambda_{\mathbb{Q}}(S)$. Proposition 3.8 implies $q \mid \tau$.
- 2. We will now show that $q=\tau$: We have shown that q is a divisor of τ . Suppose that $q\neq \tau$ then q is the product of some but not all of t_1,\ldots,t_n . We can assume without loss of generality that t_1 is not a divisor of q. We know that S is a covering set of \mathcal{T}_{t_1} and $\gcd(t_1,q)=1$, hence qS is also a covering set of \mathcal{T}_{t_1} and therefore not tori-transparent. Theorem 2.9 implies that $\Lambda_{\mathbb{Z}}(qS)=\emptyset$. On the other hand, we know that $\frac{p}{q}\in\Lambda_{\mathbb{Q}}(s)$, hence $p\in\Lambda_{\mathbb{Z}}(qS)$ in contradiction to $\Lambda_{\mathbb{Z}}(qS)=\emptyset$. Hence $q=\tau$.
- 3. We will next show that

$$\Lambda_{\mathbb{Q}}(S) \subset \left\{ \frac{1}{c} \cdot \frac{p}{\tau} \mid c \in \mathbb{Z}_+ \right\} :$$

Consider an irreducible fraction $\frac{p'}{q'}$ in $\Lambda_{\mathbb{Q}}(S)$. We know that the irreducible fraction $\frac{p}{q} = \frac{p}{\tau}$ is the maximum of $\Lambda_{\mathbb{Q}}(S)$. Proposition 3.8 implies that $p' \mid p$ and $\tau \mid q'$, hence there exists $c \in \mathbb{Z}_+$ such that

$$\frac{p'}{q'} = \frac{1}{c} \cdot \frac{p}{\tau}.$$

4. We will now show that

$$\left\{\frac{1}{c} \cdot \frac{p}{\tau} \middle| c \in \mathbb{Z}_+\right\} \subset \Lambda_{\mathbb{Q}}(S) :$$

Circumscribed Circles in Integer Geometry

Let $c \in \mathbb{Z}_+$. We know that $\frac{p}{\tau} \in \Lambda_{\mathbb{Q}}(S)$, hence $p \in \Lambda_{\mathbb{Z}}(\tau S)$ and therefore $\Lambda_{\mathbb{Z}}(\tau S) \neq \emptyset$. Theorem 2.9 implies that the set τS is tori-transparent. It follows that the set $c(\tau S)$ is also tori-transparent. Theorem 2.9 implies that $1 \in \Lambda_{\mathbb{Q}}(c\tau S)$ and therefore $\frac{1}{c} \in \Lambda_{\mathbb{Q}}(\tau S)$. We know that $p, \frac{1}{c} \in \Lambda_{\mathbb{Q}}(\tau S)$, hence $\frac{p}{c} \in \Lambda_{\mathbb{Q}}(\tau S)$ according to Proposition 3.7. Therefore $\frac{p}{c\tau} \in \Lambda_{\mathbb{Q}}(S)$.

5. Finally, we will show that the greatest common divisor of all integer distances between pairs of points in S is a multiple of p: We know that $\frac{p}{q} = \frac{p}{\tau} \in \Lambda_{\mathbb{Q}}(S)$, hence $p \in \Lambda_{\mathbb{Z}}(\tau S)$ and therefore τS has a circumscribed circle of radius p. It follows that the integer distance between any two points in τS is a multiple of p. We know that $\gcd(p,\tau) = \gcd(p,q) = 1$, hence the integer distance between any two points in S is a multiple of p.

Remark 3.11. Let *S* be a finite integer set. Then

$$\Lambda_{\mathbb{Z}}(S) = \Lambda_{\mathbb{Q}}(S) \cap \mathbb{Z}.$$

In the case $\Lambda_{\mathbb{Z}}(S) \neq \emptyset$, we additionally get the equality

$$\max(\Lambda_{\mathbb{Z}}(S)) = \max(\Lambda_{\mathbb{Q}}(S)).$$

Remark 3.12. There is a similarity between the expression for the rational circumscribed spectrum in Theorem 3.10 and some formulas for coefficients of Ehrhart polynomials, see for example [BR15].

Note that while Theorem 3.10 states that the greatest common divisor of all integer distances between pairs of points in S is a multiple of p, it is not necessarily equal to p as can be seen in the following example:

Example 3.13. Consider the set

$$S = \{(0,0), (2,0), (0,2), (2,2)\}.$$

Oleg Karpenkov, Anna Pratoussevitch, Rebecca Sheppard

On the one hand, the set S is tori-transparent, so Theorem 3.10 implies that there exists a divisor p of all integer distances between pairs of points in S such that

$$\Lambda_{\mathbb{Q}}(S) = \left\{ \frac{p}{c} \mid c \in \mathbb{Z}_+ \right\}.$$

The greatest common divisor of all integer distances between points in S is g=2, hence either p=1 and $\Lambda_{\mathbb{Z}}(S)=\{1\}$ or p=g=2 and $\Lambda_{\mathbb{Z}}(S)=\{1,2\}$. On the other hand, we have $S=2\hat{S}$, where

$$\hat{S} = \{(0,0), (1,0), (0,1), (1,1)\}.$$

Now \hat{S} is a covering set of \mathcal{T}_2 , hence Theorem 2.9 implies $1 \notin \Lambda_{\mathbb{Z}}(\hat{S})$ and therefore $2 \notin \Lambda_{\mathbb{Z}}(S)$. Thus $p = 1 \neq g$.

To give a more precise description of circumscribed spectra, we will need the following definition:

Definition 3.14. An integer set S is called *primitive* if it is not shift-divisible by k for any integer k > 1.

Remark 3.15. Note that a set is primitive if and only if the greatest common divisor of the distances between all pairs of its points equals to one.

Theorem 3.16. Let S be a finite integer set. Let x be an integer point, g an integer and \hat{S} a primitive set such that $S = x + g\hat{S}$. Let $\{t_1, ..., t_n\}$ be the set of all primes t such that \hat{S} is a covering set of \mathcal{T}_t . Let $\tau = \prod_{i=1}^n t_i$. Then the rational circumscribed spectrum of S is

$$\Lambda_{\mathbb{Q}}(S) = \left\{ \frac{1}{c} \cdot \frac{g}{\tau} \mid c \in \mathbb{Z}_+ \right\}.$$

If \hat{S} *is tori-transparent then* $\tau = 1$ *and*

$$\Lambda_{\mathbb{Q}}(S) = \left\{ \frac{g}{c} \mid c \in \mathbb{Z}_+ \right\}.$$

Proof. Theorem 3.10 implies that there exists $p \in \mathbb{Z}_+$ such that

$$\Lambda_{\mathbb{Q}}(\hat{S}) = \left\{ \frac{1}{c} \cdot \frac{p}{\tau} \,\middle|\, c \in \mathbb{Z}_+ \right\},\,$$

Circumscribed Circles in Integer Geometry

and that p is a divisor of all integer distances between pairs of points in \hat{S} . The set \hat{S} is primitive, hence the greatest common divisor of all integer distances between pairs of points in \hat{S} is equal to 1 and therefore p = 1. It follows that

$$\Lambda_{\mathbb{Q}}(\hat{S}) = \left\{ \frac{1}{c} \cdot \frac{1}{\tau} \,\middle|\, c \in \mathbb{Z}_+ \right\}$$

and therefore

$$\Lambda_{\mathbb{Q}}(S) = \Lambda_{\mathbb{Q}}(g\hat{S}) = g \cdot \Lambda_{\mathbb{Q}}(\hat{S}) = \left\{ \frac{1}{c} \cdot \frac{g}{\tau} \middle| c \in \mathbb{Z}_+ \right\}.$$

Definition 3.17. The *primorial* d# of $d \in \mathbb{Z}_+$ is defined as the product of all prime numbers smaller or equal to d.

Proposition 3.18. Let S be a finite integer set and k = |S| then

$$\frac{1}{|\sqrt{k}|\#} \in \Lambda_{\mathbb{Q}}(S).$$

Proof. Let k = |S|. Theorem 3.10 implies that $\frac{1}{n\tau} \in \Lambda_{\mathbb{Q}}(S)$ for every $n \in \mathbb{Z}_+$, where $\tau = \prod_{i=1}^n t_i$ and $\{t_1, \dots, t_n\}$ is the set of all primes t such that S is a covering set of \mathcal{T}_t . Note that if S is a covering set of an integer torus \mathcal{T}_t then $t^2 = |\mathcal{T}_t| \le |S| = k$ and therefore $t \le \sqrt{k}$. It follows that $\{t_1, \dots, t_n\}$ is a subset of the set of all primes smaller or equal to \sqrt{k} , hence τ is a divisor of $\lfloor \sqrt{k} \rfloor \#$, i.e. $\lfloor \sqrt{k} \rfloor \# = n\tau$ for some $n \in \mathbb{Z}_+$. Therefore

$$\frac{1}{|\sqrt{k}|^{\#}} = \frac{1}{n\tau} \in \Lambda_{\mathbb{Q}}(S).$$

Example 3.19. Let $a, b \ge 2$ be integers. The circumscribed spectra of the integer set

$$G_{a,b} = \{1, \dots, a\} \times \{1, \dots, b\}$$

are given by

$$\Lambda_{\mathbb{Z}}(G_{a,b}) = \emptyset, \quad \Lambda_{\mathbb{Q}}(G_{a,b}) = \left\{ \frac{1}{c} \cdot \frac{1}{(\min(a,b))\#} \,\middle|\, c \in \mathbb{Z}_+ \right\}.$$

To prove this, note that $G_{a,b}$ is a primitive set. Theorem 3.16 implies that

$$\Lambda_{\mathbb{Q}}(G_{a,b}) = \left\{ \frac{1}{c} \cdot \frac{1}{\tau} \mid c \in \mathbb{Z}_+ \right\},\,$$

where $\{t_1, \dots, t_n\}$ is the set of all primes t such that $G_{a,b}$ is a covering set of \mathcal{T}_t and $\tau = \prod_{i=1}^n t_i$. The set $G_{a,b}$ is a covering set for an integer torus \mathcal{T}_t if and only if $1 \le t \le \min(a,b)$. Hence the set $\{t_1, \dots, t_n\}$ consists of all primes smaller or equal to $\min(a,b)$ and therefore $t_1 = \min(a,b)$. Finally, $t_2 = t_3 = t_4$.

4 Circumscribed Circles of Polygons

We define an *integer circumscribed circle of a polygon P* as the integer circumscribed circle of the set of vertices of *P* in the sense of Definition 2.1. Note that an integer circle is an integer circumscribed circle of *P* if and only if all vertices of *P* are on the circle (see Figure 1). We define a *rational circumscribed circle of a polygon P* as the rational circumscribed circle of the set of vertices of *P* in the sense of Definition 3.2.

In this section we summarise the implications of the results of Theorem 3.16 for integer and rational circumscribed circles of polygons.

4.1 Circumscribed Circles of Segments and Triangles

An integer segment or triangle always admits a unit integer circumscribed circle.

Proposition 4.1. Let S be an integer segment or triangle. Let g be the greatest common divisor of all integer distances between pairs of vertices of S. Then the integer circumscribed spectrum $\Lambda_{\mathbb{Z}}(S)$ consists of all positive divisors of g and

$$\Lambda_{\mathbb{Q}}(S) = \left\{ \frac{g}{c} \mid c \in \mathbb{Z}_+ \right\}.$$

In particular if S is a primitive segment or triangle then

$$\Lambda_{\mathbb{Z}}(S) = \{1\}, \quad \Lambda_{\mathbb{Q}}(S) = \left\{\frac{1}{c} \mid c \in \mathbb{Z}_+\right\}.$$

Proof. There exist an integer point x and a primitive polygon \hat{S} such that $S = x + g\hat{S}$. The set of vertices of \hat{S} consists of at most three points and therefore is tori-transparent.

Theorem 3.16 implies that

$$\Lambda_{\mathbb{Q}}(S) = \left\{ \frac{g}{c} \mid c \in \mathbb{Z}_+ \right\}.$$

It follows that $\Lambda_{\mathbb{Z}}(S) = \Lambda_{\mathbb{Q}}(S) \cap \mathbb{Z}$ consists of all positive divisors of g.

We obtain the following corollary:

Corollary 4.2. If an integer set S has a integer circumscribed circle of radius r then the integer distance between any two points of S is a multiple of r.

Proof. Consider $A, B \in S$. Any integer circumscribed circle of S is in particular an integer circumscribed circle of the segment AB, hence the integer length of the segment AB is divisible by r.

Let us recall the Euclidean Extended Sine Rule: for a triangle *ABC* we have

$$\frac{|AB|}{\sin \angle BCA} = \frac{|BC|}{\sin \angle CAB} = \frac{|CA|}{\sin \angle ABC} = 2R,$$

where *R* is the radius of the circumscribed circle.

As was shown in [Kar08], the first two of these equalities hold in lattice geometry:

$$\frac{1\ell(AB)}{|\sin \angle BCA|} = \frac{1\ell(BC)}{|\sin \angle CAB|} = \frac{1\ell(CA)}{|\sin \angle ABC|}.$$

Proposition 4.1 tells us that there is no natural generalisation for the last equality. Indeed, the circumscribed spectrum depends entirely on the integer length of the edges of the triangle and does not depend on the angles.

For instance consider two triangles, one with vertices (0,0), (1,0), (0,1) and another with vertices (0,0), (1,2), (2,1). For both triangles, all edges are of unit integer length. The sets of integer sines of the angles of these triangles are distinct, for the first triangle all integer sines are equal to 1 while for the second triangle all integer sines of the angles are equal to 3. Nevertheless the circumscribed spectra for both triangles coincide.

4.2 Circumscribed Circles of Quadrangles

We have seen that every triangle has an integer circumscribed circle, however this is no longer true for quadrangles as the following example shows.

Definition 4.3. An integer polygon P is *empty* if the only lattice points contained in P are the vertices.

Proposition 4.4. An empty integer strictly convex quadrilateral does not have a integer circumscribed circle.

Proof. Note that every empty integer strictly convex quadrilateral is integer congruent to the coordinate square S_1 with vertices (0,0), (1,0), (1,1) and (0,1). The square S_1 is a covering set of \mathcal{T}_2 , hence it is not tori-transparent. Theorem 2.9 implies that S_1 does not admit integer circumscribed circles of any radius.

However some quadrangles have integer circumscribed circles.

Example 4.5. The quadrilateral with vertices A = (0,0), B = (1,0), C = (0,1) and D = (2,2) has a unit circumscribed circle centred at (1,1).

The situation is similar to the Euclidean geometry, where a quadrangle has a circumscribed circle if and only if its opposite angles add up to π . The lattice version of this rule is as follows:

Proposition 4.6. An integer quadrangle has an integer circumscribed circle if and only if the set of its vertices is not a covering set of \mathcal{T}_2 .

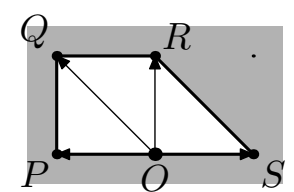
Proof. Theorem 2.9 implies that a quadrangle admits an integer circumscribed circle if and only if its set of vertices V is tori-transparent, i.e. is not a covering set of any integer torus \mathcal{T}_t for $t \geq 2$. The set V cannot be a covering set of \mathcal{T}_t for t > 2 since $|V| = 4 < t^2 = |\mathcal{T}_t|$. Hence the set V is tori-transparent if and only if it is not a covering set of \mathcal{T}_2 .

Circumscribed Circles in Integer Geometry

Remark 4.7. The conditions for a quadrangle to admit a circumscribed circle can be stated in terms of the parity of the six integer distances between its pairs of vertices as follows: An integer quadrangle admits an integer circumscribed circle if and only if at least one of the integer distances between its vertices is even.

On the other hand, the existence of an integer circumscribed circle is not determined solely by the integer angles of the integer quadrangle. For example, the angles of the quadrangles with vertices A(0,0), B(0,1), C(1,1), D(1,0) and P(-1,0), Q(-1,1), R(0,1), S(1,0) are congruent to each other, however the latter one admits a circumscribed circle, for example one centred at the origin O(0,0), while the former one does not.





4.3 Circumscribed Circles of General Polygons

In fact, the argument used in the proof of Proposition 4.6 holds for all *n*-gons with $n \le 8$:

Proposition 4.8. An integer n-gon with $n \le 8$ has an integer circumscribed circle if and only if the set of its vertices is not a covering set of \mathcal{T}_2 .

In general, the following statement holds:

Proposition 4.9. An integer n-gon admits an integer circumscribed circle if and only if its vertices are not a covering set of \mathcal{T}_t for every $t \leq \sqrt{n}$.

Acknoledgements

Grant support for R.S.: This work was supported by a Vacation Bursary of the London Mathematical Society.

We would like to thank the anonymous referee for their helpful suggestions.

References

- [Ayo74] R. Ayoub. Euler and the zeta function. *The American Mathematical Monthly*, 81:1067–1086, 1974. 18
- [BKD23] J. Blackman, O. Karpenkov, and J. Dolan. Multidimensional integer trigonometry. *Commun. Math.*, 31(2):1–26, 2023. 22
- [BR15] M. Beck and S. Robins. *Computing the continuous discretely*. Undergraduate Texts in Mathematics. Springer, New York, second edition, 2015. Integer-point enumeration in polyhedra, With illustrations by David Austin. 33
- [HW08] G. H. Hardy and E. M. Wright. *An introduction to the theory of numbers*. Oxford University Press, Oxford, sixth edition, 2008. Revised by D. R. Heath-Brown and J. H. Silverman, With a foreword by Andrew Wiles. 18
- [Kar08] O. Karpenkov. Elementary notions of lattice trigonometry. *Mathematica Skandinavica*, 102:161–205, 2008. 22, 37
- [Kar09] O. Karpenkov. On irrational lattice angles. *Funct. Anal. Other Math.*, 2(2-4):221–239, 2009. 22
- [Kar13] O. Karpenkov. Geometry of Continued Fractions. Springer Nature, 2013. 22
- [Kar22] O. Karpenkov. *Geometry of Continued Fractions*. Springer Nature, 2 edition, 2022. 20
- [MGO19] S. Morier-Genoud and V. Ovsienko. Farey boat: continued fractions and triangulations, modular group and polygon dissections. *Jahresber. Dtsch. Math.-Ver.*, 121(2):91–136, 2019. 18
- [Ser] C. Series, Continued fractions and hyperbolic geometry, LMS Summer School, Notes, 2015.
 http://homepages.warwick.ac.uk/~ masbb/HypGeomandCntdFractions-2.pdf . 18

Circumscribed Circles in Integer Geometry

AUTHORS

Oleg Karpenkov
Department of Mathematical Sciences
University of Liverpool
Liverpool L69 7ZL, United Kingdom
email: karpenk@liverpool.ac.uk

Anna Pratoussevitch
Department of Mathematical Sciences
University of Liverpool
Liverpool L69 7ZL, United Kingdom
email:annap@liverpool.ac.uk

Rebecca Sheppard

Department of Mathematical Sciences
University of Liverpool
Liverpool L69 7ZL, United Kingdom

email: rshepp@liverpool.ac.uk



Arnold Mathematical Journal Volume 11, Issue 3, 2025



Arithmetic on *q*-deformed rational numbers

Takeyoshi Kogiso Kengo Miyamoto Xin Ren Michihisa Wakui Kohji Yanagawa

Received 10 Mar 2024; Accepted 21 Nov 2024

Abstract:

Recently, Morier-Genoud and Ovsienko introduced a q-deformation of rational numbers. More precisely, for an irreducible fraction $\frac{r}{s} > 0$, they constructed coprime polynomials $\mathcal{R}_{\frac{r}{s}}(q)$, $\mathcal{S}_{\frac{r}{s}}(q) \in \mathbb{Z}[q]$ with $\mathcal{R}_{\frac{r}{s}}(1) = r$, $\mathcal{S}_{\frac{r}{s}}(1) = s$. Their theory has a rich background and many applications. By definition, if $r \equiv r' \pmod{s}$, then $\mathcal{S}_{\frac{r}{s}}(q) = \mathcal{S}_{\frac{r'}{s}}(q)$. We show that $rr' \equiv -1 \pmod{s}$ implies $\mathcal{S}_{\frac{r}{s}}(q) = \mathcal{S}_{\frac{r'}{s}}(q)$, and it is conjectured that the converse holds if s is prime (and $r \not\equiv r' \pmod{s}$). We also show that s is a multiple of 3 (resp. 4) if and only if $\mathcal{S}_{\frac{r}{s}}(\zeta) = 0$ for $\zeta = (-1 + \sqrt{-3})/2$ (resp. $\zeta = i$). We give applications to the representation theory of quivers of type A and the Jones polynomials of rational links.

AMS Classification: 05A30, 11A55, 16G20, and 57K14

Key words and phrases: q-deformed rational numbers, q-continued fractions, quivers, and Jones polynomials, and rational knots.

1 Introduction

The q-deformation of a positive integer n, which is given by

$$[n]_q = \frac{1-q^n}{1-q} = q^{n-1} + q^{n-2} + \dots + q + 1,$$

is a very classical subject of mathematics. Recently, Morier-Genoud and Ovsienko [MO20] introduced the q-deformation $[\alpha]_q$ of a rational number α based on some combinatorial properties of rational numbers. They further extended this notion to arbitrary real numbers [MO22] by some number-theoretic properties of irrational numbers. These works are related to many directions including Teichmüller spaces [FC99], the 2-Calabi-Yau category of type A_2 [BBL23], the Markov-Hurwitz approximation theory [Ko22, LL22, LMOV21, R22(a)], the modular group and Picard groups [LeM21, MOV24, O21], Jones polynomials of rational knots [KW19(a), LS19, NT20, MO20, BBL23, R22(b)], and combinatorics on fence posets [MSS21, Kan22, KR23].

For an irreducible fraction $\frac{r}{s} > 0$, we have

$$\left[\frac{r}{s}\right]_q = \frac{\mathcal{R}_{\frac{r}{s}}(q)}{\mathcal{S}_{\frac{r}{s}}(q)} \text{ for } \mathcal{R}_{\frac{r}{s}}(q), \mathcal{S}_{\frac{r}{s}}(q) \in \mathbb{Z}_{>0}[q] \text{ with } \mathcal{R}_{\frac{r}{s}}(1) = r \text{ and } \mathcal{S}_{\frac{r}{s}}(1) = s.$$

There are many ways to compute $[\alpha]_q$ (see Section 2 for details). For example, we have

$$\left[\frac{6}{5}\right]_q = \frac{[6]_q}{[5]_q} = \frac{q^5 + q^4 + q^3 + q^2 + q + 1}{q^4 + q^3 + q^2 + q + 1}, \quad \left[\frac{7}{5}\right]_q = \frac{q^4 + 2\,q^3 + 2\,q^2 + q + 1}{q^3 + 2\,q^2 + q + 1},$$

and observe that the denominators of $\frac{6}{5}$ and $\frac{7}{5}$ are the same 5, but the denominator polynomials of their q-deformation are different. In general, the following problem arises. When dose the equation $\mathcal{S}_{\frac{r}{s}}(q) = \mathcal{S}_{\frac{r'}{s}}(q)$ hold for two irreducible fractions $\frac{r}{s}$ and $\frac{r'}{s}$? By definition, we have $\mathcal{S}_{\alpha+n}(q) = \mathcal{S}_{\alpha}(q)$ for $n \in \mathbb{Z}$, and hence $r \equiv r' \pmod{s}$ implies $\mathcal{S}_{\frac{r}{s}}(q) = \mathcal{S}_{\frac{r'}{s}}(q)$. However, there are more subtle relations.

Example 1.1. (1) The table of $S_{\alpha}(q)$ for irreducible fractions α of the form $\frac{r}{17}$ is the following.

$$A = [17]_q = q^{16} + q^{15} + \dots + q + 1$$

$$B = q^9 + 2q^8 + 2q^7 + 2q^6 + 2q^5 + 2q^4 + 2q^3 + 2q^2 + q + 1$$

$$C = q^7 + 2q^6 + 3q^5 + 3q^4 + 3q^3 + 2q^2 + 2q + 1$$

$$D = q^7 + 2q^6 + 3q^5 + 4q^4 + 3q^3 + 2q^2 + q + 1$$

$$E = q^6 + 2q^5 + 4q^4 + 4q^3 + 3q^2 + 2q + 1$$

r (mod 17)	1,16	2,8	3, 11	4	5, 10	6, 14	7, 12	9, 15	13
$S_{\frac{r}{17}}(q)$	A	В	С	D	E	C^{\vee}	E^{\vee}	B^{\vee}	D^{\vee}

Here, for $f(q) \in \mathbb{Q}[q]$, $f^{\vee}(q)$ denotes its reciprocal polynomial $q^{\deg(f)}f(q^{-1})$. For example, we have

$$E^{\vee} = q^6 + 2q^5 + 3q^4 + 4q^3 + 4q^2 + 2q + 1.$$

(2) Next, we give the table of $S_{\alpha}(q)$ for irreducible fractions α of the form $\frac{r}{23}$.

$$A = [23]_q = q^{22} + q^{21} + \dots + q + 1$$

$$B = q^{12} + 2q^{11} + 2q^{10} + 2q^9 + 2q^8 + 2q^7 + 2q^6 + 2q^5 + 2q^4 + 2q^3 + 2q^2 + q + 1$$

$$C = q^9 + 2q^8 + 3q^7 + 3q^6 + 3q^5 + 3q^4 + 3q^3 + 2q^2 + 2q + 1$$

$$D = q^8 + 2q^7 + 3q^6 + 4q^5 + 4q^4 + 3q^3 + 3q^2 + 2q + 1$$

$$E = q^7 + 3q^6 + 4q^5 + 5q^4 + 4q^3 + 3q^2 + 2q + 1$$

$$F = q^7 + 2q^6 + 4q^5 + 5q^4 + 5q^3 + 3q^2 + 2q + 1$$

r (mod 23)	1,22	2, 11	3, 15	4, 17	5,9	6, 19	7, 13	8, 20	10,16	14, 18	12, 21
$S_{\frac{r}{23}}(q)$	A	В	C	D	E	D^{\vee}	F	C^{\vee}	F^{\vee}	E^{\vee}	B^{\vee}

From these examples, the third author of the present paper and Takeshi Sakurai, who were supervised by the first author, proposed the following conjecture in their master theses [R21, S21]. This is the main motivation of the present paper.

Conjecture 1.2 (Arithmetic conjecture). Let p be an odd prime integer. For two positive integers a, b which are coprime to p, $\mathcal{S}_{\frac{a}{p}}(q) = \mathcal{S}_{\frac{b}{p}}(q)$ if and only if $ab \equiv -1 \pmod{p}$ or $a \equiv b \pmod{p}$.

The necessity part of Conjecture 1.2 really requires the assumption that p is prime. In fact, $\mathcal{S}_{\frac{5}{24}}(q) = \mathcal{S}_{\frac{11}{24}}(q)$ holds, while $5 \cdot 11 \not\equiv -1 \pmod{24}$. See Subsection 2.2 for detail. On the other hand, without the assumption that p is prime, we can show the sufficiency (so the essential part of the conjecture is its necessity). We give two different proofs in Sections 3 and 4.

The proof given in Section 3 is rather direct. Combining an argument here and a combinatorial result in [KR23], we can show that $S_{\frac{r}{s}}(q)$ is palindromic if and only if $r^2 \equiv 1 \pmod{s}$. Recall that $f(q) \in \mathbb{Z}[q]$ is said to be palindromic, if $f^{\vee}(q) = f(q)$.

The proof given in Section 4 uses the q-deformation $(a,b)_p \in \mathbb{Z}[q]$ of a pair (a,b) of positive and coprime integers introduced in the previous work [W22] of the fourth author. In Section 5 we study on behavior of $\mathcal{R}_{\alpha}(q)$ and $\mathcal{S}_{\alpha}(q)$ under the operations $\mathfrak{i},\mathfrak{r},\mathfrak{i}\mathfrak{r}$ on the positive rational numbers α , which are introduced in [KW19(a)].

For a given rational number $\alpha \in \mathbb{Q} \cap (1, \infty)$, the regular continued fraction expansion of α determines a quiver Q of type A. In [MO20, Thoerem 4], they provided a method for computing $\mathcal{R}_{\alpha}(q)$ (and $\mathcal{S}_{\alpha}(q)$) by using combinatorial enumeration with the quiver Q. Specifically, the coefficients of q^k in $\mathcal{R}_{\alpha}(q)$ coincides with the number of marking of circles to k vertices of Q so that there is no arrow from a marked vertex to an unmarked vertex. Thus, one representation-theoretic view of $\mathcal{R}_{\alpha}(q)$ is that it counts the number of submodules of the largest dimensional indecomposable module M over the path algebra kQ, where k is a field. Namely, the coefficients of q^k in $\mathcal{R}_{\alpha}(q)$ is equal to the number of k-dimensional submodules of M. In Section 6, we give a formula for computing $\mathcal{R}_{\alpha}(q)$.

In Section 7, we extend the result [MO20, Proposition 1.8] which states that $S_{\alpha}(-1)$

and $\mathcal{R}_{\alpha}(-1)$ belong to $\{0,\pm 1\}$. First, we will show that

$$\mathcal{R}_{\alpha}(\omega), \, \mathcal{S}_{\alpha}(\omega) \in \{0, \pm 1, \pm \omega, \pm \omega^2\} \quad \text{for} \quad \omega = \frac{-1 + \sqrt{-3}}{2}$$

and

$$\mathcal{R}_{\alpha}(i), \, \mathcal{S}_{\alpha}(i) \in \{0, \pm 1, \pm i, \pm (1+i), \pm (1-i)\}.$$

Hence, for an irreducible fraction $\frac{r}{s}$, $\mathcal{S}_{\frac{r}{s}}(q) \in \mathbb{Z}[q]$ can be divided by $[3]_q = q^2 + q + 1$ (resp. $[4]_q = q^3 + q^2 + q + 1$) if and only if s is a multiple of 3 (resp. 4). Inspired by this fact, we conjecture that if p is a prime integer then $\mathcal{S}_{\frac{q}{p}}(q) \in \mathbb{Z}[q]$ is irreducible over \mathbb{Q} (Conjecture 7.9).

In Section 8, we give an application of the observations in the previous section. For the rational link $L(\alpha)$ associated with $\alpha \in \mathbb{Q}$ (for example, see [KL02]), the Jones polynomial $V_{L(\alpha)}(t) \in \mathbb{Z}[t^{\pm 1}] \cup t^{\frac{1}{2}}\mathbb{Z}[t^{\pm 1}]$ has the normalized form $J_{\alpha}(q) \in \mathbb{Z}[q]$ ([LS19]). Since $J_{\alpha}(q)$ for $\alpha > 1$ can be expressed using $\mathcal{R}_{\alpha}(q)$ and $\mathcal{S}_{\alpha}(q)$ by [MO20, Proposition A.1], one can study the special values of $J_{\alpha}(q)$ at $q = -1, i, \pm \omega$. There are several classical results on the special values of the Jones polynomials $V_L(t)$ for general links L, and most of the facts given in this section easily follow from these results. However, we give a new explanation using q-deformed rationals.

Acknowledgments

We would like to thank Professor Mikami Hirasawa for helpful comments and references on results on existence of the Arf invariants of rational links. We would also like to thank Professors Sophie Morier-Genoud, Valentin Ovsienko, and Taizo Kanenobu for their encouragements of our research. We are grateful to the referee for useful suggestions for improving the manuscript.

2 Preliminaries

Throughout this paper, for a real number $x \in \mathbb{R}$, the symbols $\lceil x \rceil$ and $\lceil x \rceil$ mean $\lceil x \rceil = \min\{n \in \mathbb{Z} \mid x \le n\}$ and $\lceil x \rceil = \max\{n \in \mathbb{Z} \mid n \le x\}$, respectively. For an irreducible fraction $\frac{r}{s}$, we always assume that s > 0. We regard $0 = \frac{0}{1}$ as an irreducible fraction.

2.1 q-deformed rational numbers

In this subsection, we review some basics on q-deformations for rational numbers introduced by Morier-Genoud and Ovsienko [MO20, MOV24]. A rational number $\alpha \in \mathbb{Q} \cap (1, \infty)$ can be represented by

$$\alpha = a_1 + \frac{1}{a_2 + \frac{1}{\ddots} + \frac{1}{a_n}}$$

with $a_1, ..., a_n \in \mathbb{Z}_{>0}$ and it can be also represented by

$$\alpha = c_1 - \frac{1}{c_2 - \frac{1}{\ddots} - \frac{1}{c_l}}$$

with $c_1, \dots, c_l \in \mathbb{Z}_{>1}$. In this case, we write $[a_1, \dots, a_n]$ and $[[c_1, \dots, c_l]]$ for these expansions, respectively. The former expansion is called a *regular continued fraction* of α , and the latter is called a Hirzebruch-Jung continued fraction (or *negative continued fraction* in this paper) of α . One can always assume that the length n of a regular continued fraction to be even, since $[a_1, \dots, a_n + 1] = [a_1, \dots, a_n, 1]$. The expression as a regular continued fraction is uniquely determined if the parity of n is specified, and that as a negative continued fraction is unique (since $c_i \geq 2$ for all i now).

For an integer a, we set:

$$M(a) := \begin{pmatrix} a & 1 \\ 1 & 0 \end{pmatrix}, \quad M^{-}(a) := \begin{pmatrix} a & -1 \\ 1 & 0 \end{pmatrix}.$$
 (2.1)

Moreover, for a finite sequence of integers $(a_1, ..., a_n)$, we set

$$M(a_1, ..., a_n) = M(a_1) \cdots M(a_n), \quad M^-(a_1, ..., a_n) = M^-(a_1) \cdots M^-(a_n).$$
 (2.2)

It follows from the definitions, we see that $M^-(a_1, ..., a_n) \in SL(2, \mathbb{Z})$, whereas $M(a_1, ..., a_n) \in SL(2, \mathbb{Z})$ if and only if n is even. These matrices are well-known as the matrices of continued fractions in elementary number theory because one has the following result.

Lemma 2.1 ([MO19, Proposition 3.1]). Let $\alpha = \frac{r}{s} > 1$ be an irreducible fraction, and assume that it is expressed by

$$\alpha = [a_1, ..., a_n] = [[c_1, ..., c_l]]$$

with $a_i \ge 1$ (i = 1, ..., n) and $c_j \ge 2$ (j = 1, ..., l). Then,

$$M(a_1, \dots, a_n) = \begin{pmatrix} r & r' \\ s & s' \end{pmatrix}, \quad M^-(c_1, \dots, c_l) = \begin{pmatrix} r & -r'' \\ s & -s'' \end{pmatrix},$$

where
$$\frac{r'}{s'} = [a_1, \dots, a_{n-1}]$$
 and $\frac{r''}{s''} = [[c_1, \dots, c_{l-1}]]$.

The q-deformation of positive rational numbers is based on the above lemma. Let q be a formal symbol. For an integer a, we define a Laurent polynomial $[a]_q \in \mathbb{Z}[q,q^{-1}]$ by

$$[a]_q := \frac{1 - q^a}{1 - q} = \begin{cases} q^{a-1} + q^{a-2} + \dots + q + 1 & \text{if } a > 0, \\ 0 & \text{if } a = 0, \\ -q^{-a} - q^{-a+1} - \dots - q^{-2} - q^{-1} & \text{if } a < 0. \end{cases}$$

By the definition of $[a]_q$, for all $a, n \in \mathbb{Z}$, the equation

$$[a+n]_q = q^n [a]_q + [n]_q$$
 (2.3)

holds. For an integer a, two q-deformations of (2.1) are defined by

$$M_q(a) := \begin{pmatrix} [a]_q & q^a \\ 1 & 0 \end{pmatrix}, \quad M_q^-(a) := \begin{pmatrix} [a]_q & -q^{a-1} \\ 1 & 0 \end{pmatrix}.$$
 (2.4)

The next proposition is a q-deformation of Lemma 2.1. Here, for regular continued fractions, we only use those of even length. The q-deformations of (2.2) are defined as follows.

$$\begin{array}{lll} M_q(a_1,\ldots,a_{2m}) & := & M_q(a_1)M_{q^{-1}}(a_2)M_q(a_3)\cdots M_{q^{-1}}(a_{2m}) \\ \\ \widetilde{M}_q(a_1,\ldots,a_{2m}) & := & q^{a_2+a_4+\cdots+a_{2m}}M_q(a_1,\ldots,a_{2m}) \\ \\ M_q^-(a_1,\ldots,a_n) & := & M_q^-(a_1)M_q^-(a_2)\cdots M_q^-(a_n). \end{array}$$

Then, the following statements hold.

Proposition 2.2 ([MO20, Propositions 4.3 and 4.9]). Let $\alpha = \frac{r}{s}$ be a rational number as given in Lemma 2.1. The polynomials $\mathcal{R}_{\alpha}(q)$, $\mathcal{S}_{\alpha}(q) \in \mathbb{Z}[q]$ given by

$$M_q^-(c_1, \dots, c_l) \begin{pmatrix} 1 \\ 0 \end{pmatrix} = \begin{pmatrix} \mathcal{R}_{\alpha}(q) \\ \mathcal{S}_{\alpha}(q) \end{pmatrix}$$

satisfy

$$\widetilde{M}_{q}(a_{1}, \dots, a_{2m}) \begin{pmatrix} 1 \\ 0 \end{pmatrix} = \begin{pmatrix} q \mathcal{R}_{\alpha}(q) \\ q \mathcal{S}_{\alpha}(q) \end{pmatrix}. \tag{2.5}$$

Moreover, the following statements hold.

- (1) $\mathcal{R}_{\alpha}(q)$ and $\mathcal{S}_{\alpha}(q)$ are coprime in $\mathbb{Z}[q]$.
- (2) We have $\mathcal{R}_{\frac{r}{s}}(1) = r$ and $\mathcal{S}_{\frac{r}{s}}(1) = s$.

Based on Proposition 2.2, the *q*-deformation of a rational number $\alpha > 1$ is defined by

$$[\alpha]_q := \frac{\mathcal{R}_{\alpha}(q)}{\mathcal{S}_{\alpha}(q)}.$$

Remark 2.3. Let $PSL_q(2, \mathbb{Z})$ be the subgroup of

$$\operatorname{PGL}\left(2,\mathbb{Z}\left[q^{\pm 1}\right]\right) = \operatorname{GL}\left(2,\mathbb{Z}\left[q^{\pm 1}\right]\right)/\{\pm q^{N}E_{2}\mid N\in\mathbb{Z}\}$$

generated by the following two matrices

$$R_q := \begin{pmatrix} q & 1 \\ 0 & 1 \end{pmatrix}, \quad L_q = \begin{pmatrix} 1 & 0 \\ 1 & q^{-1} \end{pmatrix}.$$

[LeM21, Proposition 1.1] states that $PSL(2, \mathbb{Z}) \cong PSL_q(2, \mathbb{Z})$. Via the equation

$$M_q(a_1,\ldots,a_{2m})=R_q^{a_1}L_q^{a_2}R_q^{a_3}L_q^{a_4}\cdots R_q^{a_{2m-1}}L_q^{a_{2m}}$$

and the classical PSL $(2, \mathbb{Z})$ action on $\mathbb{Q} \cup \left\{ \left(\frac{1}{0} \right) \right\}$, [MOV24] gives an insightful interpretation of q-deformed rationals. We can also use negative continued fractions for this interpretation.

For an integer $n \ge 2$, since n = [[n]] as a negative continued fraction, we have the following philosophically trivial equations

$$\mathcal{R}_n(q) = [n]_q$$
 and $\mathcal{S}_n(q) = 1$. (2.6)

Morier-Genoud and Ovsienko pointed out that the definition of q-deformed rational number $[\alpha]_q$ can be extended to the case where $\alpha \le 1$ including the negative rational numbers by the following formulas, see [MO20, page 3]:

$$[\alpha + 1]_q = q[\alpha]_q + 1. \tag{2.7}$$

However, for $\alpha < 0$, $\mathcal{R}_{\alpha}(q)$ is not an ordinary polynomial but a Laurent polynomial. Similarly, for $0 < \alpha < 1$, $\mathcal{R}_{\alpha}(q)$ is a polynomial, but $\mathcal{R}_{\alpha}(0) = 0$ (if $\alpha \geq 1$, we have $\mathcal{R}_{\alpha}(0) = 1$). It can be easily verified that (2.5) holds for all $\alpha \in \mathbb{Q}$, that is, without assuming that $\alpha > 1$.

Lemma 2.4. For a rational number α and an integer n, we have

$$\mathcal{R}_{\alpha+n}(q) = q^n \mathcal{R}_{\alpha}(q) + [n]_{\alpha} \mathcal{S}_{\alpha}(q)$$
 and $\mathcal{S}_{\alpha+n}(q) = \mathcal{S}_{\alpha}(q)$,

equivalently, $[\alpha + n]_q = q^n [\alpha]_q + [n]_q$. In particular, we have

$$S_{\alpha}(q) = S_{\alpha+1}(q)$$
 and $\mathcal{R}_{\alpha}(q) = q^{-1}(\mathcal{R}_{\alpha+1}(q) - S_{\alpha+1}(q)).$ (2.8)

Proof. It suffices to show that $[\alpha + n]_q = q^n [\alpha]_q + [n]_q$. For $n \ge 1$, this is easily shown by induction on n using (2.7). For $n \ge 1$, replacing α by $\alpha - n$, we have $[\alpha]_q = q^n [\alpha - n]_q + [n]_q$. Hence

$$[\alpha - n]_a = q^{-n}[\alpha]_a - q^{-n}[n]_a = q^{-n}[\alpha]_a + [-n]_a.$$

Lemma 2.5. Let a, x be positive and coprime integers with $1 \le a \le x$, and express x as the form x = ca + r for some $c, r \in \mathbb{Z}$ with $0 \le r < a$. Then the following equations hold:

$$\mathcal{R}_{\frac{x}{a}}(q) = [c+1]_q \mathcal{R}_{\frac{a}{a-r}}(q) - q^c \mathcal{S}_{\frac{a}{a-r}}(q),$$
 $\mathcal{S}_{\frac{x}{a}}(q) = \mathcal{R}_{\frac{a}{a-r}}(q).$

Proof. Note that it follows from the equations (2.6) and (2.8) that $\mathcal{R}_1(q) = \mathcal{S}_1(q) = 1$. If a = 1, then r = 0. Thus, we have

$$[c+1]_q \mathcal{R}_{\frac{a}{a-r}}(q) - q^c \mathcal{S}_{\frac{a}{a-r}}(q) = [x+1]_q \mathcal{R}_1(q) - q^x \mathcal{S}_1(q) = [x]_q = \mathcal{R}_{\frac{x}{a}}(q).$$

The second equation obviously holds when a = 1.

If a > 1, then r > 0, and thus $\frac{a}{a-r} > 1$. By x = ca + r,

$$\frac{x}{a} = \frac{(c+1)a + r - a}{a} = c + 1 - \frac{1}{\frac{a}{a-r}}.$$

So, if $\frac{a}{a-r}$ is expressed as $\frac{a}{a-r}=[[c_1,\ldots,c_l]]$, then $\frac{x}{a}=[[c+1,c_1,\ldots,c_l]]$ and

$$\begin{split} M_q^-(c+1,c_1,\ldots,c_l) \begin{pmatrix} 1 \\ 0 \end{pmatrix} &= M_q^-(c+1) M_q^-(c_1,\ldots,c_l) \begin{pmatrix} 1 \\ 0 \end{pmatrix} \\ &= \begin{pmatrix} [c+1]_q \mathcal{R}_{\frac{a}{a-r}}(q) - q^c \mathcal{S}_{\frac{a}{a-r}}(q) \\ &\mathcal{R}_{\frac{a}{a-r}}(q) \end{pmatrix}. \end{split}$$

This leads to the equations in the lemma.

By Lemmas 2.4 and 2.5, we have

$$\{\mathcal{S}_{\alpha}(q) \mid \alpha \in \mathbb{Q}\} = \{\mathcal{S}_{\alpha}(q) \mid \alpha \in \mathbb{Q} \cap (1,2]\} = \{\mathcal{R}_{\alpha}(q) \mid \alpha \in \mathbb{Q} \cap (1,\infty)\}.$$

Lemma 2.6. For coprime positive integers a, x with $1 \le a \le x$, we have

$$\mathcal{R}_{\frac{a}{x}}(q) = \mathcal{R}_{\frac{x}{x-a}}(q) - \mathcal{S}_{\frac{x}{x-a}}(q), \tag{2.9}$$

51

$$S_{\frac{a}{x}}(q) = \mathcal{R}_{\frac{x}{x-a}}(q). \tag{2.10}$$

Arnold Mathematical Journal, Vol.11(3), 2025

Proof. Express $\frac{x}{x-a}$ as the negative continued fraction $\frac{x}{x-a} = [[c_1, \dots, c_l]]$. Then $\frac{a}{x} + 1 = [[2, c_1, \dots, c_l]]$, and

$$\begin{pmatrix} \mathcal{R}_{\frac{a}{x}+1}(q) \\ \mathcal{S}_{\frac{a}{x}+1}(q) \end{pmatrix} = M_q^-(2)M_q^-(c_1,\ldots,c_l) \begin{pmatrix} 1 \\ 0 \end{pmatrix} = \begin{pmatrix} [2]_q & -q \\ 1 & 0 \end{pmatrix} \begin{pmatrix} \mathcal{R}_{\frac{x}{x-a}}(q) \\ \mathcal{S}_{\frac{x}{x-a}}(q) \end{pmatrix}.$$

This equation and Lemma 2.4 yield the equation (2.10) and

$$q\mathcal{R}_{\frac{q}{x}}(q) + \mathcal{S}_{\frac{q}{x}}(q) = [2]_q \mathcal{R}_{\frac{x}{x-q}}(q) - q\mathcal{S}_{\frac{x}{x-q}}(q)$$
 (2.11)

The equation (2.9) can be obtained by substituting (2.10) to (2.11).

2.2 The arithmetic conjecture on q-deformed rational numbers

Conjecture 1.2 is the central problem of the present paper. In this subsection, we collect a few remarks on this conjecture.

If Conjecture 1.2 holds for an odd prime p, then we have

$$\#\{\mathcal{S}_{\frac{a}{p}}(q) \mid a \in \mathbb{Z}\} = \begin{cases} \frac{p+1}{2} & (p \equiv 1 \pmod{4}), \\ \frac{p-1}{2} & (p \equiv 3 \pmod{4}). \end{cases}$$
 (2.12)

To see this, recall the result of elementary number theory that there is some $a \in \mathbb{Z}$ with $a^2 \equiv -1 \pmod{p}$ if and only if $p \equiv 1 \pmod{4}$. Thus, if $p \equiv 1 \pmod{4}$, then

$$\{1,\ldots,p-1\}=\{a_1,\ldots,a_{\frac{p-3}{2}},b_1,\ldots,b_{\frac{p-3}{2}},c,d\},$$

where $a_i b_i \equiv -1 \pmod{p}$ for each i and $c^2 \equiv d^2 \equiv -1 \pmod{p}$. If $p \equiv 3 \pmod{4}$,

$$\{1,\ldots,p-1\}=\{a_1,\ldots,a_{\frac{p-1}{2}},b_1,\ldots,b_{\frac{p-1}{2}}\}$$

holds, where $a_ib_i\equiv -1\pmod p$ for each i. In the present assumption, we have $\mathcal{S}_{\frac{a_i}{p}}(q)=\mathcal{S}_{\frac{b_i}{p}}(q)$ for each i, and this is the only case when $\mathcal{S}_{\frac{a}{p}}(q)=\mathcal{S}_{\frac{b}{p}}(q)$ holds for distinct $a,b\in\{1,\dots,p-1\}$. Hence Conjecture 1.2 implies (2.12). However, in Theorem 3.5 below, we will

prove the sufficiency of the conjecture (without assuming that p is prime). So $\mathcal{S}_{\frac{a_i}{p}}(q) = \mathcal{S}_{\frac{b_i}{p}}(q)$ actually holds, and (2.12) is equivalent to Conjecture 1.2.

Next, we remark that the assumption that p is prime is really necessary for the necessity part of Conjecture 1.2. In fact, $\frac{5}{24} = [0,4,1,4]$ and $\frac{11}{24} = [0,2,5,2]$ satisfy

$$S_{\frac{5}{24}}(q) = S_{\frac{11}{24}}(q) = q^8 + 2q^7 + 3q^6 + 4q^5 + 4q^4 + 4q^3 + 3q^2 + 2q + 1$$

by Proposition 2.2 and (2.8), while $5 \cdot 11 + 1 = 56$ is not divisible by 24.

The following table shows composite numbers p and pairs of natural numbers (a,b) $(1 < a < b < p \le 111)$ which do not satisfy the necessity of Conjecture 1.2. Note that if p admits a pair (a,b) with this property then it admits other pairs. For example, (p-b,p-a) is also such a pair by Lemma 3.1 below.

p	(a,b)	p	(a,b)
24	(5,11)	84	(19,25)
51	(11,20)	91	(19,32)
57	(13,16)	99	(17,28)
60	(11,19)	105	(23,38)
63	(13,20)	110	(19,41)
78	(17,29)	111	(25,34)

On the other hand, the sufficiency part of Conjecture 1.2 holds without the assumption that p is prime. In Sections 3 and 4, we will prove this in two ways.

2.3 Closures of a quiver and q-deformed rational numbers

By a quiver we mean a tuple $Q=(Q_0,Q_1,s,t)$ consisting of two sets Q_0,Q_1 and two maps $s,t:Q_1\to Q_0$. Each element of Q_0 (resp. Q_1) is called a vertex (resp. an arrow). For an arrow $\alpha\in Q_1$, we call $s(\alpha)$ (resp. $t(\alpha)$) the source (resp. the target) of α . We will commonly write $a\stackrel{\alpha}{\to} b$ or $\alpha:a\to b$ to indicate that an arrow α has the source a and the target b. A quiver Q is *finite* if two sets Q_0 and Q_1 are finite sets. The *opposite quiver* of Q, say Q^\vee , is defined by $Q^\vee=(Q_0,Q_1,t,s)$.

Let Q be a finite quiver. A subset $C \subset Q_0$ is a *closure* if there is no arrow $\alpha \in Q_1$ such that $s(\alpha) \in C$ and $t(\alpha) \in Q_0 \setminus C$. A closure C is an ℓ -closure if the number of elements of C is ℓ . The number of ℓ -closures is denoted by $\rho_{\ell}(Q)$. Then the polynomial

$$\operatorname{cl}(Q) := \sum_{\ell=0}^{n} \rho_{\ell}(Q) q^{\ell} \in \mathbb{Z}[q],$$

where $n = |Q_0|$, is called the *closure polynomial* of Q.

Obviously, the constant term and the coefficient of the leading term of cl(Q) are 1, including the extremal case $cl(\emptyset) = 1$. We remark that, for any ℓ , the equation

$$\rho_{\ell}(Q) = \rho_{n-\ell}(Q^{\vee}) \tag{2.13}$$

holds. For a polynomial $f(q) \in \mathbb{Z}[q]$, we define a polynomial $f^{\vee}(q)$ by

$$f^{\vee}(q) = q^{\deg(f)} f(q^{-1}),$$

which is called the *reciprocal polynomial* of f(q). By (2.13), we have

$$\operatorname{cl}(Q)^{\vee} = \operatorname{cl}(Q^{\vee}). \tag{2.14}$$

For a tuple of integers $\mathbf{a}:=(a_1,a_2,\dots,a_s)$ with $a_1,a_s\geq 0,\,a_2,\dots,a_{s-1}>0,$ we set the quiver

$$Q(\mathbf{a}) := \underbrace{\circ \longleftarrow \circ \cdots \circ \longleftarrow \circ}_{a_1 \, \text{left arrows}} \underbrace{\longrightarrow \circ \cdots \circ \longrightarrow}_{a_2 \, \text{right arrows}} \underbrace{\longrightarrow \circ \cdots \circ \longleftarrow}_{a_3 \, \text{left arrows}} \longrightarrow \cdots,$$

with the left-right distinction. We understand that if $a_1=0$, then

$$Q(\mathbf{a}) := \underbrace{\longrightarrow \circ \cdots \circ \longrightarrow \circ}_{a_2 \text{ right arrows}} \underbrace{\longleftarrow \circ \cdots \circ \longleftarrow \circ}_{a_3 \text{ left arrows}} \longrightarrow \cdots.$$

Note that $|Q(\mathbf{a})_0| = a_1 + a_2 + \cdots + a_s + 1$, and, for $\mathbf{a} = (a_1, a_2, \dots, a_s)$, the equation

$$\operatorname{cl}(Q(0,\mathbf{a})) = \operatorname{cl}(Q(\mathbf{a}))^{\vee} \tag{2.15}$$

holds since $Q(0, \mathbf{a}) \simeq Q(\mathbf{a})^{\vee}$ as quivers. Here we have cl(Q(0, 0)) = cl(Q(0)) = 1 + q.

Remark 2.7. We note that the closure polynomial $cl(Q(\mathbf{a}))$ of a quiver $Q(\mathbf{a})$ can be realized with the *rank polynomials of a finite fence poset*, which is more common in combinatorics (see [MSS21] and [KR23] for detail).

Lemma 2.8. For $\mathbf{a} = (a_1, a_2, ..., a_s)$, we put $\mathbf{a}^{\text{pal}} := (a_s, a_{s-1}, ..., a_1)$. Then, there is an isomorphism of quivers

$$Q(\mathbf{a}^{\mathsf{pal}}) \simeq \left\{ egin{array}{ll} Q(\mathbf{a}) & \textit{if s is even,} \\ Q(\mathbf{a})^{\vee} & \textit{if s is odd.} \end{array}
ight.$$

Therefore, we have

$$cl(Q(\mathbf{a}^{pal})) = \begin{cases} cl(Q(\mathbf{a})) & \text{if s is even,} \\ cl(Q(\mathbf{a}))^{\vee} & \text{if s is odd.} \end{cases}$$

Proof. First, we assume that s is even. Then, the direction of the i-th arrow of $Q(\mathbf{a})$ from the left is the opposite of that of the i-th arrow of $Q(\mathbf{a}^{\text{pal}})$ from the right end. Thus, $Q(\mathbf{a}^{\text{pal}})$ is the " π -rotation" of $Q(\mathbf{a})$, and hence $Q(\mathbf{a}) \simeq Q(\mathbf{a}^{\text{pal}})$ as quivers. We leave the case n is odd to the reader as an easy exercise.

According to [MO20, Section 3], Morier-Genoud and Ovsienko gave a combinatorial interpretation of the coefficients in $\mathcal{R}_{\alpha}(q)$ and $\mathcal{S}_{\alpha}(q)$.

Let $\alpha > 1$ be a rational number, and write α as the regular continued fraction $\alpha = [a_1, a_2, ..., a_{2m}]$. Then, we set

$$Q_{\alpha}^{\mathcal{R}} := Q(a_1 - 1, a_2, \dots, a_{2m-1}, a_{2m} - 1),$$

$$Q_{\alpha}^{\mathcal{S}} := \begin{cases} Q(0, a_2 - 1, a_3, \dots, a_{2m-1}, a_{2m} - 1) & \text{if } m > 1, \\ Q(0, a_2 - 2) & \text{if } m = 1. \end{cases}$$

Here, if $a_2 = 1$ and m > 1 (resp. $a_2 = 2$ and m = 1, $a_2 = 1$ and m = 1), we understand that $Q_{\alpha}^{S} = Q(a_3, \dots, a_{2m-1}, a_{2m} - 1)$ (resp. $Q_{\alpha}^{S} = Q(0)$, $Q_{\alpha}^{S} = \emptyset$). The quiver Q_{α}^{S} is obtained by deleting the first a_1 arrows from Q_{α}^{R} .

Remark 2.9. If $\alpha \notin \mathbb{Z}$ and $\alpha > 1$, the above construction of $Q_{\alpha}^{\mathcal{R}}$ and $Q_{\alpha}^{\mathcal{S}}$ also works for the expression as a regular continued fraction of *odd* length.

Following the notation used in [MO20], we will use the symbols $\rho_{\ell}(\alpha)$ and $\sigma_{\ell}(\alpha)$ to denote the numbers of ℓ -closures of $Q_{\alpha}^{\mathcal{R}}$ and $Q_{\alpha}^{\mathcal{S}}$, respectively.

Theorem 2.10 ([MO20, Theorem 4]). Let $\alpha > 1$ be an irreducible fraction. Then, the following equations hold:

$$\mathcal{R}_{\alpha}(q) = \sum_{\ell>0} \rho_{\ell}(\alpha) q^{\ell} \left(= \operatorname{cl}(Q_{\alpha}^{\mathcal{R}}) \right), \tag{2.16}$$

$$S_{\alpha}(q) = \sum_{\ell > 0} \sigma_{\ell}(\alpha) q^{\ell} \left(= \operatorname{cl}(Q_{\alpha}^{\mathcal{S}}) \right). \tag{2.17}$$

2.4 Farey neighbors and Farey sums

In this subsection, we recall the definitions of Farey neighbors and Farey sums.

Two irreducible fractions $\frac{x}{a}$, $\frac{y}{b}$ are said to be *Farey neighbors* if ay - bx = 1. Here we regard $\infty = \frac{1}{a}$ as an irreducible fraction.

For two irreducible fractions $\frac{x}{a}$, $\frac{y}{b}$, the operation \sharp is defined as follows:

$$\frac{x}{a}\sharp \frac{y}{b} := \frac{x+y}{a+b}.$$

If $\frac{x}{a}$, $\frac{y}{b}$ are Farey neighbors, then $\frac{x}{a} \sharp \frac{y}{b}$ is called the *Farey sum* of $\frac{x}{a}$ and $\frac{y}{b}$. The Farey sum of two irreducible fractions is also irreducible. Farey neighbors have the following fundamental properties.

Lemma 2.11. *The following assertions hold.*

- (1) Any non-negative rational number can be obtained from $\frac{0}{1}$ and $\frac{1}{0}$ applying \sharp in finitely many times.
- (2) For any positive rational number $\alpha \in (0, \infty)$, there uniquely exist Farey neighbors $\frac{x}{a}, \frac{y}{b}$ such that $\alpha = \frac{x}{a} \sharp \frac{y}{b}$. The pair $(\frac{x}{a}, \frac{y}{b})$ is called the Farey parent of α , and the fraction $\frac{x}{a}$ (resp. $\frac{y}{b}$) is called the left parent (resp. the right parent).

For proof of the above lemma, see [A13, Theorem 3.9] or [KW19(b), Lemma 3.5].

Let α and β be two fractions with $\alpha, \beta \geq 1$. If $\alpha \sharp \beta = [[c_1, ..., c_l]]$, then the equation

$$[\alpha \sharp \beta]_q = \frac{\mathcal{R}_{\alpha}(q) + q^{c_l - 1} \mathcal{R}_{\beta}(q)}{\mathcal{S}_{\alpha}(q) + q^{c_l - 1} \mathcal{S}_{\beta}(q)}$$
(2.18)

holds, see [MO20, Theorem 3].

3 A proof of the sufficiency of the conjecture

In this section, without the assumption that p is a prime number, we will show that $ab \equiv -1 \pmod{p}$ implies $\mathcal{S}_{\frac{a}{p}}(q) = \mathcal{S}_{\frac{b}{p}}(q)$, that is, the sufficiency part of Conjecture 1.2 holds. Recall that $\mathcal{S}_{\alpha+n}(q) = \mathcal{S}_{\alpha}(q)$ for all $\alpha \in \mathbb{Q}$ and $n \in \mathbb{Z}$.

In the rest of the paper, p means a (not necessarily prime) integer with $p \ge 2$, unless otherwise specified.

Lemma 3.1. Let $\frac{a}{p}$, $\frac{b}{p}$ be irreducible fractions with $a \equiv -b \pmod{p}$. We may assume that $\frac{a}{p} - \left\lfloor \frac{a}{p} \right\rfloor \leq \frac{1}{2}$, and hence $\frac{a}{p} = [a_1, a_2, \dots, a_k]$ with $a_2 \geq 2$ as a regular continued fraction. Then we have $\frac{b}{p} = [b_1, 1, a_2 - 1, a_3, \dots, a_k]$, where $b_1 = \left\lfloor \frac{b}{p} \right\rfloor$.

Proof. Since the assertion only depends on the decimal parts of $\frac{a}{p}$ and $\frac{b}{p}$, we may assume that $0 < \frac{a}{p} \le \frac{b}{p} < 1$. Then we have b = p - a,

$$\frac{a}{p} = \frac{1}{p} = \frac{1}{\frac{p}{a}} = \frac{1}{\frac{p-aa_2}{a}}$$

and

$$\frac{b}{p} = \frac{p-a}{p} = \frac{1}{\frac{p}{p-a}} = \frac{1}{1 + \frac{a}{p-a}} = \frac{1}{1 + \frac{1}{\frac{p-a}{a}}} = \frac{1}{1 + \frac{1}{\frac{p-a}{a}}}.$$

If k > 2, we have $\frac{p - aa_2}{a} = [a_3, a_4, ..., a_k]$, and the assertion follows.

Proposition 3.2. Let $\frac{a}{p}$, $\frac{b}{p}$ be irreducible fractions with $a \equiv -b \pmod{p}$. Then we have $\mathcal{S}_{\frac{a}{p}}(q) = \mathcal{S}_{\frac{b}{p}}^{\vee}(q)$.

Proof. We may assume that $1 < \frac{a}{p}, \frac{b}{p} < 2$, and $\frac{a}{p} = [1, a_2, \dots, a_k]$ with $a_2 \ge 2$. Then we have $\frac{b}{p} = [1, 1, a_2 - 1, a_3, \dots, a_k]$ by Lemma 3.1. With the notation of the previous section, we have

$$Q_{\frac{a}{p}}^{s} = Q(0, a_2 - 1, a_3, \dots, a_k - 1)$$
 and $Q_{\frac{b}{p}}^{s} = Q(a_2 - 1, a_3, \dots, a_k - 1)$

(by Remark 2.9, we do not have to care about the parity of the length of the regular continued fraction). Hence we have $Q_{\frac{b}{a}}^{s} = (Q_{\frac{a}{n}}^{s})^{\vee}$ by (2.15), and

$$\mathcal{S}_{\frac{b}{p}}(q) = \operatorname{cl}(Q_{\frac{b}{p}}^{\mathcal{S}}) = \operatorname{cl}((Q_{\frac{a}{p}}^{\mathcal{S}})^{\vee}) = \operatorname{cl}(Q_{\frac{a}{p}}^{\mathcal{S}})^{\vee} = \mathcal{S}_{\frac{a}{p}}^{\vee}(q)$$

by Theorem 2.10 and (2.15).

The following lemma is a variant of "Palindrome Theorem" (for example, see [KL02, Theorem 4]) for continued fractions. We will give a direct proof here for the reader's convenience.

Lemma 3.3. Let $\frac{a}{p}$, $\frac{b}{p}$ be irreducible fractions with $\frac{a}{p} = [a_1, a_2, a_3, ..., a_n]$ as a regular continued fraction. Set $b_1 := \left\lfloor \frac{b}{p} \right\rfloor$. Then $\frac{b}{p} = [b_1, a_n, a_{n-1}, ..., a_2]$ if and only if $ab \equiv (-1)^n \pmod{p}$.

Proof. Clearly, it suffices to show the case $a_1 = b_1 = 0$. First, assume that $\frac{b}{p} = [0, a_n, \dots, a_2]$. By Lemma 2.1, we have

$$\begin{pmatrix} a & k \\ p & l \end{pmatrix} = \begin{pmatrix} 0 & 1 \\ 1 & 0 \end{pmatrix} \begin{pmatrix} a_2 & 1 \\ 1 & 0 \end{pmatrix} \cdots \begin{pmatrix} a_n & 1 \\ 1 & 0 \end{pmatrix}$$

for some $k, l \in \mathbb{Z}$. Hence we have

$$\begin{pmatrix} p & l \\ a & k \end{pmatrix} = \begin{pmatrix} a_2 & 1 \\ 1 & 0 \end{pmatrix} \begin{pmatrix} a_3 & 1 \\ 1 & 0 \end{pmatrix} \cdots \begin{pmatrix} a_n & 1 \\ 1 & 0 \end{pmatrix}.$$

Taking the transpose of both sides, we get

$$\begin{pmatrix} p & a \\ l & k \end{pmatrix} = \begin{pmatrix} a_n & 1 \\ 1 & 0 \end{pmatrix} \begin{pmatrix} a_{n-1} & 1 \\ 1 & 0 \end{pmatrix} \cdots \begin{pmatrix} a_2 & 1 \\ 1 & 0 \end{pmatrix}.$$

Hence we have

$$\begin{pmatrix} l & k \\ p & a \end{pmatrix} = \begin{pmatrix} 0 & 1 \\ 1 & 0 \end{pmatrix} \begin{pmatrix} a_n & 1 \\ 1 & 0 \end{pmatrix} \cdots \begin{pmatrix} a_2 & 1 \\ 1 & 0 \end{pmatrix},$$
 (3.1)

and it implies that $\frac{l}{p} = [0, a_n, ..., a_2] = \frac{b}{p}$, and hence l = b. The determinant of the right side of (3.1) is $(-1)^n$, so that of the left side is also. It implies that $ab - pk = (-1)^n$, and hence $ab \equiv (-1)^n \pmod{p}$.

The converse implication follows from the above observation and the uniqueness of the solution of $\overline{a} \cdot x = \pm \overline{1}$ in $\mathbb{Z}/p\mathbb{Z}$.

Proposition 3.4. Let $\frac{a}{p}$, $\frac{b}{p}$ be irreducible fractions with $ab \equiv 1 \pmod{p}$. Then we have $\mathcal{S}_{\frac{a}{p}}(q) = \mathcal{S}_{\frac{b}{p}}^{\vee}(q)$.

Proof. We may assume that $1 < \frac{a}{p}, \frac{b}{p} < 2$. If $\frac{a}{p} = [1, a_2, \dots, a_{2m}]$, then $\frac{b}{p} = [1, a_{2m}, \dots, a_2]$ by Lemma 3.3. Hence we have

$$Q_{\frac{b}{p}}^{\mathcal{S}} = Q(a_{2m}-1, a_{2m-1}, \dots, a_2-1)^{\vee} \simeq Q(a_2-1, a_3, \dots, a_{2m}-1) = (Q_{\frac{a}{p}}^{\mathcal{S}})^{\vee}$$

by Lemma 2.8. So the assertion follows from Theorem 2.10 and (2.15).

The following implies the sufficiency of Conjecture 1.2.

Theorem 3.5. Let p be a positive integer. For irreducible fractions $\frac{a}{p}$, $\frac{b}{p}$ with $ab \equiv -1 \pmod{p}$, we have $\mathcal{S}_{\frac{a}{p}}(q) = \mathcal{S}_{\frac{b}{p}}(q)$.

Proof. The assertion follows from Propositions 3.2, 3.4 and the fact that $f^{\vee\vee}(q) = f(q)$ for general $f(q) \in \mathbb{Z}[q]$.

We note that, for the numerator $\mathcal{R}_{\frac{r}{s}}(q)$ for $\frac{r}{s} > 1$, a similar result holds. See Lemma 4.1 below.

Regarding $Q_{\alpha}^{\mathcal{S}}$ as a finite poset, Kantarcı Oğuz and Ravichandran [KR23] intensely studied $\mathcal{S}_{\alpha}(q)$ from a purely combinatorial point of view. Among other things, they showed that $\mathcal{S}_{\alpha}(q)$ is always unimodal. Here we apply another result of their. A polynomial f(q) is said to be *palindromic* if $f^{\vee}(q) = f(q)$.

Theorem 3.6. For an irreducible fraction $\frac{r}{s}$, $\mathcal{S}_{\frac{r}{s}}(q)$ is palindromic if and only if $r^2 \equiv 1 \pmod{s}$.

Proof. Let $\mathbf{b} = (b_1, \dots, b_k)$ be an integer sequence such that $b_1, b_k \ge 0, b_2, \dots, b_{k-1} > 0$ and k is odd. [KR23, Theorem 1.3 (c)], which was first conjectured in [MSS21], states that $\operatorname{cl}(Q(\mathbf{b}))$ is palindromic if and only if $b_i = b_{k+1-i}$ for all $1 \le i \le k$.

Set $\frac{r}{s}=[a_1,\ldots,a_{2m}]$. By the above mentioned result, the q-polynomial $\mathcal{S}_{\frac{r}{s}}(q)=\text{cl}(Q(a_2-1,a_3,\ldots,a_{2m}-1)^{\vee})$ is palindromic if and only if

$$a_i = a_{2m+2-i}$$
 for all $2 \le i \le 2m$. (3.2)

By Lemma 3.3, the condition (3.2) holds if and only if $a^2 \equiv 1 \pmod{p}$.

Corollary 3.7. *The following hold.*

- (1) For an irreducible fraction $\frac{a}{p^n}$ such that p is an odd prime, $\mathcal{S}_{\frac{a}{p^n}}(q)$ is palindromic, if and only if $a \equiv \pm 1 \pmod{p^n}$, if and only if $\mathcal{S}_{\frac{a}{p^n}}(q) = [p^n]_q = 1 + q + \dots + q^{p^n-1}$.
- (2) For $n \ge 2$, $\mathcal{S}_{\frac{a}{2^n}}(q)$ is palindromic if and only if $a \equiv \pm 1 \pmod{2^n}$ or $a \equiv 2^{n-1} \pm 1 \pmod{2^n}$.

Proof. (1) The latter equivalence is clear, so we prove the former. By Theorem 3.6, it is sufficient to show that $a^2 \equiv 1 \pmod{p^n}$ implies $a \equiv \pm 1 \pmod{p^n}$. If $a^2 \equiv 1 \pmod{p^n}$, then p^n divides (a+1)(a-1). Since p is an odd prime, p does only divide one of a+1 and a-1. In fact, if p divides both a+1 and a-1, then p divides 2, which is a contradiction. This means that all p copies of p that appear in the prime decomposition of p0 must come from either p1 or p2. Thus, p3 divides either p3 or p4 and p5 divides either p6 divides either p8 divides either p9.

(2) Since 4 cannot divide both a+1 and a-1 at the same time, an argument similar to the above works.

Combining the above results with Chinese remainder theorem, for a general s, we can easily detect all r such that $\mathcal{S}_{\frac{r}{s}}$ is palindromic (equivalently, $r^2 \equiv 1 \pmod{s}$).

Corollary 3.8. For an irreducible fraction $\frac{r}{s} > 1$, $\mathcal{R}_{\frac{r}{s}}(q)$ is palindromic if and only if $s^2 \equiv 1 \pmod{r}$.

Proof. By (2.10), we have $\mathcal{R}_{\frac{r}{s}}(q) = \mathcal{S}_{\frac{r-s}{r}}(q)$. Hence we have

$$\mathcal{R}_{\frac{r}{s}}(q)$$
 is palindromic $\iff \mathcal{S}_{\frac{r-s}{r}}(q)$ is palindromic $\iff (r-s)^2 \equiv 1 \pmod{r}$ $\iff s^2 \equiv 1 \pmod{r}$,

where the second equivalence follows from Corollary 3.6.

4 Another proof of the sufficiency of the conjecture

In [W22], the fourth author introduced the q-deformed integers derived from pairs of positive and coprime integers. In this section, by using them we give the second proof of the sufficiency of Conjecture 1.2. To do this we need the following interpretation of the conjecture.

Lemma 4.1. *Conjecture 1.2 is equivalent to the following statement.*

(*) Let p be an odd prime integer. For two integers a, b with $1 \le a < b < p$, $\mathcal{R}_{\frac{p}{a}}(q) = \mathcal{R}_{\frac{p}{b}}(q)$ if and only if $ab \equiv -1 \pmod{p}$.

Proof. This follows from Lemmas 2.4 and 2.6.

Definition 4.2 ([W22, Definition 4.3]). For a pair (a,b) of positive and coprime integers we define a polynomial $(a,b)_q$ in q with integer coefficients by

$$(a,b)_{q} := \begin{cases} (a-r,r)_{q} + q(a,b-a)_{q} & \text{if } a < b, \\ (a-b,b)_{q} + q^{\left\lceil \frac{a}{b} \right\rceil}(r,b-r)_{q} & \text{if } a > b, \end{cases}$$

$$(4.1)$$

where r is the remainder when b is divided by a in case where a < b, and when a is divided by b in case where a > b, and also $(1, n)_q = (n, 1)_q := [1 + n]_q$ for any non-negative integer n.

The polynomial $(a, b)_q$ is convenient to compute $[\alpha \sharp \beta]_q$.

Theorem 4.3 ([W22, Theorem 4.4]). If $\alpha = \frac{x}{a}$, $\beta = \frac{y}{b} \ge 1$ are Farey neighbors, then

$$S_{\alpha \sharp \beta}(q) = (a, b)_{q}, \quad \mathcal{R}_{\alpha \sharp \beta}(q) = (x, y)_{q}.$$

Thus, we have

$$[\alpha \sharp \beta]_q = \frac{(x,y)_q}{(a,b)_q}.$$

Any rational number $\alpha > 0$ is associated with a link $L(\alpha)$ in the 3-sphere \mathbb{S}^3 which is given by the diagram $D(\alpha)$ below, and such a link is called a *rational link* or *two-bridge link*. If α belongs to the open interval (0,1), then the diagram $D(\alpha)$ is given as in Figure 1 after the expression of $\alpha = [0, a_1, \dots, a_n]$ with odd n.

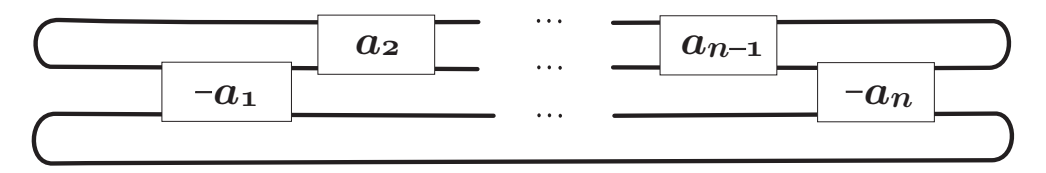


Figure 1: the diagram $D(\alpha)$ of rational link

where

If $\alpha > 1$, then $D(\alpha)$ is defined by $D(\alpha) := D(\alpha^{-1})$, and if $\alpha = 1$, then $D(\alpha) = \square$. For a negative rational number α , a rational link $L(\alpha)$ and its diagram $D(\alpha)$ are defined in the same way as the positive case. Then we see that the link $L(\alpha)$ is the mirror image of $L(-\alpha)$. However, for any $\alpha \in \mathbb{Q}$, there is some $\beta \in \mathbb{Q} \cap (1, \infty)$ such that $L(\alpha)$ and $L(\beta)$ are isotopic. See, for example, [KL02, Theorem 2]. In this sense, we may assume that $\alpha > 1$.

As a useful isotopy invariant for an oriented link L in \mathbb{S}^3 , the Jones polynomial $V_L(t)$ [J85, Kau87], which is valued in $\mathbb{Z}[t^{\pm \frac{1}{2}}]$, is well-studied. Lee and Schiffler [LS19] introduced

the following normalization $J_{\alpha}(q)$ of the Jones polynomial $V_{\alpha}(t) := V_{L(\alpha)}(t)$ of a rational link $L(\alpha)$:

$$J_{\alpha}(q) := \pm t^{-h} V_{\alpha}(t)|_{t=-q^{-1}}, \tag{4.2}$$

where $\pm t^h$ is the leading term of $V_{\alpha}(t)$. This indicates the normalization such that the constant term is 1 as a polynomial in q. We note that

$$J_1(q) = 1, \quad J_{\frac{1}{0}}(q) = q.$$

By Lee and Schiffler [LS19], it is known that the Jones polynomial $V_{\alpha}(t)$ can be recovered from $J_{\alpha}(q)$. By [MO20, Proposition A.1] and the equation (2.18), we see that, for a rational number $\alpha > 1$, the normalized Jones polynomial $J_{\alpha}(q)$ can be computed by

$$J_{\alpha}(q) = q\mathcal{R}_{\alpha}(q) + (1 - q)\mathcal{S}_{\alpha}(q). \tag{4.3}$$

Using this formula, the fourth author showed the following.

Theorem 4.4 ([W22, Theorem 5.3]). Let (a, p) be a pair of coprime integers with $1 \le a < p$. Then

$$(a, p)_q = J_{\frac{p}{a}}(q) + q(a - r, r)_q, \tag{4.4}$$

where r is the remainder when p is divided by a.

The equation (4.4) corresponds to the equation $J_{\frac{r}{s}}(q) = \mathcal{R}' - q\mathcal{S}'$ in [MO20, p.45] under the setting $\frac{r}{s} = \frac{p}{a}$. In fact, since $\mathcal{S}' = \mathcal{S}_{\frac{p}{a}}(q)$ and $\mathcal{R}' = q\mathcal{R}_{\frac{p}{a}}(q) + \mathcal{S}_{\frac{p}{a}}(q)$ as shown in [MO20, p.45], we have $\mathcal{S}' = (a-r,r)_q$ by (4.6) below and $\mathcal{R}' = q(a,p-a)_q + (a-r,r)_q = (a,p)_q$ by (4.1) and (4.5) below.

As an application of Theorem 4.4 we have:

Theorem 4.5 ([W22, Theorem 5.4]). Let (a, p) be a pair of coprime integers with $1 \le a \le p$, and r the remainder when p is divided by a. Then, the following equations hold.

$$\mathcal{R}_{\frac{p}{a}}(q) = (a, p - a)_q,\tag{4.5}$$

$$\mathcal{S}_{\frac{p}{a}}(q) = (a - r, r)_q. \tag{4.6}$$

By using the above theorem, one can give another proof of Theorem 3.5, that is, the sufficiency of Conjecture 1.2.

Another proof of Theorem 3.5. Since $ab \equiv -1 \pmod{p}$, there is some $m \in \mathbb{Z}$ with mp-ab = 1. Since $1 \le a \le b < p$, we have $0 \le m < a$. Thus, $\left(\frac{a}{m}, \frac{p-a}{b-m}\right)$ is the Farey parents of $\frac{p}{b}$. By using Theorem 4.3, we have

$$\mathcal{R}_{\frac{p}{b}}(q) = (a, p - a)_q.$$

(See also the proof of [KW22, Theorem 3.2].) Combining this equation with (4.5), we get $\mathcal{R}_{\frac{p}{a}}(q) = \mathcal{R}_{\frac{p}{b}}(q)$.

Remark 4.6. By Corollary 3.8 and (4.5), $(a,b)_q$ is palindromic if and only if $a^2 \equiv 1 \pmod{a+b}$. Combining this observation with Theorem 4.3, one can show the following. For a positive irreducible fractions $\frac{c}{z}$ whose Farey parent is $(\frac{a}{x},\frac{b}{y})$, $\mathcal{S}_{\frac{c}{z}}(q)$ is palindromic, if and only of $x^2 \equiv 1 \pmod{x+y}$ (equivalently, $y^2 \equiv 1 \pmod{x+y}$).

5 Three operations on the positive rational numbers and qdeformed rational numbers

In the study of Conway-Coxeter friezes of zigzag-type developed by the first and the fourth authors [KW19(b), KW19(a)] crucial three operators $\mathfrak{i},\mathfrak{r},\mathfrak{i}\mathfrak{r}$ on the positive rational numbers are introduced. In this section we examine effect of the operators $\mathfrak{i},\mathfrak{r},\mathfrak{i}\mathfrak{r}$ on $\mathcal{R}_{\alpha}(q),\mathcal{S}_{\alpha}(q)$.

Let $\alpha = \frac{z}{c} > 0$ be an irreducible fraction. In the case where $\alpha \in (0,1)$, irreducible fractions $i(\alpha)$, $r(\alpha)$, $(ir)(\alpha)$ in the interval (0,1) are defined as follows [KW19(a)]:

$$i(\alpha) := \frac{c-z}{c} (= 1 - \alpha), \quad r(\alpha) := \frac{a}{c}, \quad ir(\alpha) := \frac{b}{c}, \tag{5.1}$$

where $(\frac{x}{a}, \frac{y}{b})$ is the Farey parent of α . Note that

$$az \equiv 1 \pmod{c}$$
 and $b \equiv -a \pmod{c}$. (5.2)

In fact, since z = x + y, c = a + b and ay - bx = 1 now, we have

$$az = a(x + y) = ax + ay = ax + 1 + bx = 1 + (a + b)x = 1 + cx.$$

Hence as operations on $\mathbb{Q} \cap (0,1)$, we have $\mathfrak{i}^2 = \mathfrak{r}^2 = \mathrm{id}$ and $\mathrm{i}\mathfrak{r} = \mathfrak{r}\mathfrak{i}$. By Theorem 3.6, for $\alpha \in \mathbb{Q} \cap (0,1)$, $\mathfrak{r}(\alpha) = \alpha$ if and only if $\mathcal{S}_{\alpha}(q)$ is palindromic.

In the case where $\alpha > 1$, $\mathfrak{i}(\alpha)$, $\mathfrak{r}(\alpha)$, and $\mathfrak{ir}(\alpha)$ are defined as follows:

$$\mathbf{i}(\alpha) := \left(\mathbf{i}(\alpha^{-1})\right)^{-1}, \qquad \mathbf{r}(\alpha) := \left(\mathbf{r}(\alpha^{-1})\right)^{-1}, \qquad (\mathbf{i}\mathbf{r})(\alpha) := \left((\mathbf{i}\mathbf{r})(\alpha^{-1})\right)^{-1}. \tag{5.3}$$

Here we also have $\mathfrak{i}^2 = \mathfrak{r}^2 = \mathrm{id}$ and $\mathfrak{i}\mathfrak{r} = \mathfrak{r}\mathfrak{i}$. Moreover, $\mathfrak{r}(\alpha) = \alpha$ if and only if $\mathcal{R}_{\alpha}(q)$ is palindromic.

By Lemmas 3.1 and 3.3, and the equation (5.2), one can show that for a positive rational number $\alpha = [0, a_2, ..., a_n],$

$$(i\mathfrak{r})(\alpha) = \begin{cases} [0, a_n, \dots, a_3, a_2] & \text{if } n \text{ is odd,} \\ [0, 1, a_n - 1, a_{n-1}, \dots, a_3, a_2] & \text{if } n \text{ is even and } a_n \ge 2, \\ [0, a_{n-1} + 1, a_{n-2}, \dots, a_3, a_2] & \text{if } n \text{ is even and } a_n = 1, \end{cases}$$

$$i(\alpha) = \begin{cases} [0, 1, a_2 - 1, a_3, \dots, a_n] & \text{if } a_2 \ge 2, \\ [0, a_3 + 1, a_4, \dots, a_n] & \text{if } a_2 = 1, \end{cases}$$

$$r(\alpha) = \begin{cases} [0, 1, a_n - 1, a_{n-1}, \dots, a_3, a_2] & \text{if } n \text{ is odd and } a_n \ge 2, \\ [0, a_{n-1} + 1, a_{n-2}, \dots, a_3, a_2] & \text{if } n \text{ is odd and } a_n = 1, \\ [0, a_n, \dots, a_3, a_2] & \text{if } n \text{ is even.} \end{cases}$$

$$(5.6)$$

$$\mathbf{i}(\alpha) = \begin{cases} [0, 1, a_2 - 1, a_3, \dots, a_n] & \text{if } a_2 \ge 2, \\ [0, a_3 + 1, a_4, \dots, a_n] & \text{if } a_2 = 1, \end{cases}$$
(5.5)

$$\mathbf{r}(\alpha) = \begin{cases} [0, 1, a_n - 1, a_{n-1}, \dots, a_3, a_2] & \text{if } n \text{ is odd and } a_n \ge 2, \\ [0, a_{n-1} + 1, a_{n-2}, \dots, a_3, a_2] & \text{if } n \text{ is odd and } a_n = 1, \\ [0, a_n, \dots, a_3, a_2] & \text{if } n \text{ is even.} \end{cases}$$
 (5.6)

Lemma 5.1. Let $\alpha \in \mathbb{Q} \cap (0, \infty)$ whose expression as a regular continued fraction is $\alpha =$

 $[a_1, a_2, ..., a_n]$. If n is odd, then

$$\beta = \begin{cases} [a_1, \dots, a_{n-1}, a_n - 1] & \text{if } a_n \ge 2, \\ [a_1, \dots, a_{n-2}] & \text{if } a_n = 1 \text{ and } n \ge 3, \\ [0] & \text{if } a_1 = 1 \text{ and } n = 1, \end{cases}$$

$$\gamma = \begin{cases} [a_1, \dots, a_{n-1}] & \text{if } n \ge 3, \\ [& \text{if } n = 1 \end{cases}$$

are Farey neighbors and $\alpha = \beta \sharp \gamma$, where [] expresses $\infty = \frac{1}{0}$. If n is even, then

$$\beta = [a_1, \dots, a_{n-1}]$$

$$\gamma = \begin{cases} [a_1, \dots, a_{n-1}, a_n - 1] & \text{if } a_n \ge 2, \\ [a_1, \dots, a_{n-2}] & \text{if } a_n = 1 \text{ and } n \ge 4, \\ [& \text{if } a_2 = 1 \text{ and } n = 2 \end{cases}$$

are Farey neighbors and $\alpha = \beta \sharp \gamma$.

Proof. Note that, as a regular continued fraction, each rational number has expressions in both odd and even lengths. It is easy to check that two definitions (the odd case and the even case) coincide.

We will prove the equation $\alpha = \beta \sharp \gamma$ by induction on n. The cases n = 0 and n = 1 are clear. Now, we suppose that the statement holds for n - 1. We only show the case $n \geq 3$ is odd and $a_n \geq 2$; the proofs in other cases are similar. Not that we have $\beta = [a_1, \ldots, a_{n-1}, a_n - 1]$ and $\gamma = [a_1, \ldots, a_{n-1}]$ now. Set $[a_2, \ldots, a_{n-1}] = \frac{r}{s}$, $[a_2, \ldots, a_{n-1}, a_n - 1] = \frac{r'}{s'}$.

By induction hypothesis, $(\frac{r}{s}, \frac{r'}{s'})$ is the Farey parents of $\frac{r+r'}{s+s'} = [a_2, a_3, ..., a_n]$. Since $\beta = \frac{r'a_1+s'}{r'}$, $\gamma = \frac{ra_1+s}{r}$ and sr'-rs'=1, β and γ are Farey neighbors. Moreover, it follows from induction hypothesis that we have

$$\beta \sharp \gamma = \frac{a_1(r+r')+s+s'}{r+r'} = a_1 + \frac{1}{\frac{r+r'}{s+s'}} = a_1 + \frac{1}{[a_2, \dots, a_n]} = [a_1, a_2, \dots, a_n] = \alpha.$$

For a quiver Q of type A, let denote by Q^{rot} the quiver obtained from Q by π -rotation. Since $Q \simeq Q^{\text{rot}}$ as quivers, their closure polynomials are same;

$$cl(Q) = cl(Q^{rot}). (5.7)$$

For $\alpha \in \mathbb{Q} \cap (1, \infty)$, the equations (5.4), (5.5) and (5.6) imply that

$$Q_{\mathbf{i}(\alpha)}^{\mathcal{R}} = (Q_{\alpha}^{\mathcal{R}})^{\vee},\tag{5.8}$$

$$Q_{(ir)(\alpha)}^{\mathcal{R}} = (Q_{\alpha}^{\mathcal{R}})^{\text{rot}},\tag{5.9}$$

$$Q_{\mathbf{r}(\alpha)}^{\mathcal{R}} = (Q_{\alpha}^{\mathcal{R}})^{\mathsf{rot}\vee} = (Q_{\alpha}^{\mathcal{R}})^{\mathsf{vrot}}.$$
 (5.10)

Except for the denominator of $\mathfrak{i}(\alpha)$, the denominator and numerator polynomials of q-deformations of $\mathfrak{i}(\alpha)$, $\mathfrak{r}(\alpha)$, $(\mathfrak{i}\mathfrak{r})(\alpha)$ are computed from that of α and its Farey parent as follows.

Theorem 5.2. Let $\alpha \in \mathbb{Q} \cap (1, \infty)$ and (β, γ) be its parents. Then, the following hold.

(1)
$$\mathcal{R}_{i(\alpha)}(q) = \mathcal{R}_{r(\alpha)}(q) = \mathcal{R}_{\alpha}^{\vee}(q)$$
 and $\mathcal{R}_{(ir)(\alpha)}(q) = \mathcal{R}_{\alpha}(q)$.

(2)
$$S_{(i\mathfrak{r})(\alpha)}(q) = \mathcal{R}_{\beta}(q)$$
, and $S_{\mathfrak{r}(\alpha)}(q) = \mathcal{R}^{\vee}_{\gamma}(q)$.

Proof. (1) By the equations (2.14) and (5.7), these follow from (5.8), (5.9), and (5.10).

(2) We write α as $\alpha = [a_1, a_2, ..., a_{2m}]$. Then, it follows from Lemma 5.1 that $\beta = [a_1, ..., a_{2m-1}]$. Since $\alpha^{-1} = [0, a_1, ..., a_{2m}] \in \mathbb{Q} \cap (0, 1)$, we have $(i\mathfrak{r})(\alpha^{-1}) = [0, a_{2m}, ..., a_1]$ by (5.4). Thus, $(i\mathfrak{r})(\alpha) = [a_{2m}, ..., a_1]$. Hence, Theorem 2.10 and (5.7) imply that

$$\begin{split} \mathcal{S}_{(\mathrm{ir})(\alpha)}(q) &= \mathrm{cl}(Q(0, a_{2m-1}-1, a_{2m-2}, \dots, a_2, a_1-1)) \\ &= \mathrm{cl}(Q(0, a_{2m-1}-1, a_{2m-2}, \dots, a_2, a_1-1)^{\mathrm{rot}}) \\ &= \mathrm{cl}(Q(a_1-1, a_2, \dots, a_{2m-2}, a_{2m-1}-1)) \\ &= \mathcal{R}_{\beta}(q). \end{split}$$

Finally, we consider $S_{\mathfrak{r}(\alpha)}(q)$. Suppose that $a_{2m} > 1$. In this case, it follows from Lemma 5.1 that $\gamma = [a_1, \dots, a_{2m-1}, a_{2m} - 1]$. By (5.6), $\mathfrak{r}(\alpha) = [1, a_{2m} - 1, a_{2m-1}, \dots, a_1]$. Thus, we have

$$\begin{split} \mathcal{S}_{\mathbf{r}(\alpha)}(q) &= \mathrm{cl}(Q(a_{2m}-2,a_{2m-1},\ldots,a_2,a_1-1)^\vee) \\ &= \mathrm{cl}(Q(a_{2m}-2,a_{2m-1},\ldots,a_2,a_1-1))^\vee \\ &= \mathrm{cl}(Q(a_{2m}-2,a_{2m-1},\ldots,a_2,a_1-1)^\mathrm{rot})^\vee \\ &= \mathrm{cl}(Q(a_1-1,a_2,\ldots,a_{2m-1},a_{2m}-2))^\vee \\ &= \mathcal{R}_\gamma^\vee(q). \end{split}$$

In the case where $a_{2m} = 1$, by the same argument the same equation is derived.

For a rational number α with $0 < \alpha < 1$, the q-deformations of $\mathfrak{i}(\alpha)$, $\mathfrak{r}(\alpha)$ and $(\mathfrak{i}\mathfrak{r})(\alpha)$ behave as follows.

Proposition 5.3. For a rational number $\alpha \in \mathbb{Q} \cap (0,1)$, we have the followings.

(1)
$$S_{\mathfrak{r}(\alpha)}(q) = S_{\alpha}^{\vee}(q) = S_{\mathfrak{t}(\alpha)}(q) = \mathcal{R}_{\alpha^{-1}}(q)$$
.

(2)
$$\mathcal{R}_{\mathfrak{i}(\alpha)}(q) = \mathcal{R}_{\alpha^{-1}}(q) - \mathcal{S}_{\alpha^{-1}}(q)$$
, $\mathcal{R}_{r(\alpha)}(q) = \mathcal{R}_{\alpha^{-1}}(q) - \mathcal{R}_{\gamma^{-1}}(q)$, where (β, γ) is the parent of α .

Proof. (1) The first (resp. second) equality follows from (5.1), (5.2), and Proposition 3.4 (resp. Proposition 3.2). To see the third equality, express $i(\alpha) = \frac{a}{x}$ as an irreducible fraction. Then we have $\alpha = \frac{x-a}{x}$ and $\alpha^{-1} = \frac{x}{x-a}$. So the equality follows from (2.10).

(2) The first equation immediately follows from (2.9). Since $\mathfrak{i}(\mathfrak{i}\mathfrak{r}(\alpha)) = \mathfrak{r}(\alpha)$ and $(\mathfrak{i}\mathfrak{r}(\alpha))^{-1} = \mathfrak{i}\mathfrak{r}(\alpha^{-1})$, replacing α by $\mathfrak{i}\mathfrak{r}(\alpha)$, the first equation yields

$$\mathcal{R}_{\mathfrak{r}(\alpha)}(q) = \mathcal{R}_{(\mathfrak{i}\mathfrak{r})(\alpha^{-1})}(q) - \mathcal{S}_{(\mathfrak{i}\mathfrak{r})(\alpha^{-1})}(q).$$

Applying Theorem 5.2, we have $\mathcal{R}_{\mathfrak{r}(\alpha)}(q) = \mathcal{R}_{\alpha^{-1}}(q) - \mathcal{R}_{\gamma^{-1}}(q)$.

As an application of Proposition 3.2 we have:

Theorem 5.4. Let $\alpha \in \mathbb{Q} \cap (1, \infty)$, and express it as a regular continued fraction $\alpha = [a_1, a_2, ..., a_n]$.

(1) If $a_1 = 1$, then

$$\mathcal{S}_{\mathfrak{i}(\alpha)}(q) = \mathcal{S}^{\vee}_{\frac{(a_2+1)(\alpha-1)+\alpha-2}{\alpha-1}}(q).$$

(2) If $a_1 \ge 2$, then

$$\mathcal{S}_{\mathfrak{i}(\alpha)}(q) = \mathcal{S}^{\vee}_{\frac{a_1(\alpha-1)+\alpha-2}{\alpha-1}}(q).$$

Proof. Set $\alpha = \frac{x}{a}$ with $1 \le a < x$. Then, $\mathcal{S}_{\mathfrak{t}(\alpha)}(q) = \mathcal{S}_{\frac{x}{x-a}}(q)$, and hence by Proposition 3.2

$$\mathcal{S}_{\frac{x}{x-a}}(q) = \mathcal{S}_{\frac{x'}{x-a}}^{\vee}(q) \tag{5.11}$$

for $x' \in \mathbb{Z}$ such that $x' \equiv -x \pmod{x-a}$ and $\left\lfloor \frac{x}{x-a} \right\rfloor = \left\lfloor \frac{x'}{x-a} \right\rfloor$.

(1) Since $a_1 = 1$, we have $\frac{a}{x-a} = [a_2, ..., a_n]$, and $0 \le a - a_2(x-a) < x - a$. As x' one can take $x' := -x + (a_2 + 3)(x - a)$. Thus by (5.11) we have

$$\begin{split} \mathcal{S}_{\frac{x}{x-a}}(q) &= \mathcal{S}_{\frac{-x+(a_2+3)(x-a)}{x-a}}^{\vee}(q) \\ &= \mathcal{S}_{\frac{-\alpha+(a_2+3)(\alpha-1)}{\alpha-1}}^{\vee}(q) \\ &= \mathcal{S}_{\frac{(a_2+1)(\alpha-1)+\alpha-2}{\alpha-1}}^{\vee}(q). \end{split}$$

(2) Since $a_1 \ge 2$, we have $\frac{x}{a} - a_1 = [0, a_2, ..., a_n]$ and $0 \le x - aa_1 < a$. In this case one can take $x' := -x + (a_1 + 2)(x - a)$. Then, by the same argument of the proof of Part (1), the assertion is derived.

6 A formula for computing closure polynomials of type A

For an irreducible fraction $\alpha > 1$, the denominator and numerator polynomials of $[\alpha]_q$ are given by closure polynomials of some quivers of type A (see Theorem 2.10). On the other hand, from a representation theoretical viewpoint, the closure polynomial of a type A quiver Q counts subrepresentations of "the full interval representation" of Q in which a field k corresponds to each vertex and the identity map corresponds to each arrow. In this section, we give an expression to calculate $\operatorname{cl}(Q)$ that explicitly gives the

number of subrepresentations of the full interval representation.

Let Q be a quiver of type A, that is, the underlying graph of Q is $A_n = 1 - 2 - 3 - \cdots - n$. A representation of Q over a field k is a system $M = (M_a, \varphi_\alpha)_{a \in Q_0, \alpha \in Q_1}$ $(M = (M_a, \varphi_\alpha)$ for short) consisting of k-vector spaces M_a $(a \in Q_0)$, and k-linear maps $\varphi_\alpha: M_{s(\alpha)} \to M_{t(\alpha)}$ $(\alpha \in Q_1)$. The dimension of M is the sum of k-dimensions of M_a . A representation $M' = (M'_a, \varphi'_\alpha)$ is said to be a subrepresentation of M if M'_a is a subspace of M_a , and $\varphi'_\alpha = \varphi_\alpha|_{M'_a}$. For two representations $M = (M_a, \varphi_\alpha)$ and $N = (N_a, \psi_\alpha)$, a morphism of representations $f: M \to N$ is a family $f = (f_a)_{a \in Q_0}$ of k-linear maps $f_a: M_a \to N_a$ such that $\psi_\alpha f_{s(\alpha)} = f_{t(\alpha)} \varphi_\alpha$ for any arrow α .

The category of finite dimensional representations of Q is denoted by $\operatorname{rep}(Q)$. It is well-known that there is an k-linear equivalence between $\operatorname{rep}(Q)$ and the category of finitely generated kQ-modules, where kQ is the path algebra of Q. For a vertex $i \in Q_0$, we denote by S(i) the corresponding simple kQ-module. For a kQ-module M, we also denote by $\operatorname{rad}(M)$, $\operatorname{top}(M)$, and $\operatorname{soc}(M)$ the Jacobson radical, the top, and the socle of M, respectively. The *support* of M is the set of composition factors, which is denoted by $\operatorname{supp}(M)$. In this subsection, any objects of $\operatorname{rep}(Q)$ are freely regarded as objects of $\operatorname{mod} kQ$. For representations of quivers, see [ASS06, Chapters II and III] for more details.

By the Gabriel theorem (for example, see [ASS06, Chapter VII, Theorem 5.10]), there is one-to-one corresponding between indecomposable objects of $\operatorname{rep}(Q)$ and positive roots of A_n , that is, pairs (i,j) with $1 \le i \le j \le n$. In this correspondence, each pair (i,j) is assigned with the interval representation $\mathbb{I}[i,j] = (M_a, \varphi_\alpha)$, where

$$M_a = \begin{cases} \mathsf{k} & \text{if } i \le a \le j, \\ \{0\} & \text{otherwise,} \end{cases} \quad \varphi_\alpha = \begin{cases} 1 & \text{if } i \le s(\alpha) \text{ and } t(\alpha) \le j, \\ 0 & \text{otherwise.} \end{cases}$$

Following this notation, $\mathbb{I}[1, n]$ is called the *full interval representation* of Q. Then, it follows from the definition of the closure polynomial that the coefficient of q^{ℓ} of cl(Q) is equal to the number of ℓ -dimensional subrepresentations of $\mathbb{I}[1, n]$.

Throughout this section, we fix a type A quiver $Q = Q(\mathbf{a})$ for some tuple $\mathbf{a} = (a_1, a_2, \dots, a_s) \in \mathbb{Z}^s_{\geq 0}$, which has n vertices, and denote by $\mathbb{I}(\mathbf{a})$ the full representation of $Q(\mathbf{a})$. It is clear that $\rho_1(Q(\mathbf{a})) = \dim_k \operatorname{soc}(\mathbb{I}(\mathbf{a}))$, which equals to the number of sinks of $Q(\mathbf{a})$. Note that the Jordan-Hölder theorem implies that any coefficients of $\operatorname{cl}(Q(\mathbf{a}))$ are greater than or equal to 1. This yields that, for any irreducible fraction $\alpha > 1$, any coefficients of the polynomials $\mathcal{R}_{\alpha}(q)$ and $\mathcal{S}_{\alpha}(q)$ are greater than 1. We also remark that the top and the socle of $\mathbb{I}(\mathbf{a})$ are given by

$$\begin{aligned} \log(\mathbb{I}(\mathbf{a})) &= \bigoplus_{k \geq 1} S(1+a_1+a_2+\cdots+a_{2k-1}) \\ \operatorname{soc}(\mathbb{I}(\mathbf{a}))) &= \begin{cases} S(1) \oplus \bigoplus_{k \geq 1} S(1+a_1+a_2+\cdots+a_{2k}) & \text{if } a_1 \neq 0, \\ \bigoplus_{k \geq 1} S(1+a_1+a_2+\cdots+a_{2k}) & \text{if } a_1 = 0. \end{cases} \end{aligned}$$

Now, we choose $1 \le k_1 < k_2 < \dots < k_t$ and $1 \le \ell_1 < \ell_2 < \dots < \ell_{t'}$ to be

$$top(\mathbb{I}(\mathbf{a})) = S(k_1) \oplus \cdots \oplus S(k_t),$$
$$soc(\mathbb{I}(\mathbf{a})) = S(\ell_1) \oplus \cdots \oplus S(\ell_{t'}).$$

Here, we put

$$\mathcal{T}_{\mathbf{a}} := \{ (k_{i_1}, \dots, k_{i_s}) \in \mathbb{Z}^s \mid 1 \le i_1 < \dots < i_s \le t, \ s \in \mathbb{N} \}.$$

A subquiver of $Q(\mathbf{a})$ of the form

$$\underbrace{\circ \longrightarrow \circ \cdots \circ \longrightarrow \circ}_{p_1 \text{ arrows}} \underbrace{- \circ \cdots \circ \longleftarrow \circ}_{p_2 \text{ arrows}}$$

is called a (p_1, p_2) -valley. For a (p_1, p_2) -valley, we define a polynomial $val_q(p_1, p_2)$ by

$$val_{q}(p_{1}, p_{2}) := cl(Q(0, p_{1}, p_{2})).$$

Observe that the equation $val_q(p_1, p_2) = val_q(p_2, p_1)$ holds by (5.7) and this can be calculated through the following.

T. Kogiso, K. Miyamoto, X. Ren, M. Wakui, K. Yanagawa

Lemma 6.1. For a (p_1, p_2) -valley with $p_1 \ge p_2$, we have

$$\operatorname{val}_q(p_1,p_2) = 1 + \sum_{k=1}^{p_2+1} kq^k + (p_2+1) \sum_{k=p_2+2}^{p_1+1} q^k + \sum_{k=p_1+2}^{p_1+p_2+1} (p_1+p_2+2-k)q^k$$

Proof. This lemma follows from direct computation.

Now, we define a sequence of pairs of integers as follows:

(i) Compute
$$\mathbf{a} - \mathbf{1} := \begin{cases} (a_1 - 1, a_2 - 1, \dots, a_s - 1) & \text{if } a_1 \neq 0, \\ (a_2 - 1, a_3 - 1, \dots, a_s - 1) & \text{if } a_1 = 0. \end{cases}$$

(ii) We put

$$(b_1,b_2,\dots,b_{2m}) := \begin{cases} (0,{\bf a}-{\bf 1},0) & \text{if } a_1 \neq 0 \text{ and } s \text{ is even,} \\ \\ (0,{\bf a}-{\bf 1}) & \text{if } a_1 \neq 0 \text{ and } s \text{ is odd,} \\ \\ ({\bf a}-{\bf 1},0) & \text{if } a_1 = 0 \text{ and } s \text{ is even,} \\ \\ ({\bf a}-{\bf 1}) & \text{if } a_1 = 0 \text{ and } s \text{ is odd.} \end{cases}$$

(iii) We set $\mathcal{J}_{\mathbf{a}} := \{(b_1, b_2), (b_3, b_4), \dots, (b_{2m-1}, b_{2m})\}$

Proposition 6.2. The number of ℓ -dimensional subrepresentations of $rad(\mathbb{I}(\mathbf{a}))$ coincides with the coefficient of q^{ℓ} of

$$\mathsf{val}_q(b_1,b_2) \cdot \mathsf{val}_q(b_3,b_4) \cdots \mathsf{val}_q(b_{2m-1},b_{2m}).$$

Proof. We show the case that $a_1 > 0$ and s is even: the proof of other cases are similar. In this case, m = t + 1 and the quiver $Q(\mathbf{a})$ is of the form:

$$\underbrace{1 \leftarrow \circ \cdots \circ \leftarrow \circ}_{b_2 \text{ arrows}} \leftarrow k_1 \rightarrow \underbrace{\circ \rightarrow \circ \cdots \circ \rightarrow \circ}_{b_3 \text{ arrows}} \leftarrow b_4 \text{ arrows} \leftarrow k_2$$

$$\rightarrow \underbrace{\circ \rightarrow \circ \cdots \circ \rightarrow \circ}_{b_5 \text{ arrows}} \leftarrow \underbrace{\circ \rightarrow \circ \cdots \circ \leftarrow \circ}_{b_6 \text{ arrows}} \leftarrow k_3 \rightarrow \cdots \leftarrow k_t \rightarrow \underbrace{\circ \rightarrow \circ \cdots \circ \rightarrow n}_{b_{2m-1} \text{ arrows}}.$$

This yields that rad(I(a)) is decomposed as

$$rad(\mathbb{I}(\mathbf{a}))) = \mathbb{I}[1, k_1 - 1] \oplus \mathbb{I}[k_1 + 1, k_2 - 1] \oplus \cdots \oplus \mathbb{I}[k_t + 1, k_t - 1] \oplus \mathbb{I}[k_t + 1, n].$$

Thus, each subrepresentation $N \subset \operatorname{rad}(\mathbb{I}(\mathbf{a}))$ is the direct sum of subrepresentations $N_1 \subset \mathbb{I}[1,k_1-1]$, $N_i \subset \mathbb{I}[k_i+1,k_{i+1}-1]$ $(i=1,\ldots,t-1)$, and $N_t \subset \mathbb{I}[k_t+1,n]$. Since the numbers of subrepresentations of $\mathbb{I}[1,k_1-1]$, $\mathbb{I}[k_i+1,k_{i+1}-1]$ $(i=1,\ldots,t-1)$, and $\mathbb{I}[k_t+1,n]$ are equal to $\operatorname{val}_q(b_1,b_2)$, $\operatorname{val}_q(b_{2i+1},b_{2i+2})$ $(i=1,\ldots,t-1)$, and $\operatorname{val}_q(b_{2m-1},b_{2m})$, respectively, the assertion follows.

For each k_i (i = 1, ..., t), a polynomial $\Delta_q(k_i)$ is defined as follows.

(i) Suppose that $a_1 > 0$. In this case, we define $\Delta_q(k_i)$ by

$$\Delta_{q}(k_{i}) := \begin{cases} q^{\ell_{i+1} - \ell_{i} + 1} [\ell_{i} - k_{i-1}]_{q} [k_{i+1} - \ell_{i+1}]_{q} & \text{if } i \neq 1, t, \\ \\ q^{\ell_{2}} [k_{2} - \ell_{2}]_{q} & \text{if } i = 1, \\ \\ q^{n - \ell_{t} + 1} [\ell_{t} - k_{t-1}]_{q} & \text{if } i = t. \end{cases}$$

(ii) Suppose that $a_1=0$. In this case, we define $\Delta_q(k_i)$ by

$$\Delta_q(k_i) := \begin{cases} q^{\ell_i - \ell_{i-1} + 1} [\ell_{i-1} - k_{i-1}]_q [k_{i+1} - \ell_i]_q & \text{if } i \neq 1, t, \\ \\ q^{\ell_1} [k_2 - \ell_1]_q & \text{if } i = 1, \\ \\ q^{n - \ell_{l-1} + 1} [\ell_{l-1} - k_{l-1}]_q & \text{if } i = t. \end{cases}$$

For each k_i , take a subset

$$\{(v_{2j-1}^{(k_i)}, v_{2j}^{(k_i)}) \mid j = 1, 2, \dots, r_{k_i}\} \subset \mathcal{J}_{\mathbf{a}}$$

such that any $(v_{2j-1}^{(k_i)}, v_{2j}^{(k_i)})$ -valley is not adjacent to vertex k_i . Then, we set

$$\widetilde{\Delta}_q(k_i) := \Delta_q(k_i) \prod_{i=1}^{r_{k_i}} \mathsf{val}(\upsilon_{2j-1}^{(k_i)}, \upsilon_{2j}^{(k_i)}).$$

Lemma 6.3. The coefficient of q^{ℓ} of $\widetilde{\Delta}_q(k_i)$ coincides with the number of ℓ -dimensional subrepresentations N of $\mathbb{I}(\mathbf{a})$ such that $S(k_i) \in \text{supp}(N)$, but $S(k_j) \notin \text{supp}(N)$ for $i \neq j$.

Proof. We only show the statement when $a_1 > 0$ and s is even; the proofs in other cases are similar.

Let $N_{(k_i)}$ be the largest dimensional subrepresentation of $\mathbb{I}(\mathbf{a})$ such that $S(k_i) \in \operatorname{supp}(N)$, but $S(k_j) \notin \operatorname{supp}(N)$ for $i \neq j$. It is sufficient to show that the coefficient of q^ℓ of $\widetilde{\Delta}_q(k_i)$ coincides with the number of ℓ -dimensional subrepresentations of $N_{(k_i)}$. Observe that $\mathbb{I}[k_{i-1}+1,k_{i+1}-1] \subset N_{(k_i)}$ and every subrepresentation of $N_{(k_i)}$ must have $\mathbb{I}[\ell_i,\ell_{i+1}]$ as a subrepresentation whose dimension is $\ell_{i+1}-\ell_i+1$. Here, if k_{i-1} (resp. k_{i+1}) is not in $Q(\mathbf{a})_0$, then we replace $k_{i-1}+1$ by ℓ_1 (resp. $k_{i+1}-1$ by ℓ_{i+1}). Now, we consider an isomorphism

$$\mathbb{I}[k_{i-1}+1,k_{i+1}-1]/\mathbb{I}[\ell_i,\ell_{i+1}] \simeq \mathbb{I}[k_{i-1}+1,\ell_i-1] \oplus \mathbb{I}[\ell_{i+1}+1,k_{i+1}-1].$$

Since the number of ℓ -dimensional subrepresentations of $\mathbb{I}[k_{i-1}+1,\ell_i-1]$ (resp. $\mathbb{I}[\ell_{i+1}+1,k_{i+1}-1]$) corresponds to the coefficient of q^ℓ of $[\ell_i-k_{i-1}]_q$ (resp. $[k_{i+1}-\ell_{i+1}]_q$), the number of ℓ -dimensional subrepresentations N' of $\mathbb{I}[k_{i-1}+1,k_{i+1}-1]$ such that $S(k_i) \in \operatorname{supp}(N')$ is the coefficient of q^ℓ of $\Delta_q(k_i)$. Remaining subrepresentations that must be counted come from subrepresentations of $\operatorname{rad}(\mathbb{I}(\mathbf{a}))/(\mathbb{I}[k_{i-1}+1,k_{i+1}-1]/S(k_i))$. Therefore, the assertion follows from Proposition 6.2.

Next, for two $k_{i_1} < k_{i_2}$, we define

$$\Delta_q(k_{i_1},k_{i_2}) := \begin{cases} \frac{\Delta_q(k_{i_1})\Delta_q(k_{i_2})}{q[\ell_{i_2}-k_{i_2-1}]_q[k_{i_1+1}-\ell_{i_1+1}]_q} & \text{if } i_2=i_1+1, \\ \Delta_q(k_{i_1})\Delta_q(k_{i_2}) & \text{otherwise.} \end{cases}$$

Inductively, for $k_{i_1} < k_{i_2} < \cdots < k_{i_r}$, we define

$$\Delta_q(k_{i_1},k_{i_2},\dots,k_{i_r}) := \begin{cases} \frac{\Delta_q(k_{i_1},k_{i_2},\dots,k_{i_r-1})\Delta_q(k_{i_r})}{q[\ell_{i_r}-k_{i_r-1}]_q} & \text{if } i_r=i_{r-1}+1, \\ \\ \Delta_q(k_{i_1},k_{i_2},\dots,k_{i_r-1})\Delta_q(k_{i_r}) & \text{otherwise.} \end{cases}$$

Take a subset

$$\{(v_{2j-1}^{(k_{i_1},\dots,k_{i_r})},v_{2j}^{(k_{i_1},\dots,k_{i_r})})\mid j=1,2,\dots,r_{(k_{i_1},\dots,k_{i_r})}\}\subset\mathcal{J}_{\mathbf{a}}$$

such that any $(v_{2j-1}^{(k_{i_1},\dots,k_{i_r})},v_{2j}^{(k_{i_1},\dots,k_{i_r})})$ -valley is not adjacent to one of vertices k_{i_1},\dots,k_{i_r} . Then, for $r=1,\dots,t$, we set

$$\widetilde{\Delta}_q(k_1,\dots,k_r) := \Delta_q(k_1,\dots,k_r) \prod_{j=1}^{r_{(k_1,\dots,k_r)}} \mathrm{val}(\upsilon_{2j-1}^{(k_1,\dots,k_r)},\upsilon_{2j}^{(k_1,\dots,k_r)}).$$

Theorem 6.4. *The equation*

$$\operatorname{cl}(Q(\mathbf{a})) = \prod_{(b_i, b_{i+1}) \in \mathcal{J}_{\mathbf{a}}} \operatorname{val}_q(b_i, b_{i+1}) + \sum_{(k_{i_1}, \dots, k_{i_s}) \in \mathcal{T}_{\mathbf{a}}} \widetilde{\Delta_q}(k_{i_1}, \dots, k_{i_s})$$

$$\tag{6.1}$$

holds.

Proof. By Proposition 6.2, the first term of the right-hand side of (6.1) counts ℓ -dimensional subrepresentations of $\operatorname{rad}(\mathbb{I}(\mathbf{a}))$. Therefore, counting the cases where each $S(k_i)$ ($i=1,\ldots,t$) belongs to the support is sufficient. By the proof of Lemma 6.3, the number of ℓ -dimensional subrepresentations N of $\mathbb{I}(\mathbf{a})$ such that $S(k_{i_1}),\ldots,S(k_{i_r})\in\operatorname{supp}(N)$ but $S_j\notin\operatorname{supp}(N)$ for $j\neq k_{i_1},\ldots,k_{i_r}$ is the coefficient of q^ℓ of $\widetilde{\Delta}_q(k_{i_1},\ldots,k_{i_r})$. Thus, the assertion follows.

Example 6.5. (1) Let $\mathbf{a} = (1, 3, 1, 1)$. Then, the quiver $Q(\mathbf{a})$ is of the form

$$Q(\mathbf{a}) = 1 \longleftrightarrow 2 \longrightarrow 3 \longrightarrow 4 \longrightarrow 5 \longleftrightarrow 6 \longrightarrow 7,$$

and $((b_1, b_2), (b_3, b_4), (b_5, b_6)) = ((0, 0), (2, 0), (0, 0))$. So, we compute

$$\begin{split} \operatorname{val}_q(0,0) \operatorname{val}_q(2,0) \operatorname{val}_q(0,0) &= q^5 + 3q^4 + 4q^3 + 4q^2 + 3q + 1, \\ \widetilde{\Delta}_q(2) &= q^5 [1]_q [1]_q \operatorname{val}_q(0,0) = q^6 + q^5, \\ \widetilde{\Delta}_q(6) &= q^3 [3]_q \operatorname{val}_q(0,0) = q^6 + 2q^5 + 2q^4 + q^3, \\ \widetilde{\Delta}_q(2,6) &= \frac{\Delta_q(2) \Delta_q(6)}{q [3]_q [1]_q} = q^7. \end{split}$$

Thus, we have

$$cl(Q(\mathbf{a})) = q^7 + 2q^6 + 4q^5 + 5q^4 + 5q^3 + 4q^2 + 3q + 1.$$

(2) Let $\mathbf{a} = (0, 3, 1, 5, 1)$. Then, the quiver $Q(\mathbf{a})$ is of the form

$$Q(\mathbf{a}) = 1 \longrightarrow 2 \longrightarrow 3 \longrightarrow 4 \longleftarrow 5 \longrightarrow 6 \longrightarrow 7 \longrightarrow 8 \longrightarrow 9 \longrightarrow 10 \longleftarrow 11$$

T. Kogiso, K. Miyamoto, X. Ren, M. Wakui, K. Yanagawa

and $((b_1, b_2), (b_3, b_4)) = ((2, 0), (4, 0))$. So, we compute

$$\begin{aligned} \operatorname{val}_q(2,0) \operatorname{val}_q(4,0) &= q^8 + 2q^7 + 3q^6 + 4q^5 + 4q^4 + 4q^3 + 3q^2 + 2q + 1, \\ \widetilde{\Delta}_q(1) &= q^4 \operatorname{val}_q(4,0) = q^9 + q^8 + q^7 + q^6 + q^5 + q^4, \\ \widetilde{\Delta}_q(5) &= q^7[3]_q = q^9 + q^8 + q^7, \\ \widetilde{\Delta}_q(11) &= q^2[5]_q \operatorname{val}_q(2,0) = q^9 + 2q^8 + 3q^7 + 4q^6 + 4q^5 + 3q^4 + 2q^3 + q^2, \\ \widetilde{\Delta}_q(1,5) &= \frac{\Delta_q(1)\Delta_q(5)}{q[3]_q} = q^{10}, \\ \widetilde{\Delta}_q(1,11) &= \Delta_q(1)\Delta_q(11) = q^{10} + q^9 + q^8 + q^7 + q^6, \\ \widetilde{\Delta}_q(5,11) &= \frac{\Delta_q(5)\Delta_q(11)}{q[5]_q} = q^{10} + q^9 + q^8, \\ \widetilde{\Delta}_q(1,5,11) &= \frac{\Delta_q(1)\Delta_q(5)\Delta_q(11)}{q^2[3]_q[5]_q} = q^{11}. \end{aligned}$$

Thus, we have

$$cl(Q(\mathbf{a})) = q^{11} + 3q^{10} + 5q^9 + 7q^8 + 8q^7 + 9q^6 + 9q^5 + 8q^4 + 6q^3 + 4q^2 + 2q + 1.$$

7 Special values of the q-deformed rational numbers

In [MO20, Proposition 1.8], it is shown that both $\mathcal{S}_{\alpha}(-1)$ and $\mathcal{R}_{\alpha}(-1)$ belong to $\{0, \pm 1\}$. From this, we see that for an irreducible fraction $\frac{r}{s}$, s is even if and only if $\mathcal{S}_{\frac{r}{s}}(q)$ is divisible by $[2]_q = 1 + q$. In this section, we extend this observation. Set

$$\omega := \frac{-1 + \sqrt{-3}}{2}.$$

Theorem 7.1. For a rational number α , we have $\mathcal{R}_{\alpha}(\omega)$, $\mathcal{S}_{\alpha}(\omega) \in \{0, \pm 1, \pm \omega, \pm \omega^2\}$.

Proof. First, we assume that $\alpha > 1$, and write $\alpha = [[c_1, \dots, c_l]]$. By Proposition 2.2, we have

$$\begin{pmatrix} \mathcal{R}_{\alpha}(\omega) \\ \mathcal{S}_{\alpha}(\omega) \end{pmatrix} = \left(M_q^-(c_1) M_q^-(c_2) \cdots M_q^-(c_l) \right) |_{q=\omega} \begin{pmatrix} 1 \\ 0 \end{pmatrix}.$$

It is easy to check that $M_q^-(c)|_{q=\omega}$ for a positive integer c is one of the following forms:

$$M_q^-(c)|_{q=\omega} = \begin{cases} X := \begin{pmatrix} 0 & -\omega^2 \\ 1 & 0 \end{pmatrix} & \text{if } c \equiv 0 \pmod{3}, \\ Y := \begin{pmatrix} 1 & -1 \\ 1 & 0 \end{pmatrix} & \text{if } c \equiv 1 \pmod{3}, \\ Z := \begin{pmatrix} -\omega^2 & -\omega \\ 1 & 0 \end{pmatrix} & \text{if } c \equiv 2 \pmod{3}. \end{cases}$$

Let G be the subgroup of $GL(2, \mathbb{C})$ generated by X, Y and Z. A direct computation shows that the equation $X^{12} = Y^6 = Z^3 = E_2$. Set

$$A := \left\{ \zeta \begin{pmatrix} 1 \\ 0 \end{pmatrix}, \zeta \begin{pmatrix} 1 \\ -\omega \end{pmatrix}, \zeta \begin{pmatrix} 1 \\ 1 \end{pmatrix}, \zeta \begin{pmatrix} 0 \\ 1 \end{pmatrix} \middle| \zeta = \pm 1, \pm \omega, \pm \omega^2 \right\} \subset \mathbb{C}^2.$$
 (7.1)

Then, easy calculation shows that A is closed under the natural action of G. Thus, for any $W \in G$, all entries of W, especially $\mathcal{R}_{\alpha}(\omega)$ and $\mathcal{S}_{\alpha}(\omega)$ for $\alpha > 1$, belong to the set $\{0, \pm 1, \pm \omega, \pm \omega^2\}$.

Let us consider the case $\alpha \le 1$. By (2.8), we have

$$\begin{pmatrix} \mathcal{R}_{\alpha}(\omega) \\ \mathcal{S}_{\alpha}(\omega) \end{pmatrix} = \begin{pmatrix} \omega^2 & -\omega^2 \\ 0 & 1 \end{pmatrix} \begin{pmatrix} \mathcal{R}_{\alpha+1}(\omega) \\ \mathcal{S}_{\alpha+1}(\omega) \end{pmatrix}.$$
(7.2)

It is easy to check that the set A is closed under the multiplication of $\begin{pmatrix} \omega^2 & -\omega^2 \\ 0 & 1 \end{pmatrix}$, so we

can show that $\begin{pmatrix} \mathcal{R}_{\alpha+1}(\omega) \\ \mathcal{S}_{\alpha+1}(\omega) \end{pmatrix} \in A$ implies $\begin{pmatrix} \mathcal{R}_{\alpha}(\omega) \\ \mathcal{S}_{\alpha}(\omega) \end{pmatrix} \in A$. Since $\alpha+n>1$ for sufficiently large n, the desired assertion follows from repeated use of the above implication.

Since the leading coefficient of $[n]_q = 1 + q + \cdots + q^{n-1}$ is 1, when we divide $f(q) \in \mathbb{Z}[q]$ by $[n]_q$, the quotient and the remainder belong to $\mathbb{Z}[q]$. It is clear that if $\mathcal{S}_{\frac{r}{s}}(q)$ can be divided by $[3]_q = 1 + q + q^2$, then $s = \mathcal{S}_{\frac{r}{s}}(1)$ is a multiple of 3. The following states that the converse is also true.

Corollary 7.2. *The following assertions hold.*

(1) If $s = S_{\frac{r}{s}}(1)$ is a multiple of 3, $S_{\frac{r}{s}}(q)$ can be divided by $[3]_q$. Moreover, for an irreducible fraction $\frac{r}{s}$, we have

$$S_{\frac{r}{s}}(\omega) = \begin{cases} 0 & \text{if } s \equiv 0 \pmod{3}, \\ 1, \omega, \omega^2 & \text{if } s \equiv 1 \pmod{3}, \\ -1, -\omega, -\omega^2 & \text{if } s \equiv 2 \pmod{3}. \end{cases}$$

(2) Similarly, we have

$$\mathcal{R}_{\frac{r}{s}}(\omega) = \begin{cases} 0 & \text{if } r \equiv 0 \pmod{3}, \\ 1, \omega, \omega^2 & \text{if } r \equiv 1 \pmod{3}, \\ -1, -\omega, -\omega^2 & \text{if } r \equiv 2 \pmod{3}. \end{cases}$$

Proof. (1) Note that $\omega^2 = -(w+1)$. By Theorem 7.1, the remainder of the polynomial $\mathcal{S}_{\frac{r}{s}}(q)$ divided by $[3]_q$ is aq+b for $a,b\in\{0,\pm1\}$ with $(a,b)\neq(1,-1),(-1,1)$. Since $s=\mathcal{S}_{\frac{r}{s}}(1)\equiv a+b\pmod{3}$, the assertion easily follows.

(2) While $\mathcal{R}_{\frac{r}{s}}(q) \in \mathbb{Z}[q,q^{-1}]$ has terms of negative degree for $\frac{r}{s} < 0$, we have $f(q) := q^{3n}\mathcal{R}_{\frac{r}{s}}(q) \in \mathbb{Z}[q]$ for $n \gg 0$. Since $f(1) = \mathcal{R}_{\frac{r}{s}}(1) = r$ and $f(\omega) = \mathcal{R}_{\frac{r}{s}}(\omega)$, we can use the argument of the proof of (1).

Example 7.3. Even if we fix s, $\mathcal{S}_{\frac{r}{s}}(\omega)$ depends on r. For example, we have $\mathcal{S}_{\frac{12}{11}}(\omega) = -\omega^2$, $\mathcal{S}_{\frac{13}{11}}(\omega) = -\omega$, $\mathcal{S}_{\frac{14}{11}}(\omega) = -\omega^2$, $\mathcal{S}_{\frac{15}{11}}(\omega) = -1$, and so on.

Corollary 7.4. For an irreducible fraction $\frac{r}{s}$, $s \equiv r \pmod{3}$ if and only if $\mathcal{R}_{\frac{r}{s}}(\omega) = \mathcal{S}_{\frac{r}{s}}(\omega)$.

Proof. By (2.8), we have $\mathcal{R}_{\frac{r}{s}-1}(q)=q^{-1}(\mathcal{R}_{\frac{r}{s}}(q)-\mathcal{S}_{\frac{r}{s}}(q))$. By Corollary 7.2, we have

$$\mathcal{R}_{\frac{r}{s}}(\omega) = \mathcal{S}_{\frac{r}{s}}(\omega) \iff \mathcal{R}_{\frac{r-s}{s}}(\omega) = 0 \iff r-s \text{ is a multiple of 3.}$$

So we are done. \Box

In the rest of this section, i means $\sqrt{-1}$.

Proposition 7.5. We have $\mathcal{R}_{\alpha}(i)$, $\mathcal{S}_{\alpha}(i) \in \{0, \pm 1, \pm i, \pm (1+i), \pm (1-i)\}$, and the remainder of $\mathcal{S}_{\alpha}(q)$ divided by $q^2 + 1$ is aq + b for $a, b \in \{0, \pm 1\}$.

Proof. It suffices to show the first assertion. The proof is similar to that of Theorem 7.1. First, assume that $\alpha > 1$. It is easy to check that $M_q^-(c)|_{q=i}$ is of the form

$$M_{q}^{-}(c)|_{q=i} = \begin{cases} X_{0} := \begin{pmatrix} 0 & i \\ 1 & 0 \end{pmatrix} & \text{if } c \equiv 0 \pmod{4}, \\ X_{1} := \begin{pmatrix} 1 & -1 \\ 1 & 0 \end{pmatrix} & \text{if } c \equiv 1 \pmod{4}, \\ X_{2} := \begin{pmatrix} 1+i & -i \\ 1 & 0 \end{pmatrix} & \text{if } c \equiv 2 \pmod{4}, \\ X_{3} := \begin{pmatrix} i & 1 \\ 1 & 0 \end{pmatrix} & \text{if } c \equiv 3 \pmod{4}. \end{cases}$$

A direct computation shows that $X_0^8 = X_1^6 = X_2^4 = X_3^{12} = E_2$. Let G' be the subgroup of $GL(2,\mathbb{C})$ generated by X_0, X_1, X_2 and X_3 . The set

$$B := \left\{ \zeta \begin{pmatrix} 1 \\ 0 \end{pmatrix}, \zeta \begin{pmatrix} 0 \\ 1 \end{pmatrix}, \zeta \begin{pmatrix} 1 \\ 1 \end{pmatrix}, \zeta \begin{pmatrix} i \\ 1 \end{pmatrix}, \zeta \begin{pmatrix} 1+i \\ 1 \end{pmatrix}, \zeta \begin{pmatrix} 1 \\ 1-i \end{pmatrix} \middle| \zeta = \pm 1, \pm i \right\}.$$

is closed under the natural action of G'. Hence all entries of any element in G' belong to $\{0, \pm 1, \pm i, \pm (1+i), \pm (1-i)\}$. Since $\mathcal{R}_{\alpha}(i)$ and $\mathcal{S}_{\alpha}(i)$ are entries of a suitable element of G', we are done.

For the case $\alpha \leq 1$, we can use the same argument as the last part of the proof of Theorem 7.1.

Theorem 7.6. For an irreducible fraction $\frac{r}{s}$, the following are equivalent.

(1) s is a multiple of 4,

T. Kogiso, K. Miyamoto, X. Ren, M. Wakui, K. Yanagawa

- (2) $S_{\frac{r}{s}}(q)$ is divisible by $[4]_q = q^3 + q^2 + q + 1$,
- (3) $S_{\frac{r}{s}}(q)$ is divisible by $q^2 + 1$.

Proof. (1) \Rightarrow (2): Let $g(q) \in \mathbb{Z}[q]$ be the remainder of $\mathcal{S}_{\frac{r}{s}}(q)$ divided by $1 + q^2$, that is,

$$\mathcal{S}_{\frac{r}{s}}(q) = f(q) \cdot (1+q^2) + g(q) \qquad (f(q) \in \mathbb{Z}[q], \deg(g) \le 1).$$

Since $[4]_q = (1+q)(1+q^2)$ and $S_{\frac{r}{s}}(-1) = 0$ by [MO20, Proposition 1.8], it suffices to show that $S_{\frac{r}{s}}(q)$ is divisible by $1+q^2$ (equivalently, g(q)=0). For a contradiction, assume that $g(q) \neq 0$. Proposition 7.5 states that $g(q)=\pm 1, \pm q, \pm (1+q), \pm (1-q)$. However, since g(1)=s-2f(1) and s is a multiple of 4, g(1) is even, and hence $g(q)\neq \pm 1, \pm q$. Finally, we have $g(q)=\pm (1+q), \pm (1-q)$.

In what follows, for $f(q) \in \mathbb{Z}[q]$, (f(q)) denotes the ideal of $\mathbb{Z}[q]$ generated by f(q), and $\mathbb{Z}[q]/(f(q))$ denotes the quotient ring. For the canonical surjections $\pi_1 : \mathbb{Z}[q] \to \mathbb{Z}[q]/(1+q)$ and $\pi_2 : \mathbb{Z}[q] \to \mathbb{Z}[q]/(1+q^2)$ (if there is no danger of confusion, we denote $\pi_i(f(q))$ by $\overline{f(q)}$), consider the ring homomorphism

$$\phi: \mathbb{Z}[q] \ni f(q) \longmapsto (\pi_1(f(q)), \pi_2(f(q))) \in (\mathbb{Z}[q]/(1+q)) \times (\mathbb{Z}[q]/(1+q^2)).$$

Since $\mathbb{Z}[q]$ is a UFD, and 1+q and $1+q^2$ are coprime, we have $\ker(\phi)=([4]_q)$. In the present situation, we have

$$\phi(\mathcal{S}_{\frac{r}{g}}(q)) = (\overline{0}, \overline{g(q)}).$$

Recall that $g(q) = \pm (1+q), \pm (1-q)$, but we have

$$\phi(\pm(1+q)) = (\overline{0}, \pm \overline{(1+q)})$$
 or $\phi(\pm(q+q^2)) = (\overline{0}, \mp \overline{(1-q)}).$

Hence, we have either

$$\pm (1+q) - S_{\frac{r}{s}}(q) \in ([4]_q) \quad \text{or} \quad \pm (q+q^2) - S_{\frac{r}{s}}(q) \in ([4]_q).$$

In both cases, $\pm 2 - \mathcal{S}_{\frac{r}{s}}(1) \in 4\mathbb{Z}$, and it means that $\mathcal{S}_{\frac{r}{s}}(1) \equiv 2 \pmod{4}$. It contradicts the assumption that $\mathcal{S}_{\frac{r}{s}}(1) \in 4\mathbb{Z}$.

 $(2) \Rightarrow (3)$: Obvious.

(3) \Rightarrow (2) : If $\mathcal{S}_{\frac{r}{s}}(q)$ is divisible by $1+q^2$, then there is some $f(q) \in \mathbb{Z}[q]$ such that $\mathcal{S}_{\frac{r}{s}}(q) = (1+q^2)f(q)$. It follows that $s = \mathcal{S}_{\frac{r}{s}}(1) = 2f(1)$ is even, and hence $\mathcal{S}_{\frac{r}{s}}(q)$ is also divisible by 1+q. Since $[4]_q = (1+q)(1+q^2)$, the assertion follows.

The next result can be proved by an argument similar to the corresponding results for $q = \omega$.

Corollary 7.7. *The following assertions hold.*

(1) We have

$$S_{\frac{r}{s}}(i) = \begin{cases} 0 & \text{if } s \equiv 0 \pmod{4}, \\ \pm (1+i), \pm (1-i) & \text{if } s \equiv 2 \pmod{4}, \\ \pm 1, \pm i & \text{if } s \equiv 1 \pmod{2}, \end{cases}$$

and

$$\mathcal{R}_{\frac{r}{s}}(i) = \begin{cases} 0 & \text{if } r \equiv 0 \pmod{4}, \\ \pm (1+i), \pm (1-i) & \text{if } r \equiv 2 \pmod{4}, \\ \pm 1, \pm i & \text{if } r \equiv 1 \pmod{2}. \end{cases}$$

(2) For an irreducible fraction $\frac{r}{s}$, we have $s \equiv r \pmod{4}$ if and only if $\mathcal{R}_{\frac{r}{s}}(i) = \mathcal{S}_{\frac{r}{s}}(i)$.

Example 7.8. It is clear that the analog of Corollaries 7.2 and 7.7 does not hold for primitive n-th roots of unity with $n \ge 5$. In fact, since $\mathcal{S}_{\frac{7}{5}}(q) = q^3 + 2q^2 + q + 1$, we have $\mathcal{S}_{\frac{7}{5}}(\zeta) \ne 0$, where ζ is a primitive 5th root of unity (i.e., a root of $q^4 + q^3 + q^2 + q + 1$). Moreover, using a computer system, we see that $\mathcal{S}_{\frac{37}{35}}(q)$ is irreducible over \mathbb{Q} , while 35 is a composite number.

Conjecture 7.9. If p is a prime integer, then $S_{\frac{a}{p}}(q)$ is irreducible over \mathbb{Q} .

Using the computer program Maple, we checked the conjecture for prime numbers up to 739. The following is another piece of evidence.

Theorem 7.10. Let p be a prime integer. If $S_{\frac{q}{p}}(q)$ is reducible in $\mathbb{Q}[q]$ (i.e., Conjecture 7.9 does not hold), all of its factors have degree at least 7.

Proof. Consider the factorization

$$\mathcal{S}_{\frac{a}{p}}(q) = \prod_{j=1}^{k} f_j(q)$$

in the polynomial ring $\mathbb{Q}[q]$. It is a classical result that we can take $f_j(q)$ from $\mathbb{Z}[q]$ for all j. Assume that $k \geq 2$. Since $f_j(1) \in \mathbb{Z}$ for all j and $p = \mathcal{S}_{\frac{q}{p}}(1) = \prod_{j=1}^k f_j(1)$ is a prime number, we may assume that $f_1(1) = p$ and $f_j(1) = 1$ for all $j \geq 2$.

Since both the leading coefficient and constant term of $\mathcal{S}_{\frac{a}{p}}(q)$ are 1, those of $f_j(q)$ are ± 1 . Since all coefficients of $\mathcal{S}_{\frac{a}{p}}(q)$ are positive, if $q=\alpha$ is a real root of the equation $\mathcal{S}_{\frac{a}{p}}(q)=0$ then $\alpha<0$. Clearly, the same is true for each $f_j(q)$, so both the leading coefficient and constant term of $f_j(q)$ are 1 (note that $f_j(1)>0$ now).

If p=2,3, the assertion is clear. So we may assume that $p\geq 5$. Since $p=\mathcal{S}_{\frac{a}{p}}(1)$ is odd, $\mathcal{S}_{\frac{a}{p}}(-1)=\prod_{j=1}^k f_j(-1)=\pm 1$. Since $f_j(-1)\in\mathbb{Z}$ for all j, we have $f_j(-1)=\pm 1$, and hence the remainder of $f_j(q)$ divided by q+1 is ± 1 . Similarly, we have $\mathcal{S}_{\frac{a}{p}}(i)=\prod_{j=1}^k f_j(i)=\pm 1, \pm i$ by Corollary 7.7. Since $f_j(i)\in\mathbb{Z}[i]$ for all j, we have $f_j(i)=\pm 1, \pm i$, and the remainder of $f_j(q)$ divided by q^2+1 is $\pm 1, \pm q$. Since $p=\mathcal{S}_{\frac{a}{p}}(1)$ is not a multiple of 3, $\mathcal{S}_{\frac{a}{p}}(\omega)=\prod_{j=1}^k f_j(\omega)=\pm 1, \pm \omega, \pm \omega^2$. Since $f_j(\omega)\in\mathbb{Z}[\omega]$ for all j, we have $f_j(\omega)=\pm 1, \pm \omega, \pm \omega^2$ by Corollary 7.2, and the remainder of $f_j(q)$ divided by q^2+q+1 is $\pm 1, \pm q, \pm (1+q)$.

Set $g(q) = q(q+1)(q^2+1)(q^2+q+1)$, and consider the natural ring homomorphism

$$\Psi: \mathbb{Z}[q]/(g(q)) \longrightarrow \mathbb{Z}[q]/(q) \times \mathbb{Z}[q]/(q+1) \times \mathbb{Z}[q]/(q^2+1) \times \mathbb{Z}[q]/(q^2+q+1).$$

Since $\mathbb{Z}[q]$ is a UFD, Ψ is injective. Let us find polynomials in $\mathbb{Z}[q]$ whose images under Ψ are characteristic.

For
$$t(q):=(q+1)(q^2+1)(q^2+q+1)$$
, we have $\Psi(t(q))=(\overline{1},\overline{0},\overline{0},\overline{0})$ and $t(1)=12$. For $u_1(q):=q(q^2+q+1),\quad u_2(q):=q^2(q^2+q+1),$ $u_3(q):=q^3(q^2+q+1),\quad u_4(q):=q(q^2+q+1)^2,$

we have

$$\Psi(u_1(q)) = (\overline{0}, -\overline{1}, -\overline{1}, \overline{0}), \quad \Psi(u_2(q)) = (\overline{0}, \overline{1}, -\overline{q}, \overline{0}),$$

$$\Psi(u_3(q)) = (\overline{0}, -\overline{1}, \overline{1}, \overline{0}), \quad \Psi(u_4(q)) = (\overline{0}, -\overline{1}, -\overline{q}, \overline{0}),$$

and $u_k(1) = 3$ for $k = 1, 2, 3, u_4(1) = 9$. For

$$v_1(q) := q(q+1)(q^2+1), \quad v_2(q) := q(q+1)^2(q^2+1), \quad v_3(q) := q^2(q+1)(q^2+1),$$

we have

$$\Psi(v_1(q)) = (\overline{0}, \overline{0}, \overline{0}, \overline{q}), \quad \Psi(v_2(q)) = (\overline{0}, \overline{0}, \overline{0}, -\overline{1}), \quad \Psi(v_3(q)) = (\overline{0}, \overline{0}, \overline{0}, -\overline{1} - \overline{q})$$

and
$$v_1(1) = v_3(1) = 4$$
, $v_2(1) = 8$.

The possible values of $\Psi(f(q))$ have been determined above, and the leading coefficient of $f_i(q)$ is 1. Hence, if deg $f_i(q) \le 6$, we have

$$f_i(q) = c_1 g(q) + t(q) + c_2 u_k(q) + c_3 v_l(q)$$

for some $c_1 = 0, 1, c_2, c_3 = \pm 1, k = 1, ..., 4$ and l = 1, 2, 3. If $j \ge 2$, $f_j(q)$ must satisfy the following conditions:

- $f_i(q) \neq 1$ and $f_i(1) = 1$.
- The leading coefficient is 1.

However, easy calculation shows that no choice of c_1, \dots, c_3, j, k satisfies these conditions. Finally, we consider $f_1(q)$. We have

$$p = f_1(1) \le g(1) + t(1) + u_k(1) + v_l(1) \le 12 + 12 + 9 + 8 = 41.$$

However, Conjecture 7.9 has been checked in this range by using Maple. \Box

8 Application to Jones polynomials of rational knots

Using the results in the previous section, we study the special values of the Jones polynomial $V_{\alpha}(t)$ and the normalized one $J_{\alpha}(q)$ of a rational link $L(\alpha)$.

T. Kogiso, K. Miyamoto, X. Ren, M. Wakui, K. Yanagawa

For a general link *L*, it is a classical fact that

$$V_L(1) = (-2)^{c(L)-1},$$

where c(L) is the number of the components of L. On the other hand, for an irreducible fraction $\frac{r}{s}$, it is well-known that $c(L(\frac{r}{s})) = 1, 2$, and $c(L(\frac{r}{s})) = 1$ if and only if r is odd. Hence we have

$$V_{\frac{r}{s}}(1) = \begin{cases} -2 & \text{if } r \text{ is even,} \\ 1 & \text{if } r \text{ is odd.} \end{cases}$$

We can explain this equation using q-deformed rationals.

Recall the equation (4.3), which states that the normalized Jones polynomial $J_{\alpha}(q)$ of a rational link $L(\alpha)$ can be computed by the following formula:

$$J_{\alpha}(q) = q \cdot \mathcal{R}_{\alpha}(q) + (1 - q) \cdot \mathcal{S}_{\alpha}(q).$$

By an argument similar to the previous section, we can show that

$$\begin{pmatrix} \mathcal{R}_{\frac{r}{s}}(-1) \\ \mathcal{S}_{\frac{r}{s}}(-1) \end{pmatrix} = \pm \begin{pmatrix} 1 \\ 0 \end{pmatrix}, \pm \begin{pmatrix} 0 \\ 1 \end{pmatrix}, \pm \begin{pmatrix} 1 \\ 1 \end{pmatrix}$$

(this is a refinement of [MO20, Proposition 1.8]). Hence we have

$$|V_{\frac{r}{s}}(1)| = |J_{\frac{r}{s}}(-1)| = \begin{cases} 2 & \text{if } r \text{ is even,} \\ 1 & \text{if } r \text{ is odd.} \end{cases}$$
(8.1)

Next, we will consider the special values of $J_{\alpha}(q)$ at $q=i,\omega,-\omega$. Many parts of the following results should be well-known, but we are interested in the relation to q-deformed rationals.

Theorem 8.1. For an irreducible fraction $\frac{r}{s} > 1$, we have

$$J_{\frac{r}{s}}(\omega) \in \{\pm 1, \pm \omega, \pm \omega^2\},$$

if r is not a multiple of 3, and

$$J_{\frac{r}{s}}(\omega) \in \{\pm (1-\omega), \pm \omega(1-\omega), \pm \omega^2(1-\omega)\},$$

if r is a multiple of 3. In particular,

$$|V_{\frac{r}{s}}(-\omega)| = |J_{\frac{r}{s}}(\omega)| = \begin{cases} \sqrt{3} & \text{if } r \text{ is a multiple of 3,} \\ 1 & \text{otherwise.} \end{cases}$$
(8.2)

Proof. The assertion easily follows from (the proof of) Theorem 7.1. By (4.3), we have

$$J_{\frac{r}{s}}(\omega) = \begin{pmatrix} \omega & 1 - \omega \end{pmatrix} \begin{pmatrix} \mathcal{R}_{\frac{r}{s}}(\omega) \\ \mathcal{S}_{\frac{r}{s}}(\omega) \end{pmatrix} \quad \text{and} \quad \begin{pmatrix} \mathcal{R}_{\frac{r}{s}}(\omega) \\ \mathcal{S}_{\frac{r}{s}}(\omega) \\ \mathcal{S}_{\frac{r}{s}}(\omega) \end{pmatrix} \in A,$$

where A is the set given in (7.1). So the assertion follows.

Remark 8.2. For a general link L, Lickorish and Millett ([LiM86, Theorem 3]) showed that

$$V_L(-\omega) = \pm i^{c(L)-1} (\sqrt{3}i)^d,$$
 (8.3)

where $d = \dim H_1(\Sigma(L); \mathbb{Z}_3)$ with $\Sigma(L)$ the double cover of the 3-sphere \mathbb{S}^3 branched over L. By (4.2), we have

$$V_{\frac{r}{s}}(-\omega) = \pm (-\omega)^h J_{\frac{r}{s}}(\omega^{-1})$$

(note that $\omega^{-1} = \omega^2 = \overline{\omega}$). Hence, comparing (8.3) with (8.2), we have

$$\dim H_1(\Sigma(L(r/s)); \mathbb{Z}_3) = \begin{cases} 1 & \text{if } r \text{ is a multiple of 3,} \\ 0 & \text{otherwise.} \end{cases}$$

The next result can be proved similarly to Theorem 8.1, but we use Proposition 7.5 this time.

Theorem 8.3. For an irreducible fraction $\frac{r}{s} > 1$, we have

$$J_{\frac{r}{s}}(i) = \begin{cases} 0 & \text{if } r \equiv 2 \pmod{4}, \\ \pm (1+i), \pm (1-i) & \text{if } r \equiv 0 \pmod{4}, \\ \pm 1, \pm i & \text{if } r \equiv 1, 3 \pmod{4}. \end{cases}$$

Remark 8.4. For a general link L, Murakami [M86] (see also [LiM86, Theorem 1]) showed that

$$V_L(i) = \begin{cases} (-\sqrt{2})^{c(L)-1}(-1)^{\mathsf{Arf}(L)} & \text{if } \mathsf{Arf}(L) \text{ exists,} \\ 0 & \text{otherwise.} \end{cases}$$

Comparing this equation with Theorem 8.3, we see that $Arf(L(\frac{r}{s}))$ exists if and only if $r \not\equiv 2 \pmod{4}$. We were unable to find this statement in literature, but it must be possible to prove it directly.

For a general link L, it is known that $V_L(\omega)=(-1)^{c(L)-1}$. Hence, for a rational link $L(\frac{r}{s})$, we have $V_{\frac{r}{s}}(\omega)=(-1)^{r-1}$ and hence

$$J_{\frac{r}{s}}(-\omega) \in \{\pm 1, \pm \omega, \pm \omega^2\}. \tag{8.4}$$

We can give a new interpretation to this equation using q-deformed rationals. Note that $M_q^-(c)|_{q=-\omega}$ is of the form

$$X_0 := \begin{pmatrix} 0 & \omega^2 \\ 1 & 0 \end{pmatrix} \qquad \text{if } c \equiv 0 \pmod{6},$$

$$X_1 := \begin{pmatrix} 1 & -1 \\ 1 & 0 \end{pmatrix} \qquad \text{if } c \equiv 1 \pmod{6},$$

$$X_2 := \begin{pmatrix} 1 - \omega & \omega \\ 1 & 0 \end{pmatrix} \qquad \text{if } c \equiv 2 \pmod{6},$$

$$X_3 := \begin{pmatrix} 1 - \omega + \omega^2 & -\omega^2 \\ 1 & 0 \end{pmatrix} \qquad \text{if } c \equiv 3 \pmod{6},$$

$$X_4 := \begin{pmatrix} -\omega + \omega^2 & 1 \\ 1 & 0 \end{pmatrix} \qquad \text{if } c \equiv 4 \pmod{6},$$

$$X_5 := \begin{pmatrix} \omega^2 & -\omega \\ 1 & 0 \end{pmatrix} \qquad \text{if } c \equiv 5 \pmod{6}.$$

By (4.3), for $\alpha = [[c_1, ..., c_l]]$, we have

$$\left(J_{\alpha}(-\omega) *\right) = \left(-\omega 1 + \omega\right) \cdot \left(M_q^-(c_1)M_q^-(c_2)\cdots M_q^-(c_l)\right)|_{q=-\omega},$$

where $\left(J_{\alpha}(-\omega) *\right)$ and $\left(-\omega *1+\omega\right)$ are 1×2 matrices, and \cdot means the product of matrices. Easy calculation shows that $\left(-\omega *1+\omega\right)=-\omega\left(1*\omega\right)$ and there exists $\zeta_i\in\{\pm 1,\pm\omega,\pm\omega^2\}$ such that

$$\begin{pmatrix} 1 & \omega \end{pmatrix} \cdot X_i = \zeta_i \begin{pmatrix} 1 & \omega \end{pmatrix}$$

for each $0 \le i \le 5$. So we can show (8.4) by induction on l.

Remark 8.5. In the above notation, the matrix X_3 is not diagonalizable, and hence $X_3^n \neq E_2$ for all positive integers n. It means that the subgroup of $GL(2,\mathbb{C})$ generated by X_3 is infinite, and hence $\{S_{\alpha}(-\omega) \mid \alpha \in \mathbb{Q}\}$ is an infinite set.

Acknowledgements.

T. Kogiso is supported by JSPS Grant-in-Aid for Scientific Research (c) 21K03169.

K. Miyamoto is supported by JSPS Grant-in-Aid for Early-Career Scientists 20K14302, 24K16885 and Grant-in-Aid for Scientific Research (A) 23H00479.

X. Ren is supported by the Kansai University Grant-in-Aid for progress of research in graduate course, 2023.

M. Wakui is supported by the Kansai University Grant-in-Aid for progress of research in graduate course, 2023.

K. Yanagawa is supported by JSPS Grant-in-Aid for Scientific Research (C) 19K03456 and by the Kansai University Grant-in-Aid for progress of research in graduate course, 2023.

References

[A13] M. Aigner, Markov's Theorem and 100 Years of the Uniqueness Conjecture, A
Mathematical Journey from Irrational Numbers to Perfect Matchings, Springer,
2013. 56

T. Kogiso, K. Miyamoto, X. Ren, M. Wakui, K. Yanagawa

- [ASS06] I. Assem, D. Simson and A. Skowroński, *Elements of the Representation Theory of Associative Algebras, vol 1, Techniques of Representation Theory*, London Math. Soc. Stud. Texts, **65**, Cambridge University Press, Cambridge, 2006. 70
- [BBL23] A. Bapat, L. Becker and A. M. Licata, q-deformed rational numbers and the 2-Calabi–Yau category of type A_2 , Forum Math. Sigma **11** (2023), Paper No. e47, 41 pp. 43
- [FC99] V. V. Fok and L. O. Chekhov, *Quantum Teichmüller spaces*, Teoret. Mat. Fiz.
 120 (1999), no. 3, 511–528; translation in Theoret. and Math. Phys. 120 (1999), no. 3, 1245–1259. 43
- [J85] V. F. R. Jones, *A polynomial invariant for knots via von Neumann algebras*, Bull. Amer. Math. Soc. (N.S.) **12** (1985), no.1, 103–111. 62
- [Kan22] E. Kantarcı Oğuz, *Oriented posets, Rank Matrices and q-deformed Markov Numbers*, Discrete Math. 348 (2025), no. 2, Paper No. 114256, 17 pp. 43
- [Kau87] L. H. Kauffman, *State models and the Jones polynomial*, Topology **26** (1987), no.3, 395–407. 62
- [KL02] L. H. Kauffman and S. Lambropoulou, *On the classification of rational knots*, Enseign. Math. (2) **49** (2003), no.3-4, 357–410. 46, 58, 62
- [Ko22] T. Kogiso, *q-deformations and t-deformations of Markov triples*, Preprint (2020), arXiv:2008.12913. 43
- [KR23] E. Kantarcı Oğuz and M. Ravichandran, *Rank polynomials of fence posets are unimodal*, Discrete Math. **346** (2023), no.2, Paper No. 113218, 20 pp. 43, 45, 55, 59, 60
- [KW19(a)] T. Kogiso and M. Wakui, *A bridge between Conway-Coxeter friezes and rational tangles through the Kauffman bracket polynomials*, J. Knot Theory Ramifications **28** (2019), no.14, 1950083, 40 pp. 43, 45, 64

- [KW19(b)] T. Kogiso and M. Wakui, Kauffman bracket polynomials of Conway Coxeter friezes, Proceedings of the Meeting for Study of Number Theory, Hopf Algebras and Related Topics, 51–79. Yokohama Publishers, Yokohama, 2019. 56, 64
- [KW22] T. Kogiso and M. Wakui, *A characterization of Conway-Coxeter friezes of zigzag type by rational links*, Osaka J. Math. **59** (2022), no.2, 341–362. 64
- [LL22] S. Labbé and M. Lapointe, *The q-analog of the Markoff injectivity conjecture* over the language of a balanced sequence, Comb. Theory $\bf 2$ (2022), no.1, Paper No.9, 25 pp. 43
- [LeM21] L. Leclere and S. Morier-Genoud, *The q-deformations in the modular group* and of the real quadratic irrational numbers, Adv. in Appl. Math. **130** (2021), Paper No. 102223, 28 pp. 43, 50
- [LMOV21] L. Leclere, S. Morier-Genoud, V. Ovsienko and A. Veselov, *On radius of convergence of q-deformed real numbers*, Mosc. Math. J. 24 (2024), no. 1, 1–19.
- [LS19] K. Lee and R. Schiffler, *Cluster algebras and Jones polynomials*, Selecta Math. (N.S.) **25** (2019), no.4, Paper No. 58, 41 pp. 43, 46, 62, 63
- [LiM86] W. B. R. Lickorish and K.C. Millett, *Some evaluations of link polynomials*, Comment. Math. Helv. **61** (1986), no.3, 349–359. 85, 86
- [MSS21] T. McConville, B. E. Sagan and C. Smyth, *On a rank-unimodality conjecture of Morier-Genoud and Ovsienko*, Discrete Math. **344** (2021), no.8, Paper No. 112483, 13 pp. 43, 55, 60
- [MO19] S. Morier-Genoud and V. Ovsienko, *Farey boat: continued fractions and triangulations, modular group and polygon dissections*, Jahresber. Dtsch. Math.-Ver. **121** (2019), no.2, 91–136. 48

T. Kogiso, K. Miyamoto, X. Ren, M. Wakui, K. Yanagawa

- [MO20] S. Morier-Genoud and V. Ovsienko, *q-deformed rationals and q-continued fractions*, Forum Math. Sigma **8** (2020), Paper No. e13, 55 pp. 43, 45, 46, 47, 49, 50, 55, 56, 57, 63, 76, 80, 84
- [MO22] S. Morier-Genoud and V. Ovsienko, *On q-deformed real numbers*, Exp. Math. **31** (2022), no.2, 652–660. 43
- [MOV24] Morier-Genoud, S., Ovsienko, V., Veselov, A. P.: Burau representation of braid groups and q-rationals, Int. Math. Res. Not. IMRN(2024), no.10, 8618–8627. 43, 47, 50
- [M86] H. Murakami, *A recursive calculation of the Arf invariant of a link*, J. Math. Soc. Japan **38** (1986), no.2, 335–338. 86
- [NT20] W. Nagai and Y. Terashima, *Cluster variables, ancestral triangles and Alexander polynomials*, Adv. Math. **363** (2020), 106965, 37 pp. 43
- [O21] V. Ovsienko, *Towards quantized complex numbers: q-deformed Gaussian integers and the Picard group*, Open Commun. Nonlinear Math. Phys. **1** (2021), 73–93. 43
- [R21] X. Ren, Some observation on q-rational numbers and q-real numbers (in Japanese), Master's thesis, Josai Univ., 2021. 45
- [R22(a)] X. Ren, On radiuses of convergence of q-metallic numbers and related q-rational numbers, Res. Number Theory 8 (2022), no.3, Paper No. 37, 14 pp.; Corrigendum to: On radiuses of convergence of q-metallic numbers and related q-rational numbers, Res. Number Theory 9 (2023), no.2, Paper No. 39, 4 pp. 43
- [R22(b)] X. Ren, On q-deformed Farey sum and a homological interpretation of q-deformed real quadratic irrational numbers, Preprint (2022), arXiv:2210.06056.

[S21] T. Sakurai, A relationship between mutation of quivers, triangulation of polygons, and q-rational numbers (in Japanese), Master's thesis, Josai Univ., 2021.

[W22] M. Wakui, *q-deformed integers derived from pairs of coprime integers and its applications*, Low dimensional topology and number theory, Springer Proc. Math. Stat., 456, 297–323. 45, 61, 62, 63

AUTHORS

Takeyoshi Kogiso

Department of Mathematics,

Josai University,

Saitama, 350-0295, Japan.

email: kogiso@josai.ac.jp

Kengo Miyamoto

Department of Computer and Information Science,

Ibaraki University,

Ibaraki, 316-8511, Japan.

email: kengo.miyamoto.uz63@vc.ibaraki.ac.jp

Xin Ren

Department of Mathematics,

Kansai University,

Osaka, 564-8680, Japan.

email: k641241@kansai-u.ac.jp

T. Kogiso, K. Miyamoto, X. Ren, M. Wakui, K. Yanagawa

Michihisa Wakui Department of Mathematics, Kansai University, Osaka, 564-8680, Japan. email: wakui@kansai-u.ac.jp

Kohji Yanagawa Department of Mathematics, Kansai University, Osaka, 564-8680, Japan.

email: yanagawa@kansai-u.ac.jp



Arnold Mathematical Journal Volume 11, Issue 3, 2025



Ancient curve shortening flow in the disc with mixed boundary condition

Mat Langford Yuxing Liu George McNamara

Received 11 Jan 2024; Accepted 10 Mar 2025

Abstract:

Given any non-central interior point o of the unit disc D, the diameter L through o is the union of two linear arcs emanating from o which meet ∂D orthogonally, the shorter of them stable and the longer unstable (under these boundary conditions). In each of the two half discs bounded by L, we construct a convex eternal solution to curve shortening flow which fixes o and meets ∂D orthogonally, and evolves out of the unstable critical arc at $t=-\infty$ and into the stable one at $t=+\infty$. We then prove that these two (congruent) solutions are the only non-flat convex ancient solutions to the curve shortening flow satisfying the specified boundary conditions. We obtain analogous conclusions in the "degenerate" case $o \in \partial D$ as well, although in this case the solution contracts to the point o at a finite time with asymptotic shape that of a half Grim Reaper, thus providing an interesting example for which an embedded flow develops a collapsing singularity.

© 2025 Mat Langford, Yuxing Liu, George McNamara

DOI: 10.56994/ARMJ.011.003.004

1 Introduction

Variational problems subject to boundary constraints are ubiquitous in pure and applied mathematics and physics. One of the simplest such problems is to find and study paths of critical (e.g. minimal) length amongst those joining a given point o in some domain Ω to its boundary $\partial\Omega$. When Ω is a Euclidean domain, such paths are, of course, straight linear arcs from o to $\partial\Omega$ which meet $\partial\Omega$ orthogonally.

While characterizing all such curves is a non-trivial problem in general (even for convex Euclidean domains, say), the "Dirichlet–Neumann geodesics" in the unit disc in \mathbb{R}^2 are easily found: when o is the origin, they are the radii; when o is not the origin, there are exactly two, and their union is the diameter through o.

One useful tool for analyzing such variational problems is the (formal) gradient flow (a.k.a. steepest descent flow), which in this case is the "Dirichlet–Neuman curve shortening flow"; this equation evolves each point of a given curve with velocity equal to the curvature vector at that point, subject to holding one endpoint fixed at o with the other constrained to $\partial\Omega$, which is met orthogonally.

While curve shortening flow is now well-studied under other boundary conditions — particularly the "periodic" (i.e. no-boundary) [And12, AB11a, AB11b, BLT20, DHS10, GH86, Gag84, Gra87, Hui98], "Neumann–Neumann" (a.k.a. free boundary) [BBC, BL23, Buc05, Ede20, Hui89, Ko, LZ, Sta96a, Sta96b] and "Dirichlet–Dirichlet" [ALT, Hui98] conditions — we are aware of no literature considering the mixed "Dirichlet–Neumann" condition.

Our main result (inspired by [BL23]) is the following classification of the convex ancient solutions which arise in the simple setting of the unit disc.

Theorem 1.1. Given any $d \in (0,1]$, there exists a convex, locally uniformly convex ancient solution $\{\Gamma_t^d\}_{t \in (-\infty,\omega_d)}$ to curve shortening flow in the unit disc D with one endpoint fixed at

Ancient CSF in the disc with mixed boundary condition

o:=(-d,0) and the other meeting ∂D orthogonally. The timeslices Γ^d_t each lie in the upper half-disc, and converge uniformly in the smooth topology as $t \to -\infty$ to the unstable critical $arc\{(x,0): x \in [-d,1]\}$; as a graph over the x-axis,

$$e^{\lambda^2 t} y(x,t) \to A \sinh(\lambda(x+d))$$
 uniformly in x as $t \to -\infty$

for some A > 0*, where* λ *is the positive solution to* $\tanh(\lambda(1+d)) = \lambda$ *.*

When d < 1, $\omega_d = +\infty$ and the timeslices converge uniformly in the smooth topology as $t \to +\infty$ to the minimizing arc $\{(x,0): x \in [-1,-d]\}$. When d=1, $\omega_d < \infty$ and the timeslices contract uniformly as $t \to \omega_d$ to the point o and, after performing a standard type-II blow-up, converge locally uniformly in the smooth topology to the right half of the downward translating Grim Reaper.

Modulo time translations and reflection about the x-axis, $\{\Gamma_t^d\}_{t \in (-\infty, \omega_d)}$ is the only non-flat convex ancient curve shortening flow subject to the same boundary conditions.

En route to proving Theorem 1.1, we establish the following convergence result (cf. [ALT, GH86, Gag84, Gra87, LZ]), which is of independent interest (see the proof of Lemma 3.1).

Theorem 1.2. Let Γ be an oriented smooth convex arc in the upper unit half-disc D_+ with left endpoint o = (-d,0), $d \in (0,1]$, where its curvature vanishes, and right endpoint on ∂D , which is met orthogonally. Suppose that the curvature of Γ increases monotonically with arclength from o. If d < 1, then the Dirichlet–Neumann curve shortening flow starting from Γ exists for all positive time t and converges uniformly in the smooth topology as $t \to \infty$ to the minimizing arc joining o to ∂D . If d = 1, then the Dirichlet–Neumann curve shortening flow starting from Γ converges uniformly to the point o as $t \to \omega < \infty$ and, after performing a standard type-II blow-up, converges locally uniformly in the smooth topology to a half Grim Reaper.

Though the curvature monotonicity hypothesis appears unnaturally restrictive in Theorem 1.2, we note that some such additional condition is required to prevent the development of self-intersections at the Dirichlet endpoint (resulting in subsequent cusplike singularities). Moreover, as Theorem 1.2 demonstrates in case the Dirichlet endpoint lies on the boundary, collapsing singularities may form at the Dirichlet endpoint even when the flow remains embedded. It is not hard to see that this can also occur when the Dirichlet endpoint lies to the interior (as a limiting case of the flow forming a cusp singularity just after losing embeddedness, say).

Acknowledgements

This work originated as an undergraduate summer research project undertaken at the ANU by YL and GM under the supervision of ML. We are grateful to the MSI for funding the project. ML thanks Julie Clutterbuck for bringing the mixed boundary value problem to his attention.

2 Preliminaries

Fix a point $o = (-d, 0) \in D$ in the unit disc $D \subset \mathbb{R}^2$, with $d \in (0, 1]$. Denote by $C_\theta \subset D$ the circular arc which passes through o and meets the boundary of D orthogonally at $(\sin \theta, \cos \theta)$; that is,

$$C_{\theta} := \{(x, y) \in D : (x - \xi)^2 + (y - \eta)^2 = r^2\},$$

where, defining $a := \frac{1}{2}(d^{-1} + d)$,

$$(\xi,\eta) := (\cos\theta,\sin\theta) + r(-\sin\theta,\cos\theta) \quad \text{and} \quad r := \frac{1 + d^2 + 2d\cos\theta}{2d\sin\theta} = \frac{a + \cos\theta}{\sin\theta}.$$

Consider also the circular arc $\check{C}_{\theta} \subset D$ which is symmetric about the *y*-axis and meets ∂D orthogonally at $(\cos \theta, \sin \theta)$. That is,

$$\check{C}_{\theta} := \{x^2 + (y - \check{\eta})^2 = \check{r}^2\},\,$$

where

$$\check{\eta} := \csc \theta$$
 and $\check{r} := \cot \theta$.

Ancient CSF in the disc with mixed boundary condition

Proposition 2.1. The family $\{\check{C}_{\theta^+(t)}\}_{t\in(-\infty,0)}$, where $\theta^+(t) := \arcsin e^{2t}$, is a supersolution to curve shortening flow. The family $\{C_{\theta^-(t)}\}_{t\in(-\infty,\omega_d)}$, where θ^- is the solution to

$$\begin{cases} \frac{d\theta}{dt} = \frac{\sin \theta}{a + \cos \theta} \\ \theta(0) = \frac{\pi}{2} \,, \end{cases} \tag{1}$$

is a subsolution to curve shortening flow.

Remark 1. Separating variables, the problem (1) becomes

$$\int_{t}^{0} dt = \int_{\theta}^{\frac{\pi}{2}} \frac{a + \cos \omega}{\sin \omega} d\omega = \int_{\omega = \theta}^{\frac{\pi}{2}} d\log \left(2 \sin^{1+a} \left(\frac{\omega}{2} \right) \cos^{1-a} \left(\frac{\omega}{2} \right) \right),$$

and hence

$$e^t = 2\sin^{1+a}\left(\frac{\theta^{-}(t)}{2}\right)\cos^{1-a}\left(\frac{\theta^{-}(t)}{2}\right).$$

In particular, for all $d \in (0,1]$, the solution certainly exists for all t < 0, with $\theta^-(t) \sim 2^{\frac{a}{1+a}} e^{\frac{t}{a+1}}$ as $t \to -\infty$. When $d \in (0,1)$, the solution exists up to time $\omega_d = +\infty$, and $\lim_{t \to +\infty} \theta^-(t) = \pi$. When d = 1, the solution exists up to time $\omega_d = \log 2$, and $\lim_{t \to \omega_d} \theta^-(t) = \pi$.

Proof of Proposition 2.1. The first claim is proved in [BL23, Proposition 2.1].

To prove the second claim, consider any monotone increasing function θ of t, and let $\gamma(u,t)=(x(u,t),y(u,t))$ be a general parametrization of $C_{\theta(t)}$. Differentiation of the equation

$$(x - \xi)^2 + (y - \eta)^2 = r^2$$

with respect to t along γ and θ yields

$$(x - \xi)(x_t - \xi_\theta \theta_t) + (y - \eta)(y_t - \eta_\theta \theta_t) = rr_\theta \theta_t.$$

Since the outward unit normal to C_{θ} at (x, y) is $\nu = \frac{1}{r}(x - \xi, y - \eta)$, this becomes

$$-\gamma_t \cdot \nu = -\left(\frac{x-\xi}{r}\xi_\theta + \frac{y-\eta}{r}\eta_\theta + rr_\theta\right)\theta_t.$$

We claim that

$$\frac{1}{r}(x-\xi,y-\eta)\cdot(\xi_{\theta},\eta_{\theta})+r_{\theta}=-\frac{y}{\sin\theta}.$$

Indeed,

$$\begin{split} &\frac{1}{r}(x-\xi,y-\eta)\cdot(\xi_{\theta},\eta_{\theta})\\ &=\frac{1}{r}\Big((x,y)-(\cos\theta,\sin\theta)-r(-\sin\theta,\cos\theta))\Big)\cdot\Big((1+r_{\theta})(-\sin\theta,\cos\theta)-r(\cos\theta,\sin\theta)\Big)\\ &=-((x,y)-(\cos\theta,\sin\theta)-r(-\sin\theta,\cos\theta)))\cdot(\cot\theta(-\sin\theta,\cos\theta)+(\cos\theta,\sin\theta))\\ &=-(x,y)\cdot(\cot\theta(-\sin\theta,\cos\theta)+(\cos\theta,\sin\theta))+1+r\cot\theta\\ &=-(x,y)\cdot(0,\csc\theta)-r_{\theta}\,, \end{split}$$

from which the claim follows.

Since, $y \leq \sin \theta$ along C_{θ} , taking θ to be the solution to the specified initial value problem yields

$$-\gamma_t \cdot \nu = \frac{y}{\sin \theta} \theta_t = \frac{y}{\sin \theta} \frac{1}{r} \le \frac{1}{r} = \kappa,$$

as claimed. \Box

Next consider $\{H_t\}_{t\in(-\infty,\infty)}$, the fundamental domain of the horizontally oriented hairclip solution to curve shortening flow centred at o; that is,

$$H_t := \{(x, y) \in [0, \infty) \times [0, \frac{\pi}{2}] : \sin(y) = e^t \sinh(x + d) \}.$$

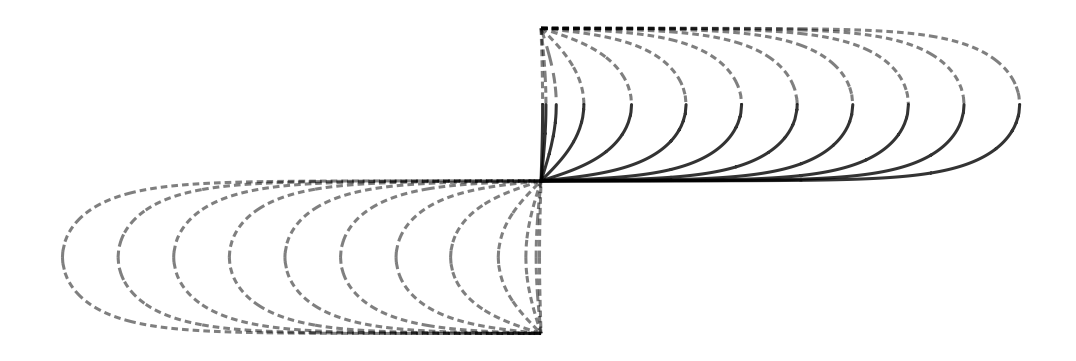


Figure 1: Some timeslices of (one period of) the "hairclip" solution.

Given any $\lambda > 0$, define $\{H_t^{\lambda}\}_{t \in (-\infty,\infty)}$ by parabolically rescaling the hairclip by λ . That is,

$$\mathrm{H}_t^{\lambda} := \lambda^{-1} \mathrm{H}_{\lambda^2 t} = \{(x, y) \in [0, \infty) \times [0, \frac{\pi}{2\lambda}] : \sin(\lambda y) = \mathrm{e}^{\lambda^2 t} \sinh(\lambda (x + d)) \}.$$

Ancient CSF in the disc with mixed boundary condition

Observe that $\{H_t^{\lambda}\}_{t \in (-\infty,\infty)}$ satisfies

$$\frac{\kappa}{\cos \theta} = \lambda \tan(\lambda y)$$
 and $\frac{\kappa}{\sin \theta} = \lambda \tanh(\lambda(x+d))$,

where $\theta \in [0, \frac{\pi}{2}]$ is the angle the tangent vector makes with the *x*-axis. From this we see, in particular, that κ is positive and monotone increasing with respect to arclength from o.

Proposition 2.2. For each $\theta \in (0, \frac{\pi}{2})$ there exists a unique pair (λ, t) such that H_t^{λ} intersects ∂D orthogonally at $(\cos \theta, \sin \theta)$.

Proof. Given any $\theta \in (0, \frac{\pi}{2})$, substituting the point $(\cos \theta, \sin \theta)$ for (x, y) in the defining equation $\sin(\lambda y) = e^{\lambda^2 t} \sinh(\lambda(x+d))$ and solving for t yields for each $\lambda \in (0, \frac{\pi}{2\sin\theta})$ the unique timeslice of the (fundamental domain of the) Hairclip solution which intersects ∂D at $(\cos \theta, \sin \theta)$; namely,

$$t = \lambda^{-2} \ln \left(\frac{\sin(\lambda \sin \theta)}{\sinh(\lambda(\cos \theta + d))} \right).$$

At that point, the normal satisfies

$$\begin{split} \nu_{\lambda}(\cos\theta,\sin\theta)\cdot(\cos\theta,\sin\theta) &= \frac{\sin(\lambda\sin\theta)\cos\theta - \tanh(\lambda(\cos\theta+d))\cos(\lambda\sin\theta)\sin\theta}{\tanh(\lambda(\cos\theta+d))\cos(\lambda\sin\theta)} \\ &= -\frac{\tan(\lambda\sin\theta)\cos\theta}{\tanh(\lambda(\cos\theta+d))}g(\lambda,\theta)\,, \end{split}$$

where

$$g(\lambda, \theta) := \tanh(\lambda(\cos \theta + d))\cot(\lambda \sin \theta)\tan \theta - 1$$
.

Observe that

$$\lim_{\lambda \searrow 0} g(\lambda, \theta) = d \cdot \sec \theta > 0, \lim_{\lambda \nearrow \frac{\pi}{2 \sin \theta}} g(\lambda, \theta) = -1 < 0$$

and

$$\frac{dg}{d\lambda} = \tan\theta \Big[(\cos\theta + d) \cot(\lambda \sin\theta) \operatorname{sech}^{2}(\lambda(\cos\theta + d)) \\ - \sin\theta \csc^{2}(\lambda \sin\theta) \tanh(\lambda(\cos\theta + d)) \Big] \\ = \frac{\tan\theta \tanh(\lambda(\cos\theta + d))}{\lambda \sin(\lambda \sin\theta)} \Big[\frac{\lambda(\cos\theta + d)}{\sinh(\lambda(\cos\theta + d))} \cos(\lambda \sin\theta) \operatorname{sech}(\lambda(\cos\theta + d)) \\ - \frac{\lambda \sin\theta}{\sin(\lambda \sin\theta)} \Big] \\ \leq \frac{\tan\theta \tanh(\lambda(\cos\theta + d))}{\lambda \sin(\lambda \sin\theta)} \Big[\cos(\lambda \sin\theta) \operatorname{sech}(\lambda(\cos\theta + d)) - 1 \Big] \\ < 0$$

for $\lambda \in (0, \frac{\pi}{2\sin\theta})$. It follows that there exists a unique λ such that

$$\nu_{\lambda}(\cos\theta,\sin\theta)\cdot(\cos\theta,\sin\theta)=0$$
.

The claim follows. \Box

Remark 2. Note that, since $\lim_{\theta \to 0} g(\lambda, \theta) = \frac{\tanh(\lambda(d+1))}{\lambda} - 1$, the function $g(\lambda, \theta)$ is non-negative at $\theta = 0$ so long as $\lambda \ge \lambda_0$, where λ_0 is the unique positive solution to the equation

$$\lambda = \tanh(\lambda(d+1))$$
.

Proposition 2.3 (A priori estimates). Let $\Gamma \subset D_+$ be a smooth, convex embedding of a closed interval with left endpoint o = (-d,0), $d \in (0,1]$, and right endpoint meeting ∂D orthogonally, and suppose that the curvature κ of Γ increases monotonically with respect to arclength from o. Denote by $\underline{\theta}$ resp. $\overline{\theta}$ the least resp. greatest value taken by the turning angle along Γ and by $\overline{\kappa} = \kappa(\overline{\theta})$ the greatest value taken by κ .

The circle $C_{\overline{\theta}}$ lies below Γ . Thus,

$$\overline{\kappa} \ge \frac{\sin \overline{\theta}}{a + \cos \overline{\theta}} \tag{2}$$

and

$$\underline{\theta} \ge \operatorname{arccot}\left(\frac{1 + a\cos\overline{\theta}}{b\sin\overline{\theta}}\right),\tag{3}$$

Arnold Mathematical Journal, Vol.11(3), 2025

where $b := \frac{1}{2}(d^{-1} - d)$ and we recall that $a := \frac{1}{2}(d^{-1} + d)$, with the right hand side taken to be zero in case d = 1.

Proof. Suppose, to the contrary, that $C_{\overline{\theta}}$ does not lie below Γ. Then some point of Γ must lie strictly below $C_{\overline{\theta}}$, and hence (since the endpoints of the two curves agree) upon translating $C_{\overline{\theta}}$ downwards, the two curves will continue to intersect until some final moment, at which they must make first order contact at some interior point $q \in \Gamma$. At this point, the curvature κ of Γ must be no less than $1/r(\overline{\theta})$ (the curvature of $C_{\overline{\theta}}$). But then, by the monotonicity of κ , κ must exceed $1/r(\overline{\theta})$ on the whole segment of Γ joining q to ∂D , in which case (since Γ and $C_{\overline{\theta}}$ make first order contact at ∂D) the point q must lie *strictly above* $C_{\overline{\theta}}$, which is absurd. So $C_{\overline{\theta}}$ must indeed lie below Γ. The first inequality is then immediate and the second is straightforward.

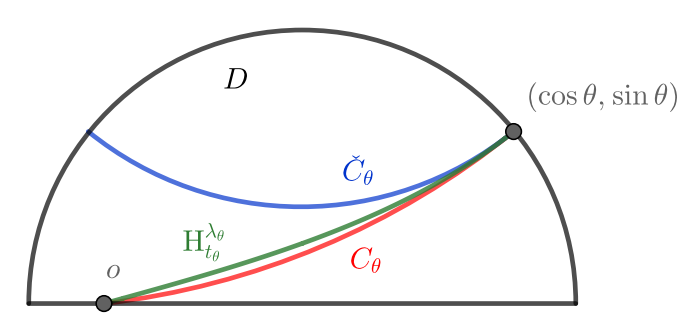


Figure 2: Scaled hairclip timeslice and circular arcs through the prescribed boundary points o and $(\cos \theta, \sin \theta)$.

3 Existence

For each $d \in (0,1]$ and $\rho \in (0,\frac{\pi}{2})$, let $\Gamma^{\rho} \subset D_{+}$ be a smooth oriented arc satisfying the following properties.

- The left endpoint of Γ^{ρ} is o=(-d,0), where its curvature vanishes, and its right endpoint meets ∂D orthogonally at $(\cos \rho, \sin \rho)$.
- Γ^{ρ} is convex.

Mat Langford, Yuxing Liu, George McNamara

– The curvature of Γ^{ρ} is monotone increasing with respect to arclength from o.

For example, we could take $\Gamma^{\rho}:=\mathrm{H}_{t_{\rho}}^{\lambda_{\rho}}\cap D$, where $(\lambda_{\rho},t_{\rho})$ are the unique choice of (λ,t) which ensure that H_{t}^{λ} meets ∂D orthogonally at $(\cos\rho,\sin\rho)$.

Lemma 3.1 (Very old (but not ancient) solutions). For each $d \in (0,1]$ and $\rho \in (0,\frac{\pi}{2})$ there exist $\alpha_{\rho} < 0$ such that $\alpha_{\rho} \to -\infty$ as $\rho \to 0$ and a smooth¹ curve shortening flow $\{\Gamma_{t}^{\rho}\}_{t \in [\alpha_{\rho}, \omega_{d})}$ in D exhibiting the following properties.

$$- \ \Gamma^{\rho}_{\alpha_{\rho}} = \Gamma^{\rho}.$$

- For each $t \in [\alpha_{\rho}, \omega_d)$, Γ_t^{ρ} is an oriented embedding of a closed interval, with left endpoint o = (-d, 0) and right endpoint meeting ∂D orthogonally.
- For each $t \in [\alpha_o, \omega_d)$, Γ_t^{ρ} is convex.
- For each $t \in [\alpha_{\rho}, \omega_d)$, the curvature of Γ_t^{ρ} is monotone increasing with respect to arclength from o.
- If d < 1, then $\omega_d = \infty$ and Γ_t^{ρ} converges uniformly in the smooth topology as $t \to \infty$ to the minimizing arc $\{(x,0): x \in [-1,-d]\}$.
- If d=1, then $\omega_d \in (0,\infty)$ and Γ_t^ρ converges uniformly as $t \to \omega_d$ to the point o, and there are sequences of times $t_j \nearrow \omega_d$, points $p_j \in \Gamma_{t_j}^\rho$, and scales $\lambda_j \nearrow \infty$ such that the sequence $\{\lambda_j(\Gamma_{\lambda_j^{-2}t+t_j}^\rho p_j)\}_{t \in [\lambda_j^2(\alpha_\rho t_j), \lambda_j^2(\omega_\rho j^{-1} t_j))}$ converges locally uniformly in the smooth topology as $j \to \infty$ to the right half of the downwards translating Grim Reaper.

Proof. Form the "odd doubling" $\check{\Gamma}^{\rho}$ of Γ^{ρ} by taking the union of Γ^{ρ} with its rotation through angle π about o. Since $\check{\Gamma}^{\rho}$ is a regular curve of class C^2 and there exists a ball B about

¹More precisely, $\{\Gamma_t^{\rho}\}_{t\in[\alpha_{\rho},\omega_d)}$ is given by a family of immersions of the interval [0,1] which is of class $C^{\infty}([0,1]\times(\alpha_{\rho},\omega_d))\cap C^{3+\beta,1+\frac{\beta}{2}}([0,1)\times[\alpha_{\rho},\omega_d))\cap C^{2+\beta,1+\frac{\beta}{2}}((0,1]\times[\alpha_{\rho},\omega_d))$ for any $\beta\in(0,1)$. Without additional compatibility conditions at the boundary points, higher regularity at the initial time may fail. However, if the curvature of Γ^{ρ} is odd resp. even at its left resp. right boundary point, then the solution will be smooth up to the left resp. right boundary point at the initial time.

Ancient CSF in the disc with mixed boundary condition

 $(\cos \rho, \sin \rho)$ (of radius 1/10, say) which is disjoint from the rotation of Γ^{ρ} through angle π about o, where Γ^{ρ} meets ∂D orthogonally, Stahl's short-time existence theorem for free boundary mean curvature flow [Sta96b, Theorem 2.1] yields a solution $\{\tilde{\Gamma}_{t}^{\rho}\}_{t\in[0,\delta)}$ to Neumann–Neumann curve shortening flow with boundary on the odd doubling of $\partial D\cap B$ for a short time $\delta>0$. Since this solution is uniquely determined by its initial condition, it must be invariant under rotation through angle π about o, and hence descend to a solution $\{\hat{\Gamma}_{t}^{\rho}\}_{t\in[0,\delta)}$ to Dirichlet–Neumann curve shortening flow in D with Dirichlet condition o and initial condition Γ^{ρ} . Denote by T the maximal time of existence of the latter.

Since the curvature of $\{\hat{\Gamma}_t^{\rho}\}_{t\in[0,T)}$ satisfies

$$\begin{cases} (\partial_t - \Delta)\kappa = \kappa^3 \\ \kappa = 0 \text{ at } o, \text{ and} \end{cases}$$

$$\kappa_s = \kappa \text{ at } \partial D,$$

where s denotes arclength from o, the maximum principle (and Hopf boundary point lemma) ensure that κ remains positive on $\hat{\Gamma}_t^{\rho} \setminus \{o\}$ for t > 0.

For similar reasons, positivity of κ_s is also preserved. Indeed, using the commutator relation

$$[\partial_t, \partial_s] = \kappa^2 \partial_s,$$

the identity $0 = \kappa_t = \Delta \kappa$ at o, and the positivity of κ away from o, we find that

$$\begin{cases} (\partial_t - \Delta)\kappa_s = 4\kappa^2 \kappa_s \\ (\kappa_s)_s = 0 \text{ at } o, \text{ and} \end{cases}$$

$$\kappa_s > 0 \text{ at } \partial D,$$

so the claim once again follows from the maximum principle.

Since $\overline{\theta}_t = \overline{\kappa} > 0$ and $\overline{\theta} < \pi$ (when d < 1, the maximum principle prevents $\hat{\Gamma}_t^{\rho}$ from ever reaching the minimizing arc — a stationary solution to the flow) we find that $\overline{\theta}$ must attain a limit as $t \to T$. We claim that this limit is π . Indeed, if $\overline{\theta} \le \theta_0 < \pi$ for all

 $t \in [0, T)$, then, representing the solution as a graph over the line $\{(-d, y) : y \in \mathbb{R}\}$, the "gradient estimate" (3) yields a uniform bound for the gradient, at least when d < 1. But then, by applying parabolic regularity theory (see, for instance, [Lie96]) to the graphical Dirichlet–Neumann curve shortening flow equation

$$\begin{cases} x_t = \frac{x_{yy}}{1 + x_y^2} & \text{in } [0, \overline{y}(t)] \\ x(0, t) = 0 \\ x_y(\overline{y}(t), t) = \cot \overline{\theta}(t), \end{cases}$$

where $\overline{y}(t) := \sin \overline{\theta}(t)$, we obtain uniform estimates for all derivatives of the graph functions $x(\cdot,t)$ (cf. [Sta96b]). To obtain corresponding estimates when d=1, we instead represent the solution as a graph over the "tilted" line through (-1,0) and $(\cos(\overline{\theta}(T)),\sin(\overline{\theta}(T)))$ and use the "gradient estimate" $\underline{\theta} \geq 0$. The Arzelà–Ascoli theorem and monotonicity of the flow now ensure that $x(\cdot,t)$ takes a smooth limit as $t \to T$, at which point the flow can be smoothly continued by the above short time existence argument, violating the maximality of T. We conclude that $\overline{\theta}(t) \to \pi$ as $t \to T$.

It now follows from (3) that $\underline{\theta}(t) \to \pi$ as $t \to T$. When d=1, we conclude that $\hat{\Gamma}_t^\rho$ contracts to o as $t \to T$. Note that in this case $T < \infty$ since the lower barriers $C_{\theta^-(t)}$ contract to o in finite time. A more or less standard "type-I vs type-II" blow-up argument (cf. [LZ]) then guarantees convergence to the half Grim Reaper after performing a standard type-II blow-up. (The flow must be type-II because the limit of a standard type-I blow-up — a shrinking semi-circle — violates the Dirichlet boundary condition.)

When d < 1, we conclude that $\hat{\Gamma}^{\rho}_t$ converges uniformly to the minimizing arc $\{(x,0): x \in [-1,-d]\}$ as $t \to T$. But then, for large enough t, $\hat{\Gamma}^{\rho}_t$ may be represented as a graph over the x-axis with small gradient, at which point parabolic regularity, short-time existence and the Arzelà–Ascoli theorem guarantee that $T = \infty$ and $\hat{\Gamma}^{\rho}_t$ converges uniformly in the smooth topology to the minimizing arc.

Finally, since $\overline{\theta}$ is monotone, there is a unique time $-\alpha_{\rho} > 0$ such that $\overline{\theta}(-\alpha_{\rho}) = \frac{\pi}{2}$; since the Neumann–Neumann circle $\check{C}_{\theta_{\rho}}$, where $\sin \theta_{\rho} = \frac{2 \sin \rho}{1 + \sin^2 \rho}$, lies above Γ^{ρ} , we find (by

Ancient CSF in the disc with mixed boundary condition

suitably time translating the upper barrier $\{\check{C}_{\theta^+(t)}\}_{t\in(-\infty,0)}$, as in [BL23]) that

$$\alpha_{\rho} < \frac{1}{2} \log \left(\frac{2 \sin \rho}{1 + \sin^2 \rho} \right).$$

Time-translating the solution $\{\hat{\Gamma}^{\rho}\}_{t\in[0,\infty)}$ by α_{ρ} now yields the desired very old (but not ancient) solution $\{\Gamma_{t}^{\rho}\}_{t\in[\alpha_{\rho},\infty)}$.

Taking the limit as $\rho \to 0$ of these very old (but not ancient) solutions yields our desired ancient solution.

Theorem 3.2. Given any $d \in (0,1]$, there exists a convex ancient Dirichlet–Neumann curve shortening flow $\{\Gamma_t\}_{t\in(-\infty,\omega_d)}$ in the upper half disc D_+ which converges uniformly in the smooth topology to the unstable critical arc $[-d,1] \times \{0\}$ as $t \to -\infty$. When d < 1, $\omega_d = \infty$ and $\{\Gamma_t\}_{t\in(-\infty,\omega_d)}$ converges uniformly in the smooth topology as $t \to +\infty$ to the minimizing arc $[-1,-d] \times \{0\}$. When d=1, $\omega_d < \infty$ and Γ_t^ρ converges uniformly as $t \to \omega_d$ to the point o, and there are a sequence of times $t_j \nearrow \omega_d$, right endpoints $p_j \in \Gamma_{t_j}^\rho$, and scales $\lambda_j \nearrow \infty$ such that the sequence $\{\lambda_j(\Gamma_{\lambda_j^{-2}t+t_j}^\rho - p_j)\}_{t\in[\lambda_j^2(\alpha_\rho - t_j),\lambda_j^2(\omega_\rho - j^{-1} - t_j))}$ converges locally uniformly in the smooth topology as $j \to \infty$ to the right half of the downwards translating Grim Reaper.

Proof. Given any sequence of angles $\rho_j \setminus 0$, consider the sequence of corresponding very old (but not ancient) solutions $\{\Gamma_t^j\}_{t\in[\alpha_j,\infty)}$ constructed in Lemma 3.1. Differentiating the Neumann boundary condition and applying the estimate (2) yields the inequality

$$\overline{\theta}_t = \overline{\kappa} \ge \frac{\sin \overline{\theta}}{a + \cos \overline{\theta}}$$

on each of these solutions. It follows, by the ODE comparison principle, that each $\{\Gamma_t^j\}_{t\in[\alpha_i,\infty)}$ satisfies

$$\overline{\theta} \le \theta^-$$
 (4)

for $t \in [\alpha_j, 0]$, where we recall that θ^- is the solution to (1). Since θ^- is independent of j, this implies uniform estimates for the gradient on any time interval of the form $[-\infty, -T]$, T > 0, when we represent $\{\Gamma_t^j\}_{t \in [\alpha_j, -T]}$ graphically over the x-axis. By parabolic regularity theory and the Arzelà–Ascoli theorem, we may then extract a smooth limit of the very old

solutions $\{\Gamma_t^j\}_{t\in(-\infty,0)}$ after passing to a subsequence. This limit is ancient, since $\alpha_\rho\to -\infty$ as $\rho\to 0$, reaches the point (0,1) at time zero (since each Γ_t^j intersects the convex domain bounded by $\check{C}_{\theta^+(t)}$ for each $t\in(-\infty,0)$), and converges uniformly in the smooth topology as $t\to -\infty$ to the unstable Dirichlet–Neumann geodesic from o due to the estimate (4) (and parabolic regularity theory). The longtime behaviour follows from the argument presented above.

3.1 Asymptotics

We now prove precise asymptotics for the height of the ancient solution constructed in Theorem 3.2, assuming the initial conditions for the old-but-not-ancient solutions $\{\Gamma_t^{\rho}\}_{t\in[\alpha_{\rho},\omega_d)}$ are given by the hairclip timeslices $\Gamma^{\rho}=\mathrm{H}_{t_{\rho}}^{\lambda_{\rho}}\cap D$.

Lemma 3.3. On each old-but-not-ancient solution $\{\Gamma_t^{\rho}\}_{t \in [\alpha_o, \omega_d)}$,

$$\frac{\kappa}{\cos \theta} \ge \lambda_{\rho} \tan(\lambda_{\rho} y).$$

Proof. Note that equality holds on the initial curve $\Gamma^{\rho} = H_{t_{\rho}}^{\lambda_{\rho}} \cap D$. Thus, given any $\mu < \lambda_{\rho}$, the function

$$w := \frac{\kappa}{\cos \theta} - \mu \tan(\mu y)$$

is strictly positive on the initial curve Γ^{ρ} , except at the left endpoint, where it vanishes. Observe that

$$w_s = \frac{\kappa_s}{\cos \theta} + \sin \theta \left(\frac{\kappa^2}{\cos^2 \theta} - \mu^2 \sec^2(\mu y) \right).$$

In particular, at the left endpoint on the initial curve,

$$w_{\rm s} = \frac{\kappa_{\rm s}}{\cos \theta} - \mu^2 \sin \theta = (\lambda_{\rho}^2 - \mu^2) \sin \theta > 0.$$

Thus (since w_s is continuous at o at time zero), if w fails to remain non-negative at positive times, then this failure must occur immediately following some *interior* time $t_* > 0$. There are three possibilities: 1. $w_s(\cdot,t_*)=0$ at the left endpoint, 2. $w(\cdot,t_*)=0$ at the right endpoint; or 3. $w(\cdot,t_*)=0$ at some interior point, p_* .

Ancient CSF in the disc with mixed boundary condition

The first of the three possibilities is immediately ruled out by the Hopf boundary point lemma.

In the second case, the Hopf boundary point lemma and the Neumann boundary condition yield, at the right endpoint,

$$0 > w_s = \frac{\kappa}{\cos \theta} + \sin \theta \left(\frac{\kappa^2}{\cos^2 \theta} - \mu^2 (1 + \tan^2(\mu y)) \right) = \mu \tan(\mu y) - \mu^2 y \ge 0,$$

which is absurd.

In the final case (having ruled out the first two), w must attain a negative interior minumum just following time t_* . But at such a point, w < 0, $w_s = 0$ and

$$0 \ge (\partial_t - \Delta)w$$

$$= \frac{(\partial_t - \Delta)\kappa}{\cos \theta} - \frac{\kappa(\partial_t - \Delta)\cos \theta}{\cos^2 \theta} + 2\left(\frac{\kappa}{\cos \theta}\right)_s \frac{(\cos \theta)_s}{\cos \theta} - (\partial_t - \Delta)(\mu \tan(\mu y)).$$

Since

$$(\partial_t - \Delta)\kappa = \kappa^3$$
, $(\partial_t - \Delta)\cos\theta = \kappa^2\cos\theta$ and $(\partial_t - \Delta)y = 0$,

we conclude that

$$0 \ge -2\left(\frac{\kappa}{\cos\theta}\right)_{s} \kappa \tan\theta + 2\mu \tan(\mu y)(\mu \tan(\mu y))_{s} \sin\theta$$

$$= 2(\mu \tan(\mu y))_{s} \sin\theta \left(\mu \tan(\mu y) - \frac{\kappa}{\cos\theta}\right)$$

$$= 2\mu^{2} \sec^{2}(\mu y) \left(\mu \tan(\mu y) - \frac{\kappa}{\cos\theta}\right)$$

$$> 0,$$

which is absurd.

Having ruled out each of the three possibilities, we conclude that $w \ge 0$ for any $\mu < \lambda_{\rho}$. The claim follows.

In the limit as $\rho \to 0$, we then obtain

$$\frac{\kappa}{\cos \theta} \ge \lambda_0 \tan(\lambda_0 y) \tag{5}$$

on the ancient solution, where $\lambda_0 = \lim_{\rho \to 0} \lambda_{\rho}$.

Mat Langford, Yuxing Liu, George McNamara

We now find that, as a graph over the *x*-axis (for *t* sufficiently negative),

$$(\sin(\lambda_0 y))_t = \lambda \cos(\lambda_0 y) y_t = \lambda_0 \cos(\lambda_0 y) \sqrt{1 + y_x^2} \kappa = \lambda_0 \cos(\lambda_0 y) \frac{\kappa}{\cos \theta} \ge \lambda_0^2 \sin(\lambda y),$$

and hence

$$\left(e^{-\lambda_0^2 t} \sin(\lambda_0 y)\right)_t \ge 0,$$

which implies that the limit

$$A(x) := \lim_{t \to -\infty} e^{-\lambda_0^2 t} y(x, t)$$

exists in $[0, \infty)$ for each $x \in (-d, 1)$.

Recall that $\theta^-(t) \sim \mathrm{e}^{\frac{t}{a+1}}$ for $t \sim -\infty$. In particular, $\overline{\theta}(t) \leq \theta^-(t)$ is integrable. We will exploit this fact to show that the limit A(x) is positive (at least near x=1). First, we shall show that $\overline{\kappa}$ is integrable.

Lemma 3.4. There exist $\rho_0 > 0$, $T > -\infty$, $C < \infty$ and $\delta > 0$ such that

$$\kappa \leq C e^{\delta t}$$
 for $t \leq T$

on each old-but-not-ancient solution $\{\Gamma_t^{\rho}\}_{t\in[\alpha_o,\omega_d)}$ with $\rho<\rho_0$.

Proof. Since

$$(\partial_t - \Delta)\sin\theta = \kappa^2\sin\theta,$$

we find that

$$(\partial_t - \Delta) \frac{\kappa}{\sin \theta} = 2\nabla \frac{\kappa}{\sin \theta} \cdot \frac{\nabla \sin \theta}{\sin \theta}.$$

So the maximum principle guarantees that the maximum of $\frac{\kappa}{\sin \theta}$ occurs at the parabolic boundary. Now, at the left boundary point, $\frac{\kappa}{\sin \theta} = 0$, while at the right,

$$\left(\frac{\kappa}{\sin\theta}\right)_{s} = \frac{\kappa}{\sin\theta} \left(\frac{\kappa_{s}}{\kappa} - \frac{\cos\theta\kappa}{\sin\theta}\right) = \frac{\overline{\kappa}}{\sin\overline{\theta}} \left(1 - \frac{\overline{\kappa}}{\tan\overline{\theta}}\right).$$

By (4), we can find $T > -\infty$ (independent of ρ) so that $\cos \overline{\theta}(t) \ge \frac{1}{2}$ for all $t \le T$. We thereby conclude that

$$\frac{\kappa}{\sin \theta} \le \max \left\{ 2, \max_{t = \alpha_{\rho}} \frac{\kappa}{\sin \theta} \right\}$$

Ancient CSF in the disc with mixed boundary condition

for all $t \le T$. Since $\max_{t=\alpha_\rho} \frac{\kappa}{\sin \theta} \le \lambda_\rho \tanh(\lambda_\rho (1+d)) \to \lambda_0^2 < 1$ as $\rho \to 0$, we find that

$$\overline{\kappa} \le 2\sin\overline{\theta} \le 2\sin\theta^-$$
 (6)

for all ρ sufficiently small. The claim follows since θ^- is comparable to $2^{1+\frac{a}{1+a}} \mathrm{e}^{\frac{t}{1+a}}$ as $t \to -\infty$.

Corollary 3.5. There exist $T > -\infty$, $C < \infty$ and $\delta > 0$ such that

$$\frac{\kappa}{v} \le \lambda_0^2 + Ce^{\delta t}$$
 for $t < T$

on the ancient solution.

Proof. Given $\rho < \rho_0$, set

$$\eta_{\rho}(t) := \lambda_{\rho}^{2} \left(\exp\left(\frac{C^{2}}{2\delta}e^{2\delta t}\right) - 1 \right),$$

where ρ_0 , C and δ are the constants from Lemma 3.4, so that

$$\frac{\eta_{\rho}'}{\lambda_{\rho}^2 + \eta_{\rho}} = C^2 e^{2\delta t}$$

and hence, for t < T,

$$\begin{split} (\partial_t - \Delta) \big(\kappa - (\lambda_\rho^2 + \eta_\rho) y \big) &= \kappa^3 - \eta_\rho' y \\ &\leq C^2 \mathrm{e}^{2\delta t} \kappa - \frac{\eta_\rho'}{\lambda_\rho^2 + \eta_\rho} (\lambda_\rho^2 + \eta_\rho) y \\ &= C^2 \mathrm{e}^{2\delta t} \big(\kappa - (\lambda_\rho^2 + \eta_\rho) y \big) \,. \end{split}$$

Since $\kappa - (\lambda_{\rho}^2 + \eta_{\rho})y = 0$ at the left endpoint and $(\kappa - (\lambda_{\rho}^2 + \eta_{\rho})y)_s = \kappa - (\lambda_{\rho}^2 + \eta_{\rho})y$ at the right endpoint, we find that

$$\kappa - (\lambda_{\rho}^2 + \eta_{\rho})y \le \exp\left(\frac{C^2}{2\delta}e^{2\delta t}\right) \left(\kappa - (\lambda_{\rho}^2 + \eta_{\rho})y\right)\Big|_{t=\alpha_{\rho}}$$

on each of the old-but-not-ancient solutions with $\rho < \rho_0$, and hence, taking $\rho \to 0$,

$$\kappa \le (\lambda_0^2 + \eta_0)y$$

on the ancient solution. The claim follows since, by the mean value theorem, we may estimate $\eta_0 \le \frac{\lambda_0^2 C^4}{4\delta^2} \mathrm{e}^{2\delta t}$ for t < 0.

By the estimate (4) and Corollary 3.5, we can find $T > -\infty$, $C < \infty$ and $\delta > 0$ such that our ancient solution satisfies

$$(\log \overline{y})_t = \frac{\overline{\kappa}}{\overline{y}\cos\overline{\theta}} \le \frac{1}{\sqrt{1 - 4C^2 e^{2\delta t}}} \frac{\overline{\kappa}}{\overline{y}} \le (1 + 8C^2 e^{2\delta t}) \frac{\overline{\kappa}}{\overline{y}} \le \lambda_0^2 + C^4 e^{2\delta t}$$

for t < T. Integrating from time t < T to time T and rearranging then yields

$$\overline{y} \ge B e^{\lambda_0^2 t}$$
, $B > 0$.

Since the gradient of the solution is bounded by $\tan \overline{\theta} \le C e^{\lambda_0^2 t}$ for $t \le T$, this guarantees that the limit $A(x) := e^{-\lambda_0^2 t} y(x,t)$ is positive for all $x > x_0$ where $x_0 < 1$.

4 Uniqueness

4.1 Unique asymptotics

Consider now any convex ancient Dirichlet–Neumann curve shortening flow $\{\Gamma_t\}_{t\in(-\infty,\omega)}$ with Dirichlet endpoint $o\in\overline{D}\setminus\{0\}$.

Lemma 4.1. Up to a time-translation, a rotation about the origin, and a reflection about the x-axis, we may arrange that

- o = (-d, 0) for some $d \in (0, 1]$,
- (0, 1) ∈ Γ₀,
- Γ_t lies in the upper half disc for all t, and
- $-\Gamma_t \to \{(x,0): x \in [-d,1]\}$ uniformly in the smooth topology as $t \to -\infty$.

Proof. Up to a time translation, we may arrange that $\omega > 0$. Up to rotation and a reflection, we may then arrange that $o = (-d,0), d \in (0,1]$, and $(\cos \overline{\theta}(0), \sin \overline{\theta}(0))$ lies in the upper half-disc. This ensures that $(\cos \overline{\theta}(t), \sin \overline{\theta}(t))$ lies in the upper half-disc for all t < 0. Indeed, if $\overline{\theta}(t_*) = 0$ for some $t_* < 0$, then convexity and the boundary conditions guarantee that $\Gamma_{t_*} = \{(x,0) : x \in [-d,1]\}$; so $\{\Gamma_t\}_{t \in (-\infty,\omega)}$ is the stationary unstable critical arc.

Ancient CSF in the disc with mixed boundary condition

Denote by Ω_t the region lying above $\Gamma_t \cup \{(0,x) : x \in [-1,-d]\}$ and set $\Omega := \bigcup_{t<\omega} \Omega_t$. The first variation formula for enclosed area yields

$$\frac{d}{dt}\operatorname{area}(\Omega_t) = -\int_{\Gamma_t} \kappa \, ds = -(\overline{\theta}(t) - \underline{\theta}(t))$$

and hence

$$\operatorname{area}(\Omega_t) = \operatorname{area}(\Omega_0) + \int_t^0 (\overline{\theta}(\tau) - \underline{\theta}(\tau)) d\tau.$$

Since $\operatorname{area}(\Omega)$ is finite, $\overline{\theta} - \underline{\theta}$ must converge to zero along some sequence of times $t_j \to -\infty$. Since $\overline{\theta} > 0$, this ensures that Ω is the upper half-disc, and hence Γ_t converges uniformly to the unstable critical arc as $t \to -\infty$. Parabolic regularity theory then guarantees smooth convergence.

Since the flow is monotone, Γ_t must then lie in the upper half disc for all t. We have thus shown, when d < 1, that $\omega = \infty$ and Γ_t converges smoothly to the minimizing arc as $t \to \infty$ and, when d = 1, that $\omega < \infty$ and Γ_t converges uniformly to o as $t \to \omega$. Up to a further time-translation, we may therefore arrange that the point (0,1) lies in Γ_0 .

Lemma 4.2. For every $t \in (-\infty, \omega)$, $\kappa_s > 0$.

Proof. Since $\kappa_s \ge 0$ at both endpoints, the claim may be obtained by applying the maximum principle exactly as in [BL23, Lemma 3.3].

Proposition 4.3. There exists $A \in [0, \infty)$ such that

$$y(x,t) = Ae^{\lambda_0^2 t} (\sinh(\lambda(x+d)) + o(1))$$
(7)

uniformly as $t \to -\infty$.

Proof. Denote by $\{\Gamma_t^*\}_{t\in(-\infty,\omega)}$ the constructed solution. Since Γ_0 and Γ_0^* both contain the point (0,1), the contrapositive of the avoidance principle guarantees that Γ_t must intersect Γ_t^* away from o at every time t<0. It follows that the value of $\underline{\theta}$ on the second solution must at no time exceed the value of $\overline{\theta}^*$ on the constructed solution. But then, applying the gradient bound (3) and estimating $\sin \overline{\theta}^* \leq A e^{\lambda_0^2 t} + o(e^{\lambda_0^2 t})$ yields

$$\frac{b}{1+a}\overline{y} \le \frac{b\sin\overline{\theta}}{1+a\cos\overline{\theta}} \le \tan\underline{\theta} \le 2\sin\underline{\theta} \le 2\sin\overline{\theta}^* \le 2(Ae^{\lambda_0^2t} + o(e^{\lambda_0^2t}))$$

as $t \to -\infty$, and hence, when d < 1,

$$\limsup_{t \to -\infty} e^{\lambda_0^2 t} \overline{y}(t) < \infty. \tag{8}$$

Since the height function y satisfies the (intrinsic) Dirichlet–Robin heat equation

$$\begin{cases} (\partial_t - \Delta)y = 0 \\ y = 0 \text{ at } o, y_s = y \text{ at } (\cos \overline{\theta}, \sin \overline{\theta}), \end{cases}$$

we may apply Alaoglu's theorem and elementary Fourier analysis as in [BL23, Proposition 3.4] to obtain (7).

When d=1, we need to work a little harder to obtain (8): at any time t<0, either $\overline{y}(t) \leq \overline{y}^*(t)$, as desired, or $\overline{y}(t) > \overline{y}^*(t)$. In the latter case, the avoidance principle and the Dirichlet condition ensure that $y^*(\cdot,t)-y(\cdot,t)$ attains a positive maximum at an interior point. Since the Dirichlet–Neumann circular arc $C_{\overline{\theta}(t)}$ lies below Γ_t (with common boundary), we can find some $t_0 > t$ and $x_0 \in (-1,\cos\overline{\theta}(t_0))$ such that the advanced arc $C_{\overline{\theta}(t_0)}$ touches Γ_t^* from above at the interior point $(x_0,y^*(x_0,t))$, and hence

$$y_{\overline{\theta}(t_0)}(x_0) = y^*(x_0, t) = :A_0 \text{ and } (y_{\overline{\theta}(t_0)})_x(x_0) = y_x^*(x_0, t) = :B_0,$$

where

$$y_{\theta}(x) = r(\theta) - \sqrt{r^2(\theta) - (x+1)^2}, \ r(\theta) := \frac{1 + \cos \theta}{\sin \theta}.$$

That is,

$$r_0 - \sqrt{r_0^2 - (x_0 + 1)^2} = A_0$$
 and $\frac{x_0 + 1}{\sqrt{r_0^2 - (x_0 + 1)^2}} = B_0$,

where $r_0 := r(\overline{\theta}(t_0))$. Rearranging, these become

$$x_0 + 1 = \frac{B_0 r_0}{\sqrt{1 + B_0^2}}$$
 and $r_0 = A_0 + \frac{x_0 + 1}{B_0} = A_0 + \frac{r_0}{\sqrt{1 + B_0^2}}$,

which together imply that

$$\left(\sqrt{1+B_0^2}-1\right)r_0=A_0\sqrt{1+B_0^2}=\frac{A_0}{x_0+1}B_0r_0.$$

Ancient CSF in the disc with mixed boundary condition

Eliminating r_0 and rearranging, we conclude that

$$\frac{A_0}{(x_0+1)B_0} = \frac{1}{1+\sqrt{1+B_0^2}}. (9)$$

We claim that this is only possible (when -t is sufficiently large) if x_0 is close to one. Indeed, the asymptotic linear analysis yields, for some $A \in (0, \infty)$,

$$\begin{cases} A_0 = y^*(x_0, t) = A e^{\lambda_0^2 t} \left(\sinh(\lambda_0(x_0 + 1)) + o(1) \right) \\ B_0 = y_x^*(x_0, t) = A \lambda_0 e^{\lambda_0^2 t} \left(\cosh(\lambda_0(x_0 + 1)) + o(1) \right) \end{cases} \text{ as } t \to -\infty.$$

(Note that, recalling (6), we may estimate $y_{xx}^* \lesssim \overline{\kappa}^* \leq 2\sin\overline{\theta}^* \leq Ce^{\lambda_0^2 t}$, which justifies the uniform C^1 convergence of $e^{-\lambda_0^2 t}y^*(\cdot,t)$.) Recalling (9), we conclude that

$$\frac{\tanh(\lambda_0(x_0+1))}{\lambda_0(x_0+1)} \to \frac{1}{2} \text{ as } t \to -\infty.$$

This implies that $x_0 = 1 - o(1)$ as $t \to -\infty$ and hence, as $t \to -\infty$,

$$\sin \overline{\theta}(t) \le \sin \overline{\theta}(t_0) = (1 + \overline{x}(t_0))r_0^{-1} \sim (1 + x_0)r_0^{-1} = \frac{B_0}{\sqrt{1 + B_0^2}} \le B_0 \sim e^{\lambda_0^2 t}$$

as desired.

4.2 Uniqueness

Uniqueness may now be established using the avoidance principle, as in [BL23, Proposition 3.5]. Combined with Theorem 3.2 and the asymptotics (7), this completes the proof of Theorem 1.1.

References

[AB11a] Ben Andrews and Paul Bryan. A comparison theorem for the isoperimetric profile under curve-shortening flow. *Comm. Anal. Geom.*, 19(3):503–539, 2011.

Mat Langford, Yuxing Liu, George McNamara

- [AB11b] Ben Andrews and Paul Bryan. Curvature bound for curve shortening flow via distance comparison and a direct proof of Grayson's theorem. *J. Reine Angew. Math.*, 653:179–187, 2011. 94
- [ALT] Paul T. Allen, Adam Layne, and Katharine Tsukahara. The Dirichlet problem for curve shortening flow. Preprint, arXiv:1208.3510v2. 94, 95
- [And12] Ben Andrews. Noncollapsing in mean-convex mean curvature flow. *Geom. Topol.*, 16(3):1413–1418, 2012. 94
- [BBC] Theodora Bourni, Nathan Burns, and Spencer Catron. Classification of convex ancient solutions to free boundary curve shortening flow in convex domains. Preprint, arXiv:2404.08824. 94
- [BL23] Theodora Bourni and Mat Langford. Classification of convex ancient free-boundary curve-shortening flows in the disc. *Anal. PDE*, 16(9):2225–2240, 2023. 94, 97, 105, 111, 112, 113
- [BLT20] Theodora Bourni, Mat Langford, and Giuseppe Tinaglia. Convex ancient solutions to curve shortening flow. *Calc. Var. Partial Differential Equations*, 59(4):133, 2020. 94
- [Buc05] John A. Buckland. Mean curvature flow with free boundary on smooth hypersurfaces. *J. Reine Angew. Math.*, 586:71–90, 2005. 94
- [DHS10] Panagiota Daskalopoulos, Richard Hamilton, and Natasa Sesum. Classification of compact ancient solutions to the curve shortening flow. *J. Differential Geom.*, 84(3):455–464, 2010. 94
- [Ede20] Nick Edelen. The free-boundary Brakke flow. *J. Reine Angew. Math.*, 758:95–137, 2020. 94
- [Gag84] M. E. Gage. Curve shortening makes convex curves circular. *Invent. Math.*, 76(2):357–364, 1984. 94, 95

Ancient CSF in the disc with mixed boundary condition

- [GH86] M. Gage and R.S. Hamilton. The heat equation shrinking convex plane curves. *J. Differ. Geom.*, 23:69–96, 1986. 94, 95
- [Gra87] Matthew A. Grayson. The heat equation shrinks embedded plane curves to round points. *J. Differential Geom.*, 26(2):285–314, 1987. 94, 95
- [Hui89] Gerhard Huisken. Nonparametric mean curvature evolution with boundary conditions. *J. Differential Equations*, 77(2):369–378, 1989. 94
- [Hui98] Gerhard Huisken. A distance comparison principle for evolving curves. *Asian J. Math.*, 2(1):127–133, 1998. 94
- [Ko] Dongyeong Ko. Existence and Morse index of two free boundary embedded geodesics on Riemannian 2-disks with convex boundary. Preprint, arXiv:2309.09896. 94
- [Lie96] Gary M. Lieberman. Second order parabolic differential equations. World Scientific Publishing Co., Inc., River Edge, NJ, 1996. 104
- [LZ] Mat Langford and Jonathan J. Zhu. A distance comparison principle for curve shortening flow with free boundary. Preprint, arXiv:2302.14258. 94, 95, 104
- [Sta96a] Axel Stahl. Convergence of solutions to the mean curvature flow with a Neumann boundary condition. *Calculus of Variations and Partial Differential Equations*, 4(5):421–441, 1996. 94
- [Sta96b] Axel Stahl. Regularity estimates for solutions to the mean curvature flow with a Neumann boundary condition. *Calculus of Variations and Partial Differential Equations*, 4(4):385–407, 1996. 94, 103, 104

Mat Langford, Yuxing Liu, George McNamara

AUTHORS

Mat Langford

Mathematical Sciences Institute,

Australian National University,

Canberra, ACT, Australia

email: mathew.langford@anu.edu.au

Yuxing Liu

Mathematical Sciences Institute,

Australian National University, Canberra,

ACT, Australia

email: yuxing.liu@anu.edu.au

George McNamara

Mathematical Sciences Institute,

Australian National University,

Canberra, ACT, Australia

email: george.mcnamara@anu.edu.au



Arnold Mathematical Journal Volume 11, Issue 3, 2025



Bouncing Outer Billiards

Andrey Gogolev Levi Keck Kevin Lewis

Received 09 Mar 2025; Accepted 22 Jul 2025

Abstract: We introduce a new class of billiard-like system, "bouncing outer billiards", which are 3-dimensional cousins of outer billiards of Neumann and Moser. We prove that the bouncing outer billiards system on a smooth convex body has at least four 1-parameter families of fixed points. We also fully describe the dynamics of bouncing outer billiards on a line segment. Finally, we carry out numerical experiments suggesting very complicated (non-ergodic) behavior for several shapes, including the square and an ellipse.

AMS Classification: 37A10, 37C05, 37C25

Key words and phrases: Billiards, outer billiards, integrable systems, periodic orbits, numerical experiments

1 Introduction

Outer billiards are dynamical systems introduced by Neumann in 1959 [Neu58] and then popularized by Moser in his lecture on stability of the solar system [Mos73, Mos78].

DOI: 10.56994/ARMJ.011.003.005

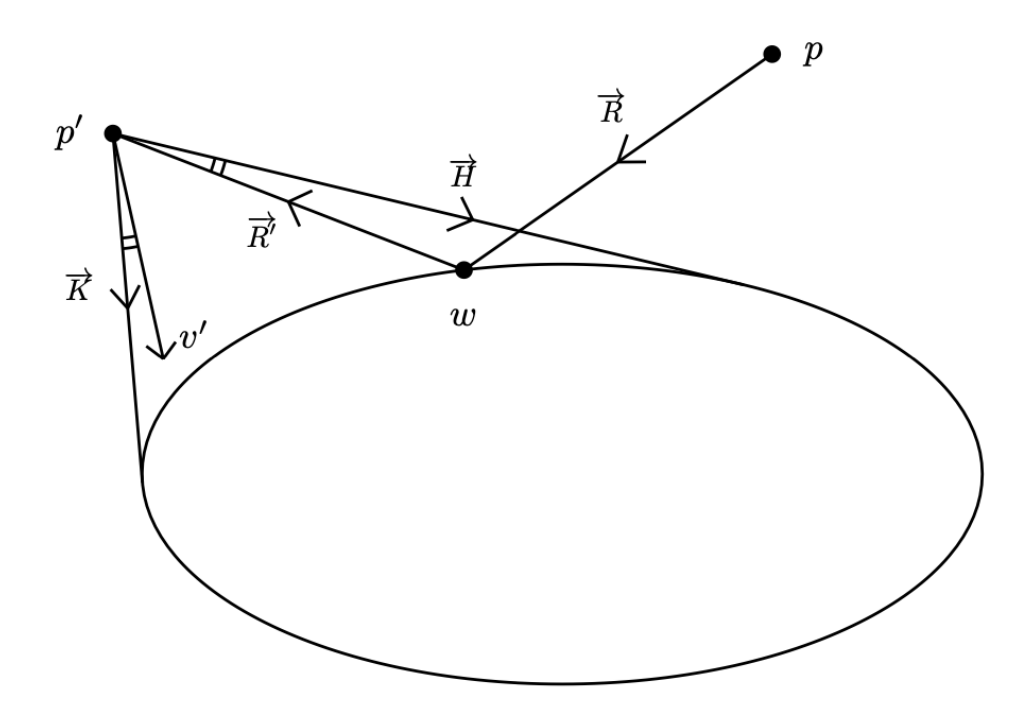


Figure 1: Bouncing Outer Billiards Dynamics

The field of outer billiards became very active about 20 years ago. In this paper, we suggest similar more complicated billiard systems called *bouncing outer billiards*, which we proceed to define.

Let $S \subset \mathbb{R}^2$ be a compact convex set with smooth boundary. The *visibility domain* V_S consists of all pairs (p, v) where $p \in \mathbb{R}^2 \setminus int(S)$, and $v \in T_p^1 \mathbb{R}^2$ is a unit vector based at p such that the ray \vec{R} spanned by v has a nonempty intersection with S.

We now define the dynamical system $F_S: V_S \to V_S$ in the following way. Given an initial condition $(p,v) \in V_S$ the corresponding ray \vec{R} reflects off the convex body at a point w as \vec{R}' in the usual way — the angle of incidence equals the angle of reflection. Next we apply the outer billiard law and consider the point $p' \in \vec{R'}$ such that $\|p - w\| = \|p' - w\|$ as indicated in Figure 1.

Finally, we will use the *visibility angle reflection rule* as follows. Let \vec{H} and \vec{K} be the rays at p' which are tangent to S. Let u be the unit vector based at p' pointing to w (in the

direction opposite to \vec{R}'). Clearly, u is inside the angle defined by \vec{H} and \vec{K} . Let v' be the reflection of u across the angle bisector of $\angle(\vec{H}, \vec{K})$ as shown on Figure 1. This completes the definition of bouncing billiard dynamics.

$$F_S(p, v) = (p', v').$$

We will drop the subscript *S* and simply write *F* when no confusion is possible.

Remark 1.1. It is easy to see that if \vec{R} is tangent to S then we have the classical outer billiard dynamics. Hence, the outer billiard is simply the restriction $F|_{\partial V_S}$ of the bouncing outer billiard to the boundary of the visibility space.

Remark 1.2 If S is not smooth, e.g. a polygon, then the angle reflection law is undefined for some initial conditions. However, such initial conditions form a set of zero Lebesgue measure since the boundary of a convex body is differentiable almost everywhere. Hence, bouncing billiard dynamics still makes sense for almost every initial condition, but the above relation to outer billiard is obscured.

Remark 1.3 S. Tabachnikov considered unfolding the outer billiard map into a family of symplectomorphisms given by the first two steps in the definition of the bouncing outer billiard [Tab95]. However, to the best of our knowledge, the visibility angle reflection rule was not considered before.

In the next section, we establish the existence of families of fixed points for bouncing outer billiards. Then, we fully describe integrable twist map dynamics of bouncing outer billiards on a line segment. Finally, we present results of our numerical explorations in the last section.

We would like to pose two questions.

Question 1.2. Does every orbit of the bouncing outer billiard on a smooth convex body remain bounded?

We were not able to detect any unbounded orbits numerically.

It is easy to check that bouncing outer billiards are conservative, that is, they preserve the Lebesgue measure on V_S (see Appendix A).

Question 1.3. *Does there exist positive volume ergodic components?*

We have found some orbits which appear to fill up 2-dimensional sets. However, in the 3-dimensional space V_S , such orbits seem to be confined to 2-dimensional surfaces.

Acknowledgements. This paper is a result of an REU project of summer 2024 at The Ohio State University. The authors are very grateful to Sergei Tabachnikov who provided several illuminating remarks on earlier drafts. The authors would like to acknowledge the support provided by the NSF grant DMS-2247747.

2 Fixed points

A natural question for any dynamical system is whether or not there exist fixed points, and if so, how to find them.

Theorem 2.1. For any convex S with C^3 boundary, the associated billiard map has uncountably many fixed points, which come in at least four local 1-parameter families.

Clearly, a point (p,v) can only be a fixed point if v is the bisector of the angle formed by the tangent rays from p to S. Therefore, given a point $p \notin S$, consider the angle given by the two tangent lines from p to S and let $v_p \in T_p\mathbb{R}^2$ be the vector spanning the angle bisector. The idea of the proof is to find a curve connecting two points, say p and q such that the ray of v_p "bounces to the left" and the ray of v_q "bounces to the right." Then, by the intermediate value theorem, there exists a fixed point (r, v_r) on such a curve.

We note right away that if ∂S has a circle subarc with constant curvature, then there is a whole 2-parameter family of fixed points in proximity of such arc. Hence we can assume, due to C^3 regularity of the boundary, that there exists a subarc of ∂S with strictly increasing curvature, as well as a subarc with strictly decreasing curvature.

The following is our main lemma.

Lemma 2.2. Let $f: [s_0, s_2] \to \partial S$ be a counter-clockwise arc-length parameterization of a subarc of ∂S along which the curvature is strictly increasing. Assume that this arc is sufficiently short so that the tangent lines at $f(s_0)$ and $f(s_2)$ intersect at a point p as indicated on Figure 2.

Then the angle bisector ray spanned by v_p will "bounce off in the direction of $f(s_0)$ ", that is, after reflecting off S, the ray will intersect the tangent segment a.

Proof. Let k(s) be the curvature at f(s), and let $K(s) = \int_{s_0}^s k(t)dt$. Since we are using arclength parameterization, K(s) is the angle between the tangent lines at $f(s_0)$ and f(s). There is a unique s_1 such that $K(s_1) = K(s_2)/2$. Then the tangent line at $f(s_1)$ is perpendicular to v_p . Hence, to prove the claim of the lemma it suffices to show that the distance from $f(s_1)$ to the tangent line b is less than the distance from $f(s_1)$ to the tangent line a. This can be expressed by the following inequality:

$$\int_{s_1}^{s_2} \sin(K(s_2) - K(s)) ds < \int_{s_0}^{s_1} \sin(K(s)) ds \tag{*}$$

To prove this inequality, we can start with the following statements by change of variables:

$$\int_{s_1}^{s_2} \sin(K(s_2) - K(s))k(s)ds = \int_0^{K(s_1)} \sin(u)du$$
$$\int_{s_0}^{s_1} \sin(K(s))k(s)ds = \int_0^{K(s_1)} \sin(v)dv$$

This gives

$$\int_{s_1}^{s_2} k(s) \sin(K(s_2) - K(s)) ds = \int_{s_0}^{s_1} k(s) \sin(K(s)) ds$$

Since curvature $k: [s_0, s_2] \to \mathbb{R}_+$ is increasing the posited inequality follows proving the lemma.

Proof of Theorem 2.1. Consider a local minimum (or maximum) of the curvature of ∂S . (By the 4-vertex theorem at least four local extrema exist.) On one side there is a short arc with increasing curvature and on the other side there is short arc with decreasing curvature. Applying the above lemma to the first arc we obtain an initial condition (p, v_p)

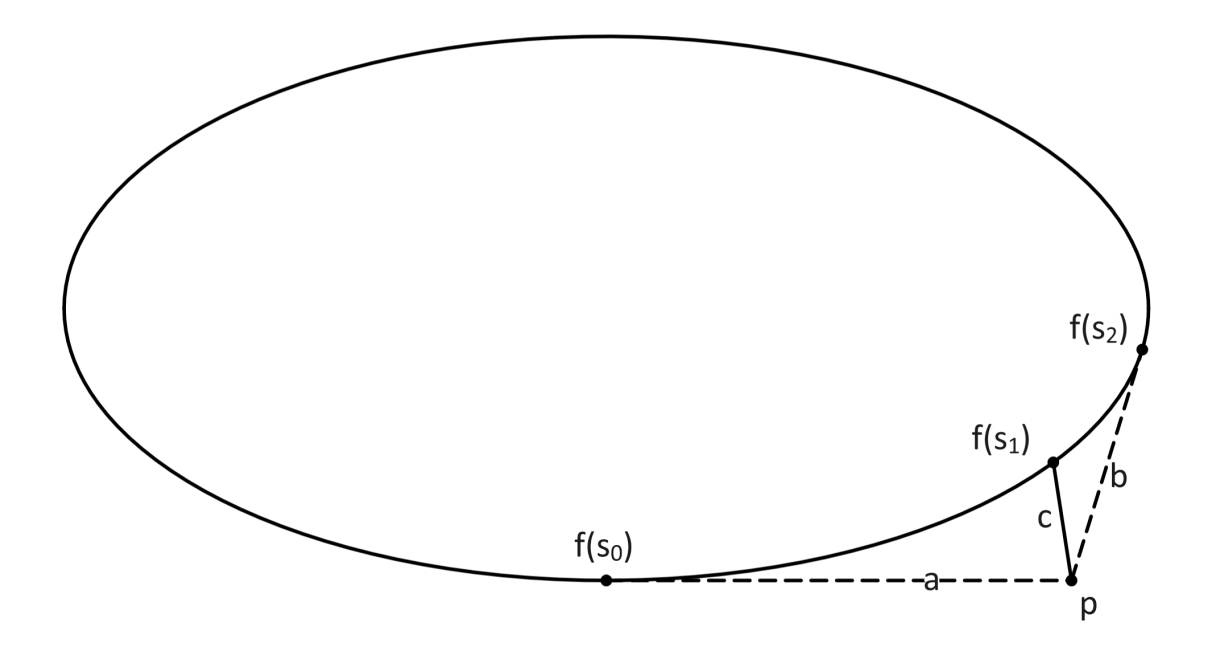


Figure 2: Fixed Point Lemma Setup

which "bounces to the left" and similarly, applying (the analogue of) the lemma to the arc with increasing curvature we obtain an initial condition (q, v_q) which "bounces to the right." It remains to connect p and q by an arc disjoint with S an apply the intermediate value theorem.

It is clear from the above proof that each vertex of ∂S yields a 1-parameter family of fixed points. These families could merge away from S. We would like to pose the following question.

Question 2.3. Let S be a convex domain with C^3 boundary. Does every closed curve around it contain at least one fixed point of the bouncing outer billiard map on S?

S. Tabachnikov considered a question of very similar flavor and eventually found a counterexample [Tab12].

3 Bouncing on a Line Segment

3.1 Parameterizing the Dynamics

This section focuses on the behavior of the bouncing outer billiards system on a line segment. Since all segments are congruent up to scaling, we only consider the segment on the x-axis from -1 to 1. For convenience, we will consider only initial points p with positive y-values, as points with negative y-values are symmetric.

Recall that we denote the visibility domain by V. Consider initial condition $(p,v) \in V$, where p = (x,y), and let $\theta = \arg(v) + \frac{\pi}{2}$. The initial conditions define a ray from the point p with slope $\tan(\theta - \frac{\pi}{2})$. Using this equation, we can derive:

$$w = (x + y \tan(\theta), 0)$$

$$p' = (x', y') = (x + 2y \tan(\theta), y)$$

Andrey Gogolev, Levi Keck, Kevin Lewis

Note that the y-coordinate of the initial point will remain constant on the orbit. From this point forward, we will refer to the y-value of the initial point as height and denote it by h.

Next, we obtain that the angle from p' to the left and right endpoints of the segment are given by $\arctan\left(\frac{1-x'}{h}\right)$ and $\arctan\left(\frac{-1-x'}{h}\right)$, respectively. Also, the angle from p' to w is given by $-\theta$. Applying the visibility angle reflection rule yields:

$$\theta' = \arctan\left(\frac{1-x'}{h}\right) + \theta + \arctan\left(\frac{-1-x'}{h}\right)$$

Summing up, the dynamics, $F(x, h, \theta) = (x', h, \theta')$ is given by:

$$x' = x + 2h \tan(\theta)$$

$$\theta' = \theta + \arctan\left(\frac{1 - x'}{h}\right) + \arctan\left(\frac{-1 - x'}{h}\right)$$
(1)

3.2 A Second Invariant

In Section 3.1, we observed that the height h is invariant. In this section, we will demonstrate the existence of a second invariant.

We define a new coordinate system in which it becomes easier to see a second invariant. First, consider the change of coordinates $g(x, h, \theta) = (w, h, d)$ given by

$$\begin{cases} w = x + h \tan(\theta) \\ d = h \tan(\theta) \end{cases}$$
 (2)

with the h-coordinate remaining unchanged. The coordinate w represents the x-value of the bounce point and the coordinate d represents the signed difference between the w and the x-value of the initial point. The inverse coordinate transformation is given by:

$$\begin{cases} x = w - d \\ \theta = \arctan\left(\frac{d}{h}\right) \end{cases}$$
 (3)

Now, we seek to understand the dynamics in these new coordinates. Let $f(w, h, d) = g \circ F \circ g^{-1}(w, h, d)$. We let f(w, h, d) be denoted by (w', h, d'), which we wish to write in terms of w, h, and d. First, combining (1) and (2) yields:

$$x' = w + d \tag{4}$$

Now, we will use (1) to rewrite the equation for d'. Following this, we simplify and use (2) and (4) to rewrite all instances of x' and $h \tan(\theta)$ in terms of w and d.

$$d' = h \tan(\theta')$$

$$= h \tan\left(\theta + \arctan\left(\frac{1 - x'}{h}\right) + \arctan\left(\frac{-1 - x'}{h}\right)\right)$$

$$= h \left(\frac{\tan(\theta) + \frac{-2x'h}{1 + h^2 - (x')^2}}{1 + \frac{2x'h}{1 + h^2 - (x')^2}}\right)$$

$$= \frac{h \tan(\theta) + h^3 \tan(\theta) - h(x')^2 \tan(\theta) - 2x'h^2}{1 + h^2 - (x')^2 + 2x'h \tan(\theta)}$$

$$= \frac{d^3 + 2h^2w + 2d^2w + dw^2 + h^2d - d}{w^2 - d^2 - h^2 - 1}$$
(5)

Finally, we can calculate w' by using the relationship w' = d' + x', which gives:

$$w' = w + d + \frac{d^3 + 2h^2w + 2d^2w + dw^2 + h^2d - d}{w^2 - d^2 - h^2 - 1}$$

$$= \frac{w^3 + d^2w + h^2w + 2dw^2 - w - 2d}{w^2 - d^2 - h^2 - 1}$$
(6)

We will now show the existence of a second invariant denoted a^2 , as a will later be shown to be the semi-axis of an ellipse.

Proposition 3.1. The quantity $a^2 := \frac{h^2 w^2 + d^2}{h^2 + d^2} \in (-1, 1)$ is preserved under dynamics. That is,

$$\frac{h^2w^2+d^2}{h^2+d^2} = \frac{h^2(w')^2+(d')^2}{h^2+(d')^2}.$$

The proof involves substituting w' and d' into the equation for a^2 to get $(a')^2 = \frac{h^2(w')^2 + (d')^2}{h^2 + (d')^2}$. After using (5) and (6) to simplify, we obtain:

Andrey Gogolev, Levi Keck, Kevin Lewis

$$(a')^2 = \frac{(h^2w^2 + d^2)(p(w, h, d))}{(h^2 + d^2)(p(w, h, d))}$$
$$= \frac{h^2w^2 + d^2}{h^2 + d^2} = a^2,$$

where

$$p(w, h, d) = d^4 + h^4 + 2d^2h^2 + 4d^3w + 6d^2w^2 + 4dh^2w$$

$$+ 4dw^3 + w^4 + 2h^2w^2 - 4dw - 2w^2 + 1 + 2h^2 - 2d^2.$$

Related to this is an equivalent invariant:

$$b^2 = \frac{h^2 w^2 + d^2}{1 - w^2} = \frac{h^2 a^2}{1 - a^2}.$$

3.3 Invariant Ellipses

In our altered coordinate system, the invariants a and b are actually the semi-axes of an invariant ellipse in the (w, h, d) coordinate system.

Proposition 3.2. Let $w, h, d \in \mathbb{R}$. Recalling the definitions $a^2 = \frac{h^2 w^2 + d^2}{h^2 + d^2}$ and $b^2 = \frac{h^2 w^2 + d^2}{1 - w^2}$, we have $\frac{w^2}{a^2} + \frac{d^2}{b^2} = 1$ (when $a^2, b^2 \neq 0$).

Proof.

$$\frac{w^2}{a^2} + \frac{d^2}{b^2} = \frac{w^2}{\frac{h^2 w^2 + d^2}{h^2 + d^2}} + \frac{d^2}{\frac{h^2 w^2 + d^2}{1 - w^2}}$$
$$= \frac{h^2 w^2 + d^2 w^2 + d^2 - d^2 w^2}{h^2 w^2 + d^2}$$
$$= 1$$

By Proposition 3.1, we have that $a^2 = (a')^2$, and by the relationship between a and b we have that $b^2 = (b')^2$. Together with Proposition 3.2, we get

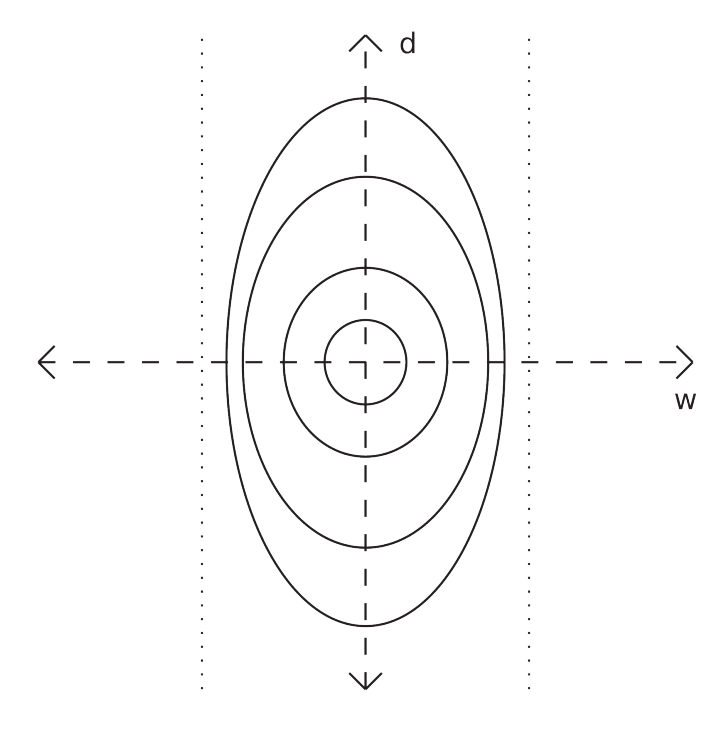


Figure 3: Several Invariant Ellipses with Height One

$$\frac{(w')^2}{a^2} + \frac{(d')^2}{b^2} = 1,$$

thus showing that any orbit belongs to an ellipse in the (w, d)-coordinate system.

Note that if a or b are equal to zero, then the other must be as well by the equation relating them. If they are both zero, we have that w=d=0 for all points in the orbit. Using (3), this implies that $x=\theta=0$ for all points in the orbit, which means such initial conditions correspond to fixed points.

3.4 Twist Dynamics

For this section, we will fix a height h and an invariant ellipse, thereby fixing invariants a and b, which are defined to be the positive square roots of a^2 and b^2 , respectively. We can parameterize the ellipse with $r(\theta) = (w, d) = (a\cos(\theta), b\sin(\theta))$. We now define the

function $\overline{f}: S^1 \to S^1$ as $\overline{f} = r^{-1} \circ f \circ r$, which allows us to view the restriction of f to our invariant ellipse as a circle diffeomorphism.

Theorem 3.3. There exists some $\varphi \in S^1$ such that $\overline{f}(\theta) = \theta + \varphi$, where $\varphi = \varphi(a)$ is a strictly increasing function, $\varphi'(a) > 0$ given by:

$$\varphi(a) = \begin{cases} \arctan(\frac{2ab}{b^2 - a^2}) + \pi & a < b \\ \arctan(\frac{2ab}{b^2 - a^2}) & a > b \end{cases}$$

$$\frac{3\pi}{2} \qquad a = b$$

with

$$\varphi'(a) = \frac{2b}{b^2 + a^2}.$$

The proof of this theorem is computational and will be included in the Appendix B.

3.5 Periodic Orbits for the Billiard on the Segment

Clearly, the middle perpendicular (the y-axis) gives a 1-parameter family of fixed points (these correspond to degenerate ellipses with a=b=0). Points of higher period are due to rational rotation numbers and come in 2-parameter families as one can vary the height as well.

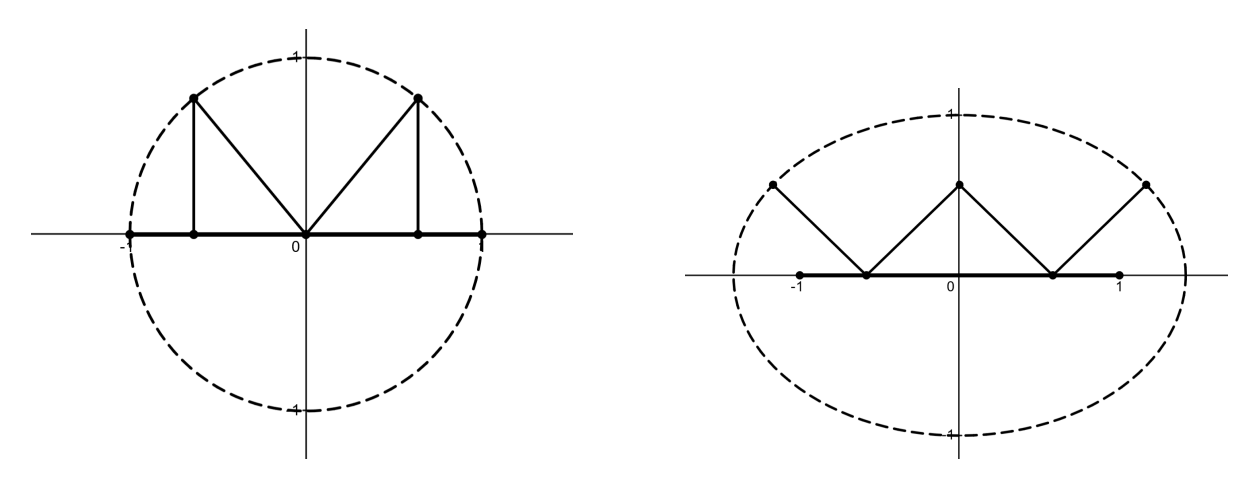


Figure 4: "M" and "W" period 4 orbits

We point out two aesthetically pleasing sub-families of period 4 orbits on Figure 4. The M-orbits fill out a semi-circle and the W-orbits fill out a semi-ellipse. For the "W" case on the right, the horizontal semi-axis is $\sqrt{2}$ and the foci of this ellipse are the ± 1 endpoints of the segment.

It is easy to calculate from the formula for the rotation number in Theorem 1.3 that for a given height h the interval of possible rotation numbers φ has the form $(\pi, \rho(h))$, where ρ is an explicit decreasing function, $\rho(h) \to 0$, $h \to \infty$; $\rho(h) \to 2\pi$, $h \to 0$. In particular, $(\pi, \rho(h)) \subset (\pi, 2\pi)$ and, hence, there are no orbits of period 2. Clearly, for all sufficiently small heights orbits of all periods ≥ 3 are present. As height increases smaller period orbits begin to disappear. For example orbits of period 4 with rotation number $\frac{3\pi}{2}$ disappear at h = 1 and orbits of period 3 with rotation number $\frac{4\pi}{3}$ disappear at $h \simeq 1.8$.

The explicit formula of Theorem 1.3 allows to explicitly calculate periodic orbits. For example, if one wished to find periodic orbits of least period 7, one can calculate parameter values that correspond to the rotation number $\frac{10\pi}{7}$.

Figure 5 depicts a family of period seven orbits of height one. Note that the depicted orbit is symmetric about the line x = 0, which unfolds into the family of asymmetric period seven orbits as indicated on the figure.

4 Numerical Simulations

4.1 Bouncing on Parabola Arcs

After fully understanding the dynamics on the segment, we can perturb the dynamics and examine how integrability is being destroyed. Probably the simplest way is to consider the unfolding of the segment into a piece of a downward-facing parabola given by $f(x) = -ax^2 + a$ { $-1 \le x \le 1$ }. We will make a slight modification to our visibility domain to make sure that bouncing billiard still makes sense.

Recall that our definition required that for (p, v) in the visibility domain, the ray

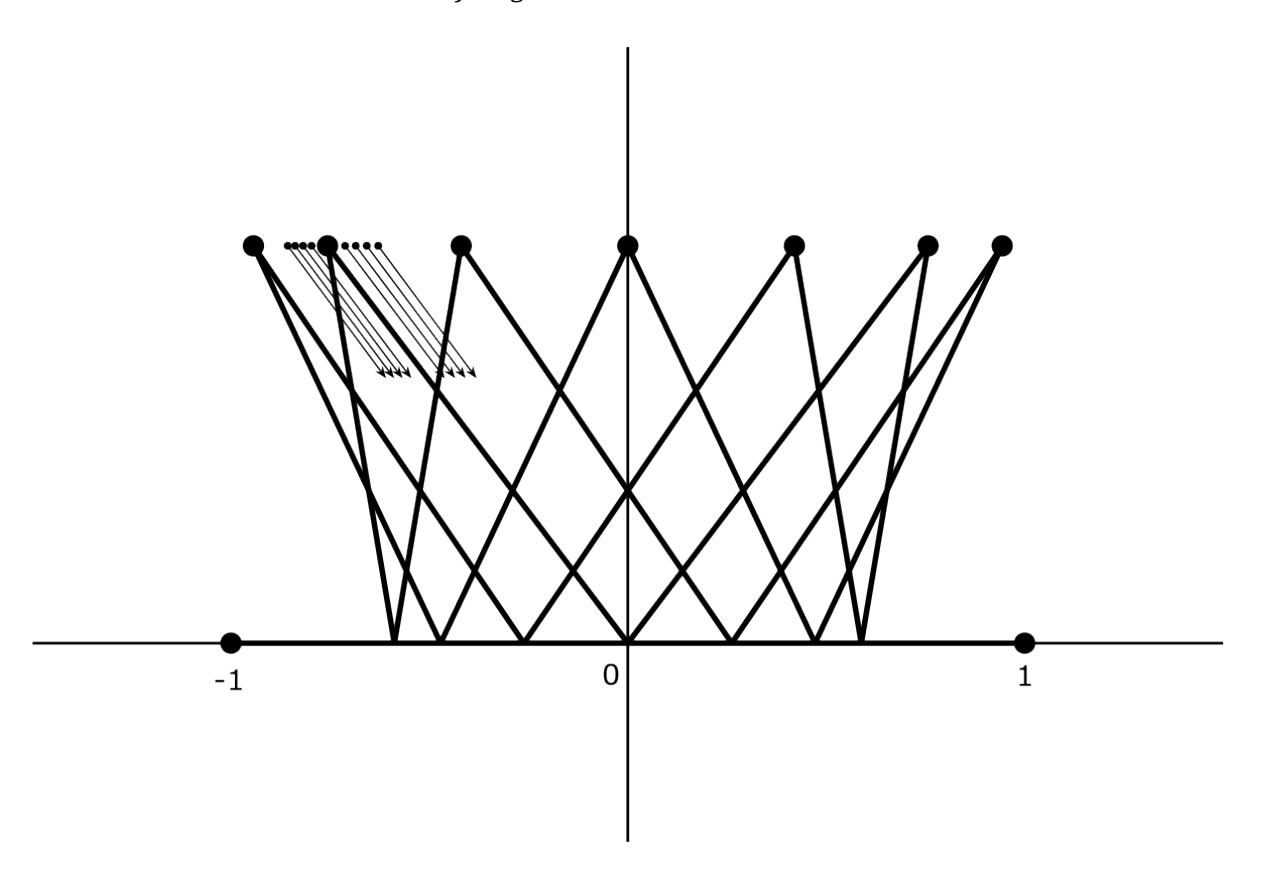


Figure 5: Family of Orbits of Period 7

spanned by v has a nonempty intersection with the boundary of the set. For the parabola, we will require that the ray has a nonempty intersection with the parabola, but we will impose the additional requirement that the segment \overline{pw} lies entirely above the parabola given by $-ax^2 + a$, where w is the closest intersection point to p of the ray and parabola. In other words, a point p must not be able to "see" the underside of the parabola. The dynamics rule remains the same, simply utilizing the newly defined visibility domain for the visibility angle reflection.

Remark 4.1. Despite the fact that our integrable model is a perfect twist map, KAM theory doesn't apply directly since we are in a 3-dimensional situation. Still, as we see below, KAM features such as elliptic islands seem to be present in our unfolding.

Figure 6 depicts some orbits on a parabola of height $\frac{3}{10}$. We observe that most of the orbits that begin close to the parabola fill invariant arcs which align themselves along the parabola (see the red orbit marked with a (2) in the figure). Others, such as the blue (1) and yellow (3) orbits, fill up periodic curves. Finally, some orbits, such as the black (4) one, exhibit more complicated behavior similar to Aubry-Mather sets with positive Lyapunov exponent.

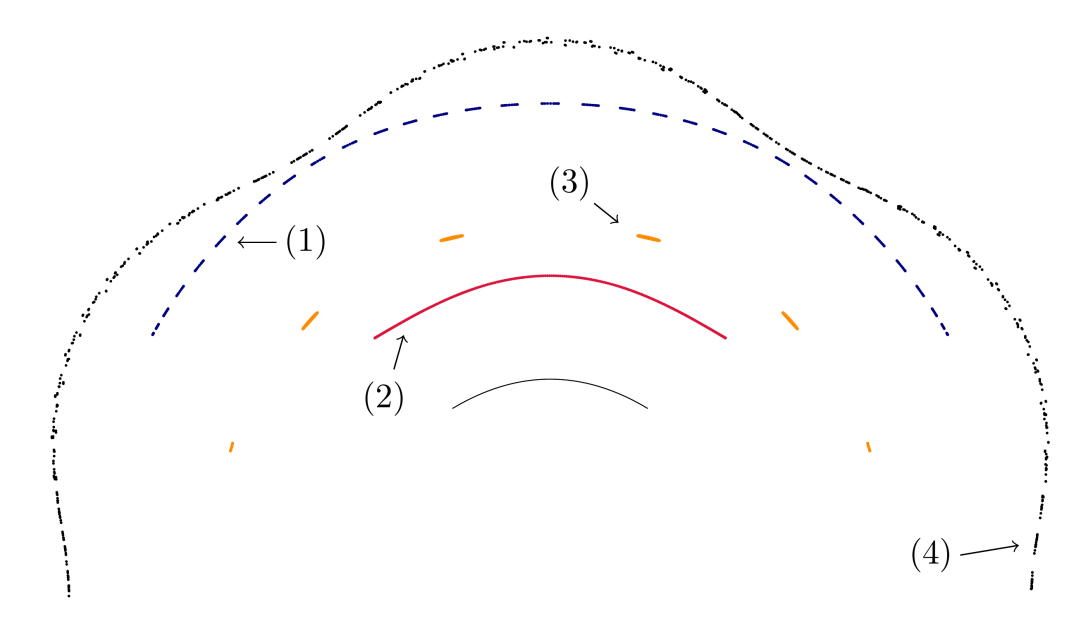


Figure 6: Orbits on Parabola of Height $\frac{3}{10}$

As we increase the height, the observed behaviors become more complicated. Figure 7 and Figure 8 depict orbits on parabolas of heights $\frac{1}{2}$ and 1, respectively. On these more extreme parabolas, we still observe periodic curves which take more complicated shapes, including non-symmetric orbits such as the blue (1) orbit on Figure 8. Additionally, with increased height, we more easily detect chaotic behavior, such as the black (4) orbits of both figures and the yellow (3) orbit of Figure 8.

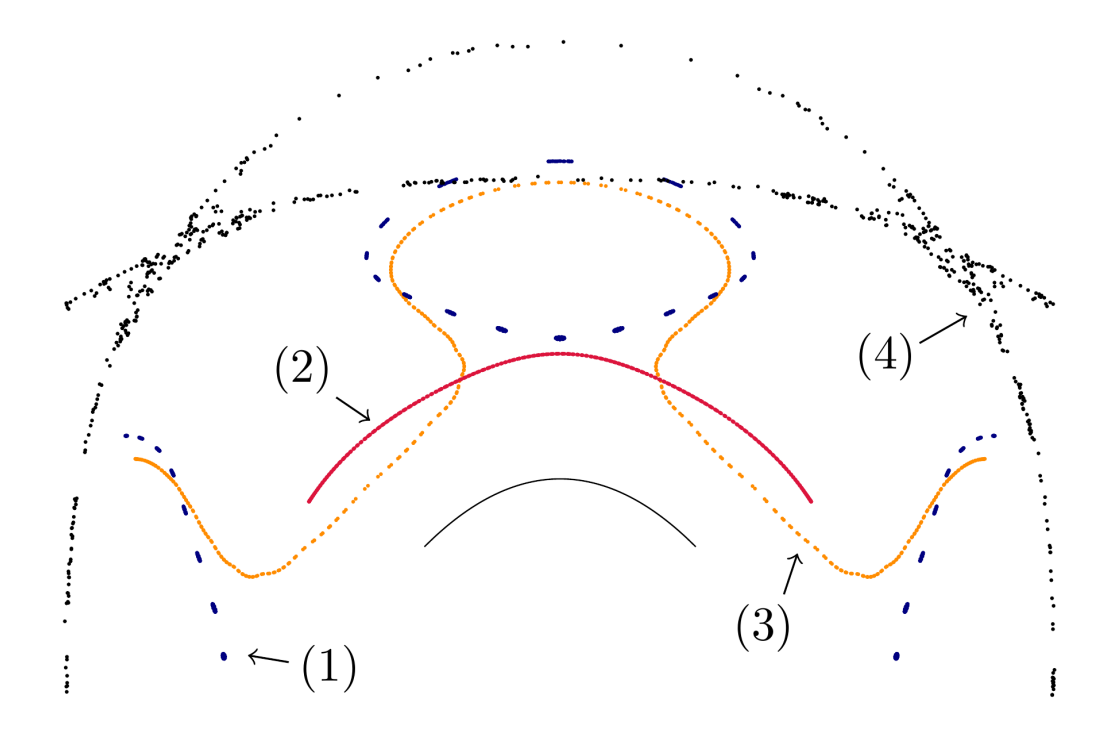


Figure 7: Orbits on Parabola of Height $\frac{1}{2}$

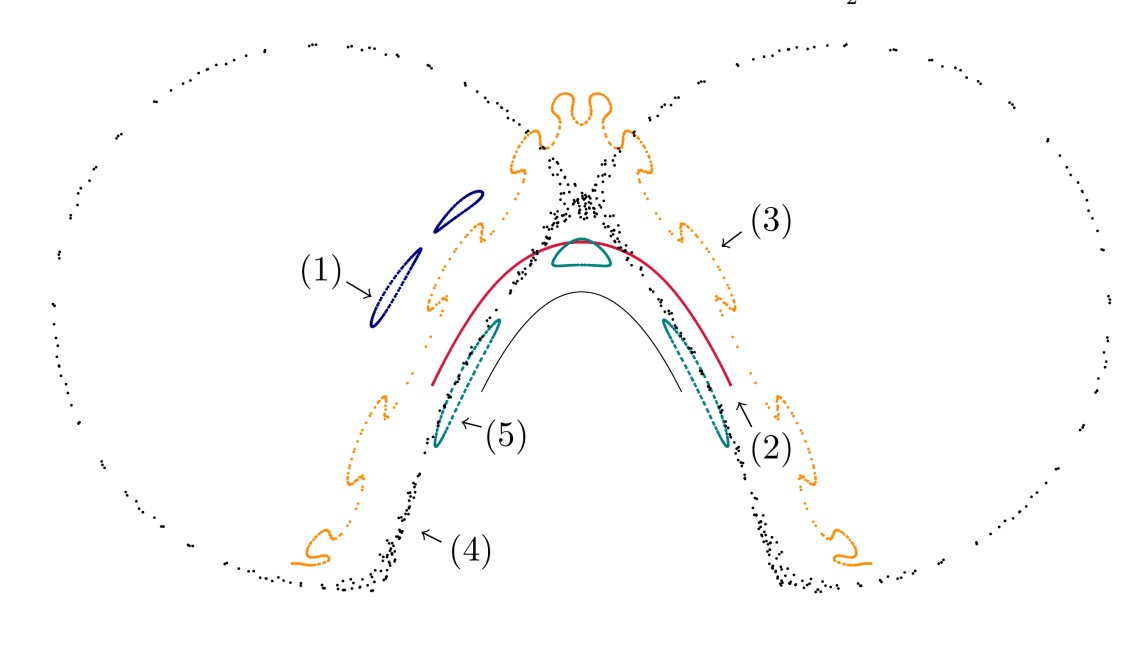


Figure 8: Orbits on Parabola of Height 1

4.2 Bouncing on the Square

It is also interesting to investigate bouncing billiards on polygons. For the sake of simplicity, we will focus solely on the system on the square. On the square, we classify observed orbits into five categories.

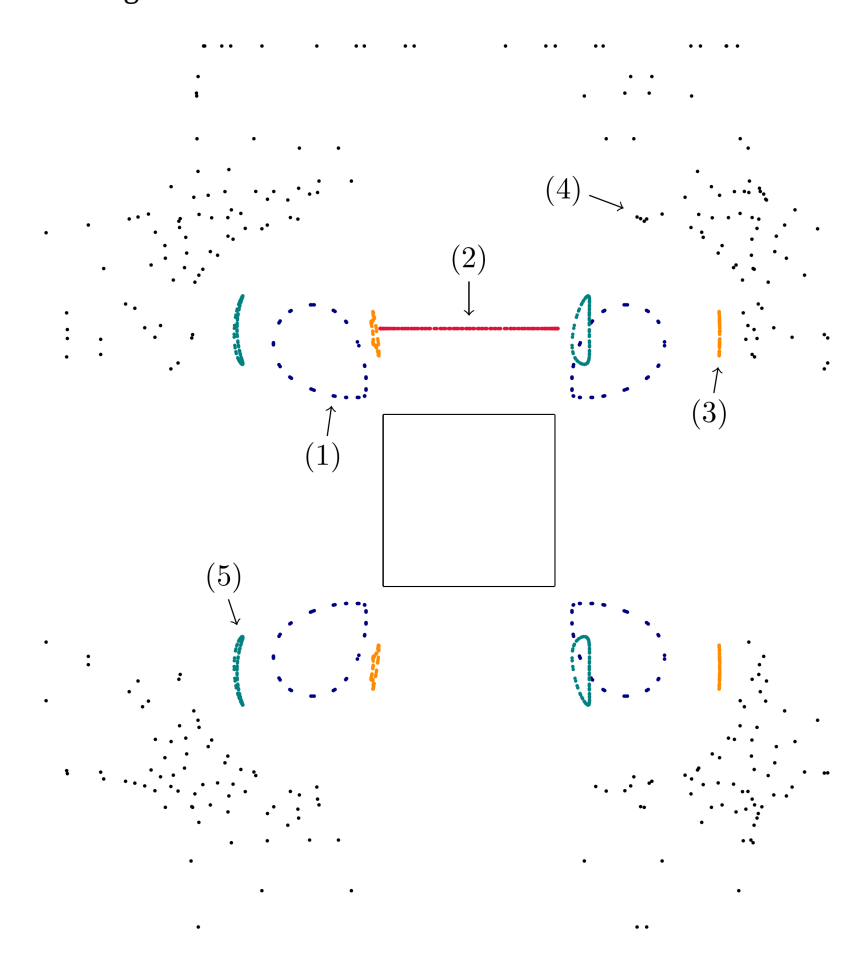


Figure 9: Orbits on a Square

The first category, such as the red (2) orbit in Figure 9, consists of points staying a fixed perpendicular distance away from one side of the square. For some such orbits, the orbit never extend in the direction parallel to that side further than the endpoints of the side. In this case, the system is identical to that on the line segment. In other cases, such orbit can extend past the corners of the square while still remaining on one side; in this

case the orbit is not the same as an orbit on the segment.

The second kind are those orbits which fill up four closed curves, with one near each corner of the square. This can be seen in the cyan (5) orbit of Figure 9. Most of these orbits observed appeared to be rotationally symmetric, but the one pictured is not.

The third kind involves what appears to be an invariant loop near each corner, but actually consists of many smaller closed curves making up the apparent larger circle. This is depicted in the blue (1) orbit of the figure.

The fourth kind is another chaotic variety. It involves a period 4 non-smooth set, possibly a Cantor set. This kind is depicted in the yellow (3) orbit of the figure.

The final class of orbits occupy all sides of the square and seem to behave chaotically such as the black (4) orbit. Such orbits appear to fill up positive area domains. However, numerics become very tricky for such orbits, as we clearly detected positive Lyapunov exponents for such orbits.

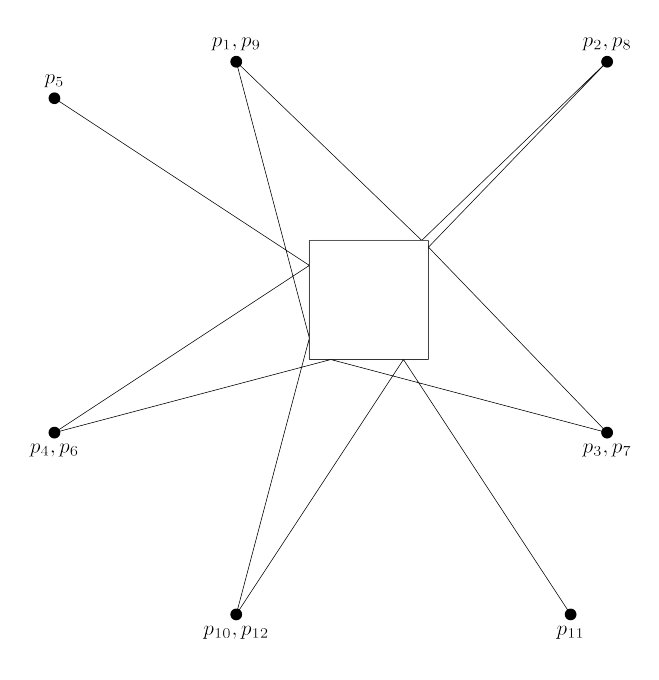


Figure 10: Period Twelve Orbit on Square with Large Eigenvalue

Another finding on the square is the existence of periodic points whose Jacobian

matrix has eigenvalues greater than one. Figure 10 shows one such example. It depicts a period twelve orbit whose Jacobian matrix has eigenvalues approximately 0.086, 1, and 11.592.

Remark 4.2. It is easy to see from the form of the differential of the bouncing outer billiard on a convex polygon that every periodic point of such a billiard has at least one eigenvalue equal to 1.

4.3 Bouncing on an Ellipse

While we fully understand the segment and the circle, in between fall ellipses, which also show very complex behavior. We consider bouncing outer billiard on the ellipse with major and minor semi-axis equal to 1 and 0.4, respectively. As expected, we can have orbits which are similar to the segment and circle, as shown in Figure 11 and Figure 12, respectively.

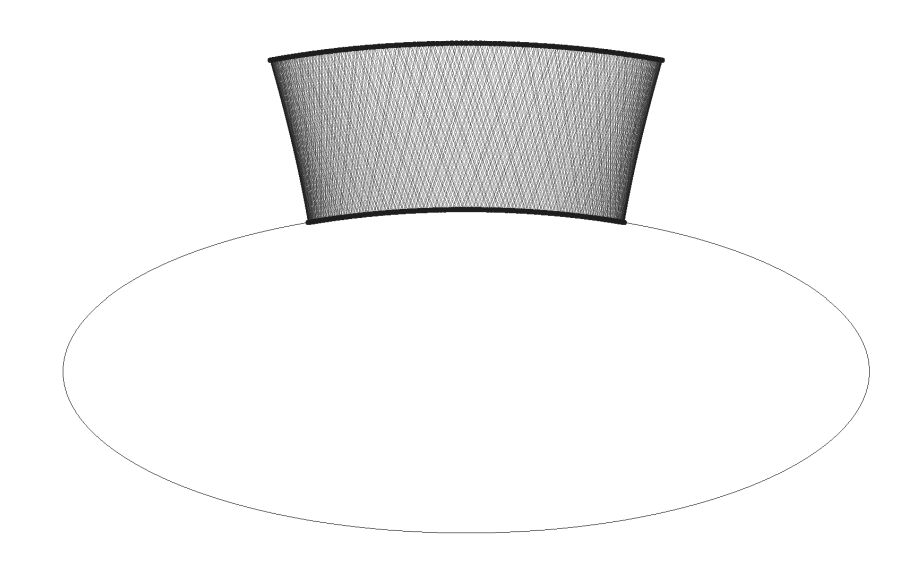


Figure 11: Segment-like behavior

Andrey Gogolev, Levi Keck, Kevin Lewis

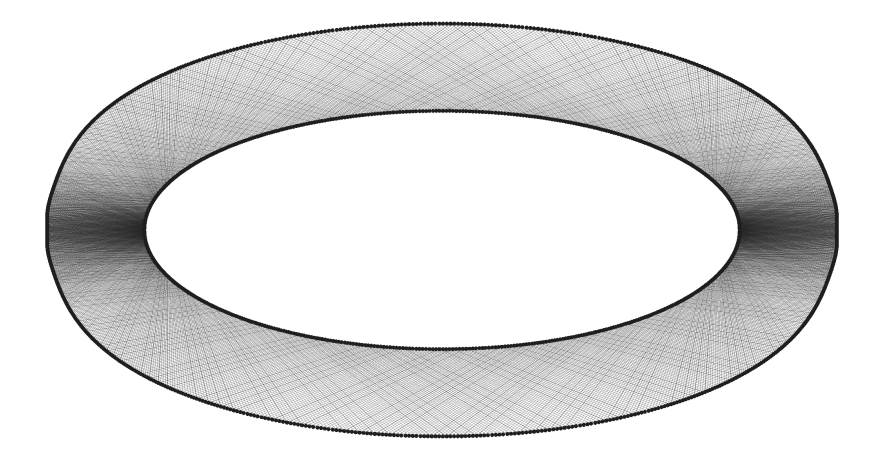


Figure 12: Circle-like behavior

We also have cases where the orbit closure fill periodic closed curves, such as those in Figure 13 and Figure 14.

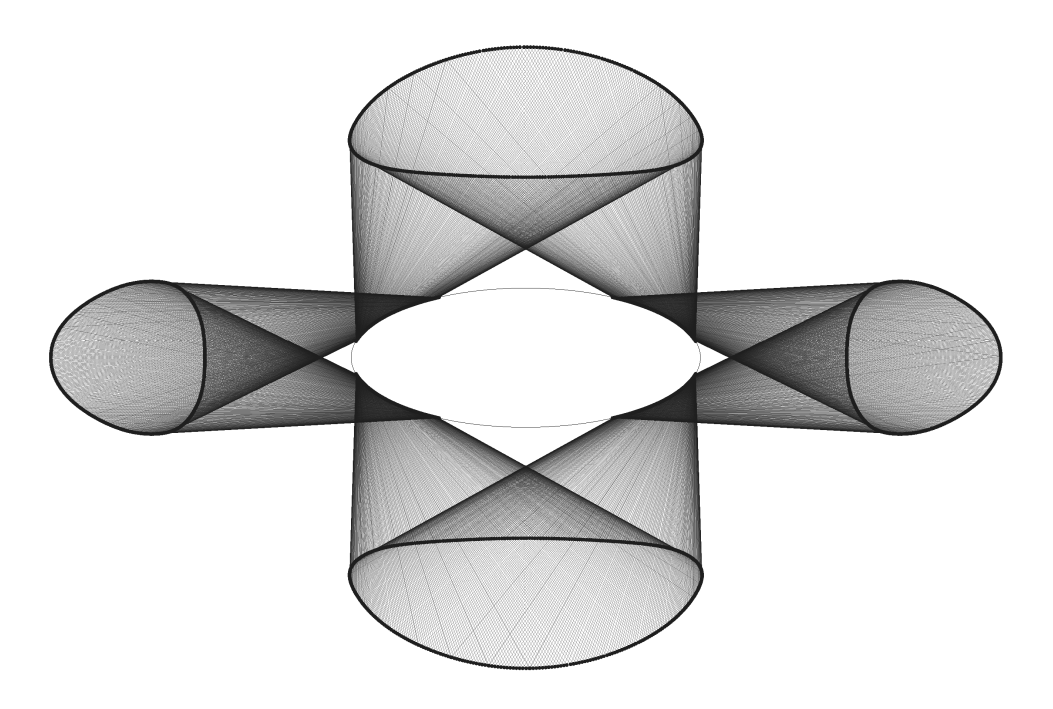


Figure 13: Four closed invariant curves

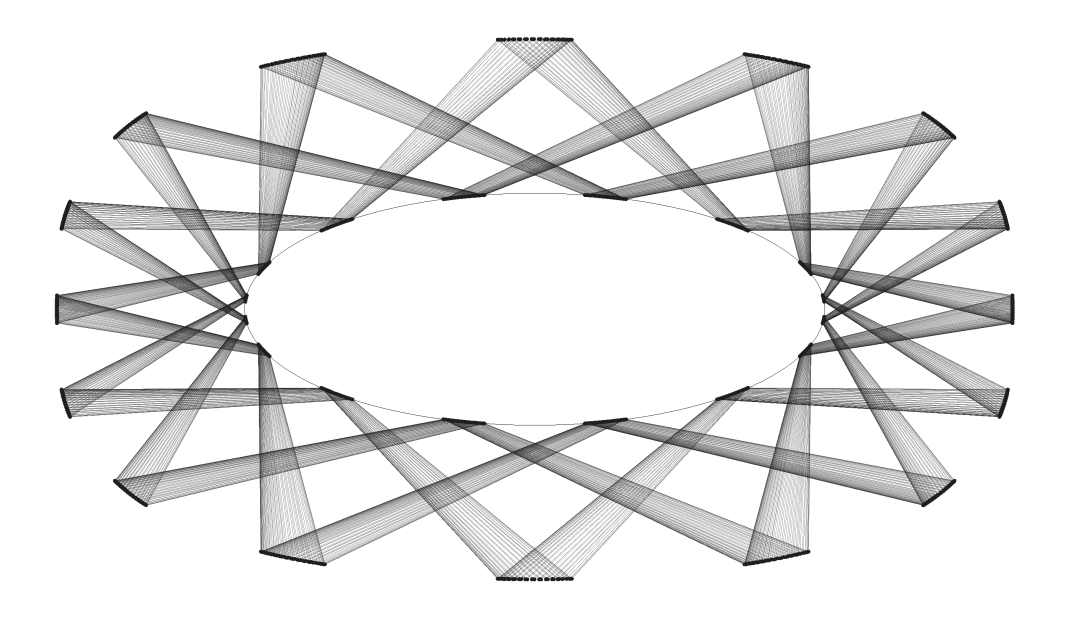


Figure 14: Many closed invariant curves

Finally, "in between" the circle-like behavior and four closed curve behavior, we detect an orbit which appears to fill up positive area domain, as shown in Figure 15.

We notice that the types of orbits we observe for the parabola arc and the ellipse are the same.

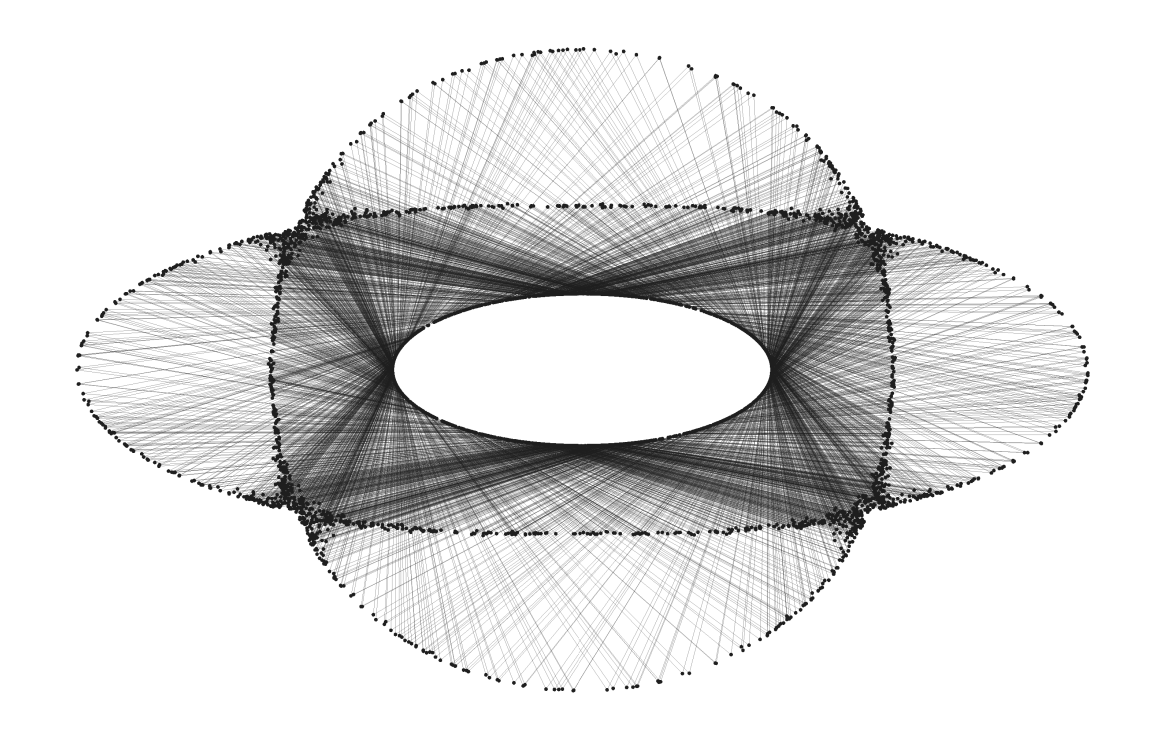


Figure 15: A chaotic orbit

Appendix A: The Conservative Property

Here we verify that bouncing outer billiard dynamics F preserves the Lebesgue measure. Let dA be the standard 2-dimensional Lebesgue measure restricted to \mathbb{R}^2 and let $d\theta$ be the Lebesgue on the circle.

Proposition 4.3. Assume that the boundary of S is a C^2 curve; then the restriction of $dA \otimes d\theta$ to V_S is an infinite measure which is invariant under F.

Remark 4.4. It is easy to verify invariance of the Lebesgue measure for polygons and seems

likely to be true for any convex S, but we haven't verified it in such generality.

Proof. We begin by noticing that the proposition holds true if S is a closed disc. Indeed, in this case it is easy to see that the visibility domain can be decomposed into circles on each of which F is a rigid rotation preserving the length (conditional measure). Hence F preserves $dA \otimes d\theta$.

Now, given a general domain S with C^2 boundary, we will verify that F_S is measure-preserving by checking that the Jacobian $JF = \det(DF)$ equals 1. Let $(p,v) \in V_S$, we can assume that (p,v) is in fact in the interior of V_S since ∂V_S has measure zero. Therefore, the ray starting at v intersect ∂S at the bounce point w transversely. This implies that infinitesimal variations of (p,v) result in infinitesimal variations of w of the same order of magnitude.

Consider the (unique) closed disc D such that ∂D is tangent to ∂S at w to the second order. Clearly, we have $F_S(p,v)=F_D(p,v)$. In fact, second-order tangency ensures that $DF_S(p,v)=DF_D(p,v)$. Indeed, to see this, first note that infinitesimal variation of (p,v) results in infinitesimal variations of w (on ∂S and ∂D), agreeing up to the second order. The angles of reflection of w are controlled by the derivatives of ∂S and ∂D at w and, hence, agree up to the first order (again due to second-order tangency at w) and the claim follows. Hence we have

$$JF_S(p, v) = \det DF_S(p, v) = \det DF_D(p, v) = 1,$$

where the last equality is by measure-preserving property of F_D pointed out at the beginning of the proof.

It is easy to show that the total Lebesgue measure of V_S is infinite when integrating in the correct order. For any angle θ , there is an infinitely long strip of constant width w of points whose rays at angle θ will hit S, where w is the length of S projected onto the axis perpendicular to θ .

Alternatively, one can verify the above proposition by a direct calculation of DF(p,v) without any reference to the disc case. Specifically, we can center the (x,y)-coordinate

Andrey Gogolev, Levi Keck, Kevin Lewis

system at the bounce point w so that the x-axis is tangent to ∂S and denote by θ the circular coordinate. We write $(p,v)=(a,b,\theta_0)$. Clearly $dA\otimes d\theta=dx\otimes dy\otimes d\theta$ and we need to verify that the Jacobian is 1 in (x,y,θ) -coordinates. Prior to the last visibility angle reflection step we have $(a,b,\theta_0)\mapsto (-a,b,-\theta_0)$ and a routine calculation gives the following expression for its derivative:

$$\begin{pmatrix} 1 + 2kb & -2ka - \frac{2a}{b} & \frac{2c^2}{b} + 2kc^2 \\ 2ka & 1 - \frac{2ka^2}{b} & \frac{2kac^2}{b} \\ -2k & \frac{2ka}{b} & -1 - \frac{2kc^2}{b} \end{pmatrix}$$

where k is the curvature at w and $c = \sqrt{a^2 + b^2}$. The determinant of this matrix is -1, which becomes 1, after composing with the reflection $\theta \mapsto const - \theta$ according to the visibility angle reflection rule.

Appendix B: Proof of Theorem 3.3

First, we will find an explicit formula for $r^{-1}(w,d)$ for w and d lying on the ellipse. We have $w=a\cos(\theta)$ and $d=b\sin(\theta)$, meaning $\tan(\theta)=\frac{ad}{hw}$. This yields:

$$\theta = r^{-1}(w, d) = \arctan\left(\frac{ad}{bw}\right) + \pi n(w) \tag{7}$$

In this formula, we use

$$n(x) := \begin{cases} 1 & x < 0 \\ 0 & x \ge 0 \end{cases}$$

to compensate for the fact that arctan only outputs between $\frac{-\pi}{2}$ to $\frac{\pi}{2}$. This explicit formula has the slight flaw that it fails for w=0. However, it can be shown separately that this case matches the behavior of all other cases. Applying r^{-1} to the right of both sides of the equation $\overline{f}=r^{-1}\circ f\circ r$ yields $\overline{f}\circ r^{-1}(w,d)=r^{-1}\circ f(w,d)=r^{-1}(w',d')$. Applying (7) yields:

$$\overline{f}(\arctan\left(\frac{ad}{bw}\right) + \pi n(w)) = \arctan\left(\frac{ad'}{bw'}\right) + \pi n(w')$$

Thus $\overline{f}(\theta) = \theta + \varphi(w, d)$, where

$$\varphi(w,d) = \arctan\left(\frac{ad'}{bw'}\right) + \pi n(w') - \arctan\left(\frac{ad}{bw}\right) - \pi n(w).$$

We will first show that $\varphi(w,d)$ is constant mod π . The terms $\pi n(w')$ and $-\pi n(w)$ are equivalent to zero mod π , so we will revisit these later.

Thus, we currently seek to show that $\arctan(\frac{ad'}{bw'}) - \arctan(\frac{ad}{bw})$ is constant $\mod \pi$. We will use the arc-tangent subtraction formula $\arctan(x) - \arctan(y) = \arctan(\frac{x-y}{1+xy}) + m\pi$, where m is either 0 or 1 depending on x and y. The term $m\pi$ is equivalent to zero $\mod \pi$ in all cases, so we will revisit this term later as well.

For the purposes of the following calculation, we will set $x = \frac{ad'}{bw'}$ and $y = \frac{ad}{bw}$. Our goal is to show that $\frac{x-y}{1+xy}$ is constant for any w and d on the fixed ellipse. First, since x and y each have a factor of $\frac{a}{b}$, which is constant for points on the ellipse, we can pull this out of the fraction:

$$\frac{x-y}{1+xy} = \left(\frac{a}{b}\right) \left(\frac{\frac{d'}{w'} - \frac{d}{w}}{1 + \frac{a^2dd'}{b^2ww'}}\right)$$

Next, multiply the numerator and denominator by b^2ww' to get:

$$\left(\frac{a}{b}\right)\left(\frac{b^2d'w - b^2dw'}{b^2ww' + a^2dd'}\right)$$

We can pull out another b^2 to bring the total constant factored out to ab:

$$(ab)\left(\frac{d'w - dw'}{b^2ww' + a^2dd'}\right)$$

After replacing w' and d' with their equivalent expressions in terms of w, h, and d, then multiplying the numerator and denominator by $(w^2 - d^2 - h^2 - 1)$, we get:

$$\frac{(ab)(2h^2w^2+2d^2)}{b^2(w^4+d^2w^2+h^2w^2+2dw^3-w^2-2dw)+a^2(d^4+2dh^2w+2d^3w+d^2w^2+d^2h^2-d^2)}$$

Andrey Gogolev, Levi Keck, Kevin Lewis

After substituting in the expressions for a^2 and b^2 , multiplying the numerator and denominator by $(1 - w^2)(h^2 + d^2)$, and simplifying, we get:

$$\frac{2ab(1-w^2)(h^2+d^2)}{d^2h^2w^2+h^4w^2+h^2w^4+d^4+d^2h^2+d^2w^2-h^2w^2-d^2}$$

Factoring the denominator yields:

$$\frac{2ab(1-w^2)(h^2+d^2)}{(h^2w^2+d^2)(h^2+d^2)-(h^2w^2+d^2)(1-w^2)}$$

Finally, dividing the numerator and denominator by $(1 - w^2)(h^2 + d^2)$ gives:

$$\frac{2ab}{\frac{h^2w^2+d^2}{1-w^2} - \frac{h^2w^2+d^2}{(h^2+d^2)}} = \frac{2ab}{b^2 - a^2}$$

Thus, we end up with the equation:

$$\varphi = \arctan\left(\frac{2ab}{b^2 - a^2}\right) mod \ \pi$$

Next, we will go back and carefully consider each of the extra terms we set aside earlier to show that φ is actually constant mod 2π . Each of these components individually may depend on w, d, a, and b, but we will show that together they only depend on a and b, which remain constant within an orbit.

We will begin with the term denoted as $m\pi$ earlier. Recall that this arose out of the extra term from the arc-tangent sum formula. Again using the definitions $x = \frac{ad'}{bw'}$ and $y = \frac{ad}{bw}$, we get that m = 0 if -xy < 1 and m = 1 if -xy > 1. This is equivalent to saying m = 0 if 1 + xy > 0 and m = 1 if 1 + xy < 0. After substituting in expressions to get 1 + xy in terms of w, h, and d as well as simplifying and factoring, we get:

$$1 + xy = \frac{(d^2 + h^2w^2)(d^2 + h^2 + w^2 - 1)}{(d^2 + h^2)(d^2w^2 + h^2w^2 + 2dw^3 + w^4 - 2dw - w^2)}$$

Since we are only concerned about the sign of 1 + xy, and $\frac{d^2 + h^2 w^2}{d^2 + h^2} \ge 0$, we can factor this out and ignore it. This leaves us with:

$$\frac{d^2 + h^2 + w^2 - 1}{d^2w^2 + h^2w^2 + 2dw^3 + w^4 - 2dw - w^2} = \frac{d^2 + h^2 + w^2 - 1}{w^2(d^2 + h^2 + w^2 - 1) + 2dw^3 - 2dw}$$

This has the same sign as its reciprocal, which after simplification becomes:

$$w^2 + \frac{2dw^3 - 2dw}{d^2 + h^2 + w^2 - 1}$$

Next, it will benefit us to rewrite d in terms of w, a, and b. Starting from the ellipse equation $\frac{w^2}{a^2} + \frac{d^2}{b^2} = 1$, we can derive the equation $d^2 = b^2 - \frac{w^2b^2}{a^2}$. Rewriting our previous expression yields:

$$w^{2} + \frac{(2w^{3} - w)\left(\pm\sqrt{b^{2} - \frac{w^{2}b^{2}}{a^{2}}}\right)}{b^{2} - \frac{w^{2}b^{2}}{a^{2}} + h^{2} + w^{2} - 1}$$

Next, we will remove h from the expression. Recall the relationship between a^2 and b^2 given by $b^2 = \frac{h^2 a^2}{1-a^2}$. From this, we can derive $h^2 = \frac{b^2 - a^2 b^2}{a^2}$. From here, we can perform a series of simplifications:

$$w^{2} + \frac{(2w^{3} - w)\left(\pm\sqrt{b^{2} - \frac{w^{2}b^{2}}{a^{2}}}\right)}{b^{2} - \frac{w^{2}b^{2}}{a^{2}} + h^{2} + w^{2} - 1} = w^{2} + \frac{2w(w^{2} - 1)\left(\pm\sqrt{b^{2} - \frac{w^{2}b^{2}}{a^{2}}}\right)}{\frac{b^{2}}{a^{2}} - \frac{w^{2}b^{2}}{a^{2}} + \frac{w^{2}a^{2}}{a^{2}} - \frac{a^{2}}{a^{2}}}$$

$$= w^{2} + \frac{2wa^{2}(w^{2} - 1)\left(\pm\sqrt{\frac{b^{2}(a^{2} - w^{2})}{a^{2}}}\right)}{(w^{2} - 1)(a^{2} - b^{2})}$$

$$= w^{2} + \frac{2wab(\pm\sqrt{a^{2} - w^{2}})}{a^{2} - b^{2}}$$

$$= \frac{a^{2}w^{2} - b^{2}w^{2} + 2wab(\pm\sqrt{a^{2} - w^{2}})}{a^{2} - b^{2}}$$

Next, we want to find the zeros of this expression with respect to w. Clearly, w=0 is a zero. To find other zeros, we will set the numerator of our expression equal to zero and assume $w \neq 0$. $a^2w^2 - b^2w^2 + 2wab(\pm\sqrt{a^2-w^2}) = 0 \implies a^2w - b^2w + 2ab(\pm\sqrt{a^2-w^2}) = 0$. After rearranging and squaring both sides, we get:

Andrey Gogolev, Levi Keck, Kevin Lewis

$$a^2 - w^2 = \frac{b^4 w^2 - 2a^2 b^2 w^2 + a^4 w^2}{4a^2 b^2}$$

Solving for *w* yields:

$$w = \pm \frac{2a^2b}{a^2 + b^2}$$

From this point forward, we will assume d is positive. The calculations play out similarly if d is negative, and the results will be given with the positive case. This means our fraction is zero when $a^2w - b^2w + 2ab\sqrt{a^2 - w^2} = 0$, removing the plus or minus present earlier. We have the possible zeros of $\pm \frac{2a^2b}{a^2+b^2}$, but determining which is a true zero will depend on the values of a and b. This is because $\sqrt{a^2 - w^2}$ becomes $\frac{a(a^2 - b^2)}{a^2+b^2}$ if a > b or $\frac{a(b^2 - a^2)}{a^2+b^2}$ if a < b. This means that if a > b we have $\frac{-2a^2b}{a^2+b^2}$ is a zero, whereas if b > a we have $\frac{2a^2b}{a^2+b^2}$ is a zero.

To find the sign of the expression, we can solve the derivatives at the zeros:

$$\frac{d}{dw} \left(\frac{a^2 w^2 - b^2 w^2 + 2wab\sqrt{a^2 - w^2}}{a^2 - b^2} \right) = \frac{2a^2 w - 2b^2 w + 2ab\sqrt{a^2 - w^2} - \frac{2abw^2}{a^2 - w^2}}{a^2 - b^2}$$
(8)

We will first analyze the derivative values for a > b. The denominator is positive in this case, and we see that the derivative is positive at w = 0. For $w = \frac{-2a^2b}{a^2+b^2}$, we have that the numerator of (8) becomes:

$$\frac{2a^2b(b^2-a^2)}{a^2+b^2} + \frac{-2abw^2}{a^2-w}$$

The second term of this expression is always negative. Since we assumed a > b, the first term is also negative, meaning the derivative is negative for this w-value.

In the case where a < b, the denominator is always negative, and we have that the derivative is negative at w = 0. For $w = \frac{2a^2b}{a^2+b^2}$, the numerator becomes:

$$\frac{2a^2b(a^2-b^2)}{a^2+b^2} + \frac{-2abw^2}{a^2-w}$$

This is again negative, but the derivative is positive, since the denominator of (8) is negative. In summary, we have the following results:

In
$$d > 0$$
 Case: If $a < b$ and $w \in (\frac{2a^2b}{a^2+b^2}, 1] \cup [-1, 0)$, then $1 + xy > 0$.
If $a < b$ and $w \in (0, \frac{2a^2b}{a^2+b^2})$, then $1 + xy < 0$.
If $a > b$ and $w \in [-1, \frac{-2a^2b}{a^2+b^2}) \cup (0, 1]$, then $1 + xy > 0$.
If $a > b$ and $w \in (\frac{-2a^2b}{a^2+b^2}, 0)$, then $1 + xy < 0$.

The case where d < 0 works similarly, with results as follows:

In
$$d < 0$$
 Case: If $a < b$ and $w \in [-1, \frac{-2a^2b}{a^2+b^2}) \cup (0, 1]$, then $1 + xy > 0$.
If $a < b$ and $w \in (\frac{-2a^2b}{a^2+b^2}, 0)$, then $1 + xy < 0$.
If $a > b$ and $w \in (\frac{2a^2b}{a^2+b^2}, 1] \cup [-1, 0)$, then $1 + xy > 0$.
If $a > b$ and $w \in (0, \frac{2a^2b}{a^2+b^2})$, then $1 + xy < 0$.

Next, we will tackle the $\pi n(w')$ term. Recall that n(w') is defined to be 1 when w' is negative and 0 otherwise. Thus, our next goal is to determine the sign of w' under all possible conditions. We will again take d>0 and present the results for the d<0 case later.

$$w' = \frac{w^3 + d^2w + h^2w + 2dw^2 - w - 2d}{w^2 - d^2 - h^2 - 1}$$

$$= \frac{w^3 - \frac{b^2w^3}{a^2} + \frac{b^2w}{a^2} + 2w^2\sqrt{b^2 - \frac{b^2w^2}{a^2}} - w - 2\sqrt{b^2 - \frac{b^2w^2}{a^2}}}{w^2 + \frac{b^2w^2}{a^2} - \frac{b^2}{a^2} - 1}$$

$$= \frac{(w^2 - 1)(a^2w - b^2w + 2ab\sqrt{a^2 - w^2})}{(w^2 - 1)(a^2 + b^2)}$$

$$= \frac{a^2w - b^2w + 2ab\sqrt{a^2 - w^2}}{a^2 + b^2}$$
(9)

We have already examined the zeros of this expression when working through the $m\pi$ term. It has a zero at $w = \frac{2a^2b}{a^2+b^2}$ when a < b and one at $\frac{-2a^2b}{a^2+b^2}$ when a > b. Notably, this expression does not have a zero at w = 0 like the previous. In this case, we have that the

Andrey Gogolev, Levi Keck, Kevin Lewis

derivative is negative at $w = \frac{2a^2b}{a^2+b^2}$ when a < b and positive at $\frac{-2a^2b}{a^2+b^2}$ when a > b.

In
$$d > 0$$
 Case: If $a < b$ and $w \in [-1, \frac{2a^2b}{a^2+b^2})$, then $w' > 0$.
If $a < b$ and $w \in (\frac{2a^2b}{a^2+b^2}, 1]$, then $w' < 0$.
If $a > b$ and $w \in (\frac{-2a^2b}{a^2+b^2}, 1]$, then $w' > 0$.
If $a > b$ and $w \in [-1, \frac{-2a^2b}{a^2+b^2})$, then $w' < 0$.

Similarly, if d < 0, we get:

In
$$d < 0$$
 Case: If $a < b$ and $w \in [-1, \frac{-2a^2b}{a^2+b^2})$, then $w' > 0$.
If $a < b$ and $w \in (\frac{-2a^2b}{a^2+b^2}, 1]$, then $w' < 0$.
If $a > b$ and $w \in (\frac{2a^2b}{a^2+b^2}, 1]$, then $w' > 0$.
If $a > b$ and $w \in [-1, \frac{2a^2b}{a^2+b^2})$, then $w' < 0$.

Finally, we have the $-\pi n(w)$ term, which requires no extra analysis since our results are currently allowed to be dependent on w.

The final step in this proof is to check how many π terms are added for each initial condition for w and d, as well as a and b values. This will be omitted since it solely involves going through each relevant interval for w and d for both the a > b and a < b case. The results are as follows:

$$\varphi = \begin{cases} \arctan(\frac{2ab}{b^2 - a^2}) + \pi & a < b \\ \arctan(\frac{2ab}{b^2 - a^2}) & a > b \\ \frac{-\pi}{2} & a = b \end{cases}$$

Taking the derivative of φ with respect to a yields:

$$\varphi'(a) = \frac{2b}{b^2 + a^2}$$

This is clearly positive for all values a > 0 since b is nonzero and positive for such a. \square

References

- [Mos73] J. Moser. *Stable and Random Motions in Dynamical Systems*, volume 77 of *Annals of Mathematics Studies*. Princeton University Press, 1973. 117
- [Mos78] J. Moser. Is the solar system stable? *Mathematical Intelligencer*, **1**:65–71, 1978.
- [Neu58] B. H. Neumann. Sharing ham and eggs. Iota., pages 14–18, 1958. 117
- [Tab95] S. Tabachnikov. On the dual billiard problem. *Adv. Math.*, 115(2):221–249, 1995.
- [Tab12] S. Tabachnikov. The (un)equal tangents problem. *The American Mathematical Monthly*, 119(5):398–405, 2012. 123

AUTHORS

Andrey Gogolev
Department of Mathematics,
The Ohio State University,
Columbus, OH, USA, 43210
email: gogolyev.1@osu.edu

Levi Keck
Department of Mathematics,
The Ohio State University,
Columbus, OH, USA, 43210
email: keck.140@osu.edu

Andrey Gogolev, Levi Keck, Kevin Lewis

Kevin Lewis
Department of Mathematics,
The Ohio State University,
Columbus, OH, USA, 43210

email: lewis.3164@osu.edu